$\mathcal{PT}$-Symmetric Hamiltonians and an Analysis of Elliptic Potential Functions in Complex Classical Mechanics

Karta Kooner
Imperial College London

September 25, 2009

Submitted in partial fulfilment of the requirements for the degree of Master of Science of the University of London

Abstract

Background to the area of $\mathcal{PT}$-symmetric Hamiltonians is presented, where the idea is put forward to replace the physically-obscure requirement for the Hamiltonian to be Hermitian with the more physical condition that the Hamiltonian merely be symmetric under the combined operations of parity reversal and time reversal — for the Hamiltonian to be $\mathcal{PT}$-symmetric. The quantum framework required to be constructed under this guideline in order to create a mechanical description of nature that preserves the remaining axioms of the quantum theory is summarized, along with the consequences that this framework appears to suggest with respect to the classical analogues of the quantum Hamiltonians is question — namely, that of classical systems extended into the complex domain.

The work done so far in examining particular classical systems where the dynamical variables are permitted to be complex is summarized, and new numerical analysis is presented of systems where the potential function is taken to be the Jacobi elliptic function $-\mathrm{cn}(x)$. Quantum behaviour seen in previous complex systems was found to be reproduced, along with other intriguing dynamics; and, although the results of the numerical simulations quickly lose accuracy within the time frame allocated for this study, it is hoped that the qualitative behaviour of the systems observed is interesting enough to prompt more detailed and extensive analysis.

1 Introduction

The quantum theory has been around since the start of the nineteenth century, and in the intervening years has undergone much work and revision; not least concerning its postulates and formalism, which have now gained widespread acceptance. However, looking at the theory's axioms it is clear that the condition that the Hamiltonian must be Hermitian is more of a mathematical nature than a physical requirement. The Hermiticity of the Hamiltonian, H, is expressed mathematically as

$$H = H^{\dagger}, \tag{1}$$

where the symbol † represents the combined operations of complex conjugation and Matrix transposition. Certainly, it appears to be a necessary requirement within the current quantum framework as a whole, where it is linked to the requirement that the time evolution operator, e^{-iHt}, be unitarity; but, in and of itself as an axiom of a physical theory it is harder to justify its presence. Where one finds difficulty in abandoning the requirement that, for example, the energy spectrum be bounded from below so that there exists a stable lowest-energy state, there appears to be less such a barrier for asking for the Hermiticity of the Hamiltonian to be dropped.

Hamiltonians that are not Hermitian are not an entirely new concept in the history of the quantum theory: they are used as a simplified and phenomenological description for the decay process [1]; and have been used to describe the ground state of a quantum system hard spheres [2], Reggeon field theory [3], and the Lee-Yang edge singularity [4]. However, as a description

for nuclear decay their use is understood to be a purely simplified and non-fundamental description from the outset, and their use as a serious attempt to describe the behaviours of a system has otherwise been criticized [6]. The problem with their use so far has been that the Hamiltonian plays a very important role in the quantum theory:

1. The Hamiltonian determines the allowed energy states of the system. The physical states, represented by the eigenfunction ψ, of the system obey the time-independent Schrödinger equation

$$H\psi = E\psi, \tag{2}$$

and span the Hilbert space of the system. The allowed energy levels of the system are determined by the eigenvalues E, which must be real and bounded from below. Here, the part played by the requirement for the Hamiltonian to be Hermitian is evident: if it were not so, the energy eigenvalues of the time-independent Schrödinger equation could not be guaranteed to be real.

2. The Hamiltonian determines the time evolution of the states and operators in the quantum theory. Any state $\psi(t)$ must also satisfy the time-dependent Schrödinger equation:

$$i\frac{\partial}{\partial t}\psi(t) = H\psi(t), \tag{3}$$

where it is assumed here, and onwards, that units have been chosen where $\hbar = 1$. Since the Hamiltonian is presumed to be time-

independent, the solution, in the Schrödinger picture, is

$$\psi(t) = e^{-iHt}\psi(0), \tag{4}$$

where e^{-iHt} is the time evolution operator. Again, the importance of the Hermiticity of the Hamiltonian is evident: it ensures that the time evolution operator is unitary.

The unitarity of the time evolution operator means that its influence drops out of the norms of states that are evolved in time, which therefore remain identical to norms of initial states. Since the norm of a state corresponds to a probability of measurement, the Hermiticity of the Hamiltonian ensures that probabilities are conserved. Although such a violation of the conservation of probability may be desirable in phenomenological models for nuclear decay, where the probability of measuring an isotope decreases with time as it decays, it is clearly *not* desirable in a fundamental description of a system.

3. The Hamiltonian incorporates the symmetries of the theory. A Hamiltonian that commutes with a linear operator A,

$$[A, H] = 0, \tag{5}$$

is said to be invariant under the transformation represented by A. Since A is a linear operator, any eigenstate of H is therefore also an eigenstate of A.

Symmetries play a fundamental role in physics and will help in the

task of constructing of a new framework that discards the axiom of the Hermiticity of the Hamiltonian.

Thus, it is evident that although the axiom of the Hermiticity of the Hamiltonian seems difficult to understand physically by itself, it plays a fundamental part in ensuring that the quantum theory as a whole satisfies the other physical requirements of an acceptable (quantum) mechanical theory: any attempts to abandon it and otherwise keep the rest of the existing framework will encounter intractable problems. However, in recent years, a quantum framework has been suggested in which the requirement for the Hamiltonian to be Hermitian has been dropped, which, importantly, otherwise leaves the remaining axioms of the quantum theory satisfied.

In 1993 D. Bessis and J. Zinn-Justin, inspired by the earlier work on the Lee-Yang edge singularity [4], began to examine the Hamiltonian,

$$H = \hat{p}^2 + i\hat{x}^3, \tag{6}$$

and noticed that some of its eigenvalues appeared to be real. Wondering whether the whole energy spectrum was in fact real they suggested their conjecture to C. M. Bender [6]. Bender noted that the Hamiltonian was not Hermitian and therefore surmised that such a hypothesis was absurd, and left it at that [6]. This was not the first time that it had been noted that such Hamiltonians had *real* energy eigenvalues: apart from the work on Reggeon field theory mentioned previously [3], Caliceti *et al.* had, based on Borel summability arguments, observed that the spectrum of a Hamiltonian similar to (6) was indeed real [5]; Andrianov had, in 1982, found evidence

that theories involving $-x^4$ potentials could have real eigenvalues [7]; and in 1992 Hollowood [8] and Scholtz *et al.* [9] had, in their own areas of research, found examples of non-Hermitian Hamiltonians with real energy spectra. However, despite the mysterious reality of the energy spectrum of these non-Hermitian Hamiltonians, it was not until 1997 having not forgotten about the Hamiltonian (6) that Bender began to seriously investigate it. Bender surmised that if the spectrum of (6) was real it was most likely due to the presence of a symmetry, and it indeed does possess $\mathcal{PT}$ symmetry — the symmetry of the combined operations of spacial reflection (also called *parity*), $\mathcal{P}$, and time reversal, $\mathcal{T}$.

The parity operator $\mathcal{P}$ is linear and, by definition, reverses the sign of the quantum position operator $\hat{x}$

$$\mathcal{P}\hat{x}\mathcal{P} = -\hat{x}, \tag{7}$$

and also the sign of the quantum momentum operator

$$\mathcal{P}\hat{p}\mathcal{P} = -\hat{p}. \tag{8}$$

The time reversal operator $\mathcal{T}$ similarly reverses the sign of the quantum momentum operator, but leaves the quantum position operator unchanged:

$$\mathcal{T}\hat{x}\mathcal{T} = \hat{x}, \tag{9}$$

$$\mathcal{T}\hat{p}\mathcal{T} = -\hat{p}. \tag{10}$$

For $\mathcal{P}$ and $\mathcal{T}$ symmetries to be consistent in the quantum theory, they must also leave the fundamental commutation relation,

$$[\hat{x}, \hat{p}] = i, \tag{11}$$

invariant, which requires the $\mathcal{T}$ operator to reverse the sign of the complex number i:

$$\mathcal{T} i \mathcal{T} = -i. \tag{12}$$

Note that equation (12) means that $\mathcal{T}$ is not a linear operator, but rather an *antilinear* operator. Furthermore, since $\mathcal{P}$ and $\mathcal{T}$ are reflection operators, their squares are equivalent to the identity operator:

$$\mathcal{P}^2 = \mathcal{T}^2 = \mathbf{1}, \tag{13}$$

and, finally, the $\mathcal{P}$ and $\mathcal{T}$ operators commute:

$$[\mathcal{P}, \mathcal{T}] = 0. \tag{14}$$

A Hamiltonian, therefore, that is $\mathcal{PT}$-symmetric will satisfy the condition

$$(\mathcal{PT}) H (\mathcal{PT}) = H, \tag{15}$$

which, using equations (13) and (14) can be readily seen to be equivalent to the condition that the Hamiltonian must commute with the $\mathcal{PT}$ operator:

$$[H, \mathcal{PT}] = 0. \tag{16}$$

Having conjectured that the reality of the energy spectrum was due to this $\mathcal{PT}$ symmetry, Bender and his former graduate student S. Boettcher decided to analyze the more general Hamiltonian

$$H = \hat{p}^2 + \hat{x}^2(i\hat{x})^\epsilon, \tag{17}$$

which is $\mathcal{PT}$-symmetric for all real values of ϵ, but only Hermitian when $\epsilon = 0$ [1]. Their work crucially relies, firstly, on the analytic continuation of eigenvalue problems [1]; and, secondly, on a powerful perturbative analysis called delta-expansion developed by Bender *et al.* [11] in order to avoid divergent perturbation series [1]. The delta-expansion analysis involves introducing a parameter that quantifies the non-linearity of a problem [6], as the parameter ϵ does in (17). Remarkably, detailed perturbative analysis and numerical studies of (17) yielded the result that for $\epsilon \geq 0$ the energy spectrum was entirely real and positive, but for $\epsilon < 0$ there existed complex eigenvalues [12]. (See *figure 1.*) The result that a $\mathcal{PT}$-symmetric, but non-Hermitian, Hamiltonian did indeed posses a real energy spectrum was enough to conjecture that it was perhaps possible to replace the axiom that the Hamiltonian be Hermitian with the more physical one that the Hamiltonian merely be $\mathcal{PT}$-symmetric.

Symmetries involving $\mathcal{P}$ and $\mathcal{T}$ are already known to exist in the homogeneous Lorentz group of spatial rotations and Lorentz boosts, and have been analyzed and suggested to exist physically before; which is why it appears to be a more reasonable constraint to place on a quantum framework than the mathematical and physically-obscure constraint of Hermiticity. The real

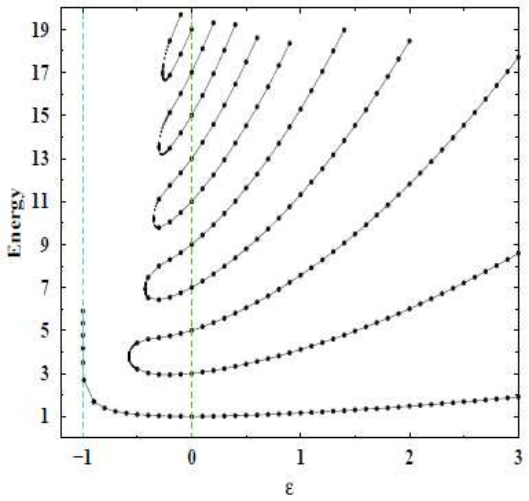

Figure 1: Energy levels of the Hamiltonian $H = \hat{p}^2 + \hat{x}^2(i\hat{x})^\epsilon$ plotted as a function of the real parameter ϵ. Note that at $\epsilon = 0$ the Hamiltonian is that of the harmonic oscillator and the energy spectrum displayed corresponds to the familiar energy levels $E_n = 2n + 1$. For the region $\epsilon \geq 0$ the spectrum is entirely real, but for $\epsilon < 0$ only a finite number of energy eigenvalues are real and an infinite number are complex (not displayed).

Lorentz group consists of four disconnected parts: firstly, those elements that are continuously connected to the identity element, and which is called the *proper orthochronous Lorentz group*; secondly, those elements in the proper orthochronous Lorentz group combined with the $\mathcal{P}$ operation; then those elements of the proper orthochronous Lorentz group combined with the $\mathcal{T}$ operator; and lastly those elements of the proper orthochronous Lorentz group combined with the $\mathcal{PT}$ operation. The latter three sets of elements are distinct and are not subgroups of the full Lorentz group since they do not contain the identity element.

However, physical theories said to be Lorentz-invariant are required to be invariant *only* under the transformations of the proper orthochronous Lorentz group, since experiments have shown that the weak interaction vi-

olates both $\mathcal{P}$ and $\mathcal{T}$ symmetry. If, however, the Lorentz group is extended into the complex domain [10] (which requires the assumption that the eigenvalues of the Hamiltonian are real and bounded from below — an assumption that we already demanded on physical grounds), the *complex* Lorentz group consists of only *two* disconnected parts: the proper orthochronous Lorentz group becomes continuously connected in group space to the elements of the proper orthochronous Lorentz group combined with the $\mathcal{PT}$ operator, and those elements that were combined with either the $\mathcal{P}$ or $\mathcal{T}$ operator now also become linked by a continuous path in group space.

What is therefore suggested is that the analysis of *complex* group theory be followed in order to justify the suggestion that it is $\mathcal{PT}$ symmetry that is fundamental to nature; and that it be conjectured that this $\mathcal{PT}$ symmetry is a more natural axiom onto which a quantum framework be constructed rather than on the axiom of the Hermiticity of the Hamiltonian.

One of the important consequences of the suggestion that the Hamiltonian need only be $\mathcal{PT}$-symmetric is that this is a weaker condition than Hermiticity [6]: many new kinds of Hamiltonians can now be studied and suggested that do not violate any of the other axioms of the quantum theory, but would otherwise have been rejected before. As of yet, no experiment has conclusively determined whether non-Hermitian Hamiltonians exist in nature, but it has been suggested that experiments in condensed matter physics may reveal evidence of non-Hermitian Hamiltonians [1]. For example, a complex crystal lattice with potential $V(x) = i \sin x$ will have a Hamiltonian

$$H = \hat{p}^2 + i \sin \hat{x}, \tag{18}$$

which has real energies despite the fact that it is non-Hermitian (precisely because it is, instead, $\mathcal{PT}$-symmetric) [1]. The wavefunction of a particle in such a lattice at the edges of the energy bands for that lattice are, however, bosonic and never fermionic, in contrast to those of ordinary crystal lattices. Thus, measurements of the energy band structure of this crystal could give clear evidence of the existence of non-Hermitian Hamiltonians [1].

Another interesting development from the suggestion of $\mathcal{PT}$-symmetric Hamiltonians is the idea of extending classical physics into the complex domain. Indeed, the Hamiltonian (17) can be though of as a complex extension of the Hamiltonian of the harmonic oscillator

$$H = \hat{p}^2 + \hat{x}^2. \tag{19}$$

It is interesting to speculate that if $\mathcal{PT}$-symmetric Hamiltonians such as (17) are indeed allowed by nature, they would appear to describe classical systems in which the force acting on the system is complex in nature. Some work has already been done on examining purely classical systems in which the motion is allowed to take place in the complex domain. Some of this work has yielded surprising results. For example, systems with a $\cos(x)$ potential with motion allowed to take place in the complex domain appear to recreate the purely quantum phenomena of tunnelling and conduction band behaviour. As such, some work has now been done and is here presented in extending this analysis to potentials with the elliptic function, $-cn(x)$, which is a doubly-periodic function (one that has two distinct periods in the complex plane).

The following sections will explain in more detail the process of extending classical mechanics into the complex domain, the framework developed to make $\mathcal{PT}$-symmetric Hamiltonians consistent with the remaining axioms of the quantum theory, and finally the work done on examples of classical systems of complex variables.

2 $\mathcal{PT}$-Symmetry and Energy Eigenvalues

In this section we shall describe how a $\mathcal{PT}$-symmetric Hamiltonian can have real energy eigenvalues, even for systems that would appear to preclude such a result such as with systems with a $-x^4$ potential term; and how they may be calculated.

2.1 Nonlinearity of the $\mathcal{PT}$ Operator, and Broken and Unbroken $\mathcal{PT}$ Symmetry

Recall the Hamiltonian (17), which was found to indeed have real energy eigenvalues, but only in the parametric region $\epsilon \geq 0$. Does this pose a problem with the assertion that $\mathcal{PT}$-symmetric Hamiltonians do have real energy spectra? The subtlety is the $\mathcal{PT}$ operator is *not* linear. Thus, although the $\mathcal{PT}$ operator commutes with the Hamiltonian, eigenstates of H are not necessarily also eigenstates of $\mathcal{PT}$ [1].

An example of the difficulties that can occur if care is not taken can be illustrated with the following argument: suppose ψ is an eigenstate of the

$\mathcal{PT}$ operator with eigenvalue λ

$$\mathcal{PT}\psi = \lambda\psi. \tag{20}$$

Since it is trivial to show that $(\mathcal{PT})^2 = \mathbf{1}$ from (13) and (14), multiplying (20) on the left by $\mathcal{PT}$, and also inserting the identity opertor to the left of ψ on the right-hand side of the equation, yields:

$$\psi = (\mathcal{PT})\lambda(\mathcal{PT})^2\psi. \tag{21}$$

Using (20) and the fact that $\mathcal{T}$ is antilinear on λ (12), we get

$$\psi = \lambda^*\lambda\psi = |\lambda|^2\psi, \tag{22}$$

which implies that $|\lambda|^2 = 1$ and that λ is a pure phase:

$$\lambda = e^{i\alpha}, \tag{23}$$

for some real α.

Now, let us *assume* that ψ is also an eigenstate of H with eigenvalue E:

$$H\psi = E\psi, \tag{24}$$

and, again, multiplying on the left by $\mathcal{PT}$ and inserting the identity operator $(\mathcal{PT})^2$ to the left of ψ on the right-hand side of the equation yields:

$$(\mathcal{PT})H\psi = (\mathcal{PT})E(\mathcal{PT})^2\psi. \tag{25}$$

Finally, using (24) and (20), along with the antilinearity of $\mathcal{T}$ on E, we find that:

$$E\lambda\psi = E^*\lambda\psi. \tag{26}$$

Since λ is nonzero from (23), it must be concluded that E is real: $E = E^*$.

However, the analysis of the energy spectrum of the Hamiltonian (17) showed that this conclusion is not correct: for any value of the parameter ϵ, where it must be remembered that the Hamiltonian is $\mathcal{PT}$-symmetric over all ϵ, the spectrum is *not* guaranteed to be entirely real (see *figure 1*). The energy eigenvalues are only real when the eigenstates of the Hamiltonian are *also* eigenstates of the $\mathcal{PT}$ operator; and the fact that the Hamiltonian and the $\mathcal{PT}$ operator commute is not sufficient to conclude this, as is normally the case for linear operators. In situations where eigenstates are common to the Hamiltonian and *also* to the $\mathcal{PT}$ operator, we say that the $\mathcal{PT}$ symmetry of the Hamiltonian is *unbroken*; and, conversely, where eigenstates of the Hamiltonian are not also eigenstates of the $\mathcal{PT}$ operator, we say that the $\mathcal{PT}$ symmetry of the Hamiltonian is *broken*. Thus, before it can be concluded that the energy spectrum of a $\mathcal{PT}$-symmetric Hamiltonian is entirely real, it must first be shown that the $\mathcal{PT}$ symmetry remains unbroken. This is not easy to show, but in 2001 Dorey *et al.* finally constructed a rigorous proof [13, 14].

Since the role that $\mathcal{PT}$-symmetric Hamiltonians could play in quantum theory was suggested in 1998, much work has been conducted on the mathematical analysis of $\mathcal{PT}$ symmetry. Such work remains of interest to the physical community, but outside the scope of this brief review. Some of the

work presented since 1998 includes that of Shin [15], Pham [16], Delabaere [17], Trinh [18], Weigert [19, 20], Mostafazadeh [22, 23, 24, 25], and Scholtz and Geyer [21].

2.2 The Complex Domain

Given the conclusions of the *section 2.1*, let us examine how we can calculate the energy eigenvalues, with a particular emphasis on understanding how to extend real quantum mechanics into the complex domain.

Starting from the Schrödinger eigenvalue problem (24), we convert the problem into an ordinary differential equation in coordinate space with the familiar substitutions:

$$\hat{x} \to x \quad \text{and} \quad \hat{p} \to -i\frac{d}{dx}. \tag{27}$$

For the Hamiltonian (17), we obtain the eigenvalue problem

$$-\psi''(x) + x^2(ix)^\epsilon\psi(x) = E\psi(x), \tag{28}$$

where we must also identify the correct boundary conditions on $\psi(x)$. This equation cannot be solved for arbitrary ϵ, but we can examine the asymptotic behaviour of $\psi(x)$ using the WKB approximation [1]: for differential equations of the form $-y''(x)+V(x)y(x) = 0$, where $V(x)$ grows as $|x| \to \infty$, y has the form

$$y(x) \sim \exp\left[\pm\int^x ds\sqrt{V(s)}\right], \tag{29}$$

for $|x| \to \infty$. Let us first examine the familiar case of $\epsilon = 0$, which corre-

sponds to the harmonic oscillator. It is evident from (29) that the asymptotic behaviour is then $\psi(x) \sim \exp(\pm\frac{1}{2}x^2)$. With the usual condition of square integrability, we are compelled to choose the solution with the negative sign in the exponent and we recover Gaussian-like solutions for large $|x|$. This result, however, also *extends into the complex plane*: if the eigenfunctions vanish exponentially on the real axis for large $|x|$, then they must also vanish in regions called *Stokes wedges*, which are wedges of opening angle $\frac{1}{2}\pi$ in the complex plane centred on the positive-real and negative-real axes [26].

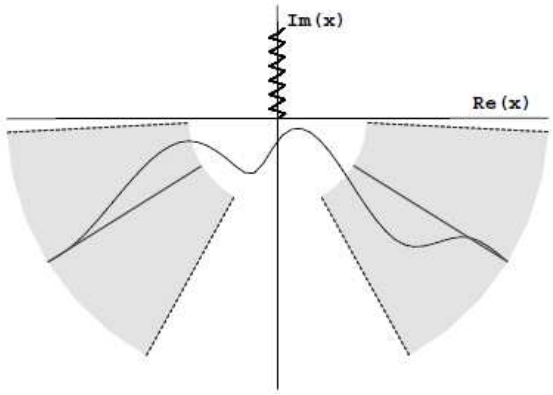

Figure 2: Stokes wedges in the complex-x plane and a suitable contour. The wedges rotate towards the negative-imaginary axis and become narrower as ϵ in (28) increases.

There are many wedges in the complex plane in which we can create a contour on which the eigenvalue problem can be posed that has $\psi(x) \to 0$ as $|x| \to \infty$; so there are many eigenvalue problems associated with (28). Thus, in order to examine the problem for arbitrary $\epsilon > 0$, we start from the harmonic oscillator case at $\epsilon = 0$ and smoothly continue ϵ to the desired value [6] (a detailed description on how to extend eigenvalue problems into the complex plane is provided in reference [27]). As the value of ϵ is increased, the

Stokes wedges become narrower and rotate downwards towards the negative-imaginary axis, and we simply choose a contour that asymptotically remains within the wedges (see *figure 2*).

It should be noted that the wedges in *figure 2* are reflections of one another in the imaginary axis. This symmetry is a manifestation of the $\mathcal{PT}$ symmetry of the Hamiltonian (17) since, for any complex x, the parity reflections maps $x \to -x$ and the time reversal maps $x \to x^*$ (12). Thus the $\mathcal{PT}$ symmetry will map $x \to -x^*$, which indeed corresponds to a reflection symmetry along the imaginary axis.

2.3 Dyson's Argument

In 1952 Freeman Dyson argued, for the first time, about analytically continuing a Hamiltonian into the complex plane in a heuristic argument for the divergence of perturbation theory in quantum electrodynamics [28]. Dyson's argument concerned rotating the electric charge e into the complex plane $e \to ie$; applied to the anharmonic oscillator Hamiltonian $H = \hat{p}^2 + g\hat{x}^4$, Dyson's argument would proceed analogously in the following manner [1]: if the parameter g were to be rotated anticlockwise in the complex-g plane from g to $-g$, the resulting potential term in the Hamiltonian would slope downwards to negative infinity. Such a potential term would have no lowest energy state. Thus, the ground state energy must have an abrupt transition from the region $g > 0$, where there exists a ground state, to the region $g < 0$, where there exists no lowest energy state; and so there must be a singularity at $g = 0$.

Dyson assumed that a potential term like $-x^4$ could not have a lowest energy state, but the Hamiltonian (17) with $\epsilon = 2$ contains precisely such a potential term, and *figure 1* shows the energy spectrum to be entirely real. The flaw in naïvely following Dyson's argument is that, although the anharmonic oscillator does indeed have a singularity at $g = 0$, the energy spectrum that an analytic continuation of the parameter g produces remains ambiguous whilst the boundary conditions remain unspecified.

The eigenvalues of the Hamiltonian $H = \hat{p}^2 - g\hat{x}^4$ depend crucially on how the parameter g is allowed to become negative, since that determines what the boundary conditions of the problem are. If one begins with the Hamiltonian $H = \hat{p}^2 + g\hat{x}^4$ and substitutes $g = |g|e^{i\theta}$, then the rotation from $\theta = 0$ to $\theta = \pi$ produces a complex ground state energy when g does become negative, as Dyson presumed. If however one begins with the Hamiltonian $H = \hat{p}^2 + gx^2(ix)^\epsilon$, then the variation of ϵ from $\epsilon : 0 \to 2$ produces the exact same resulting Hamiltonian with a negative g parameter, but the energy spectrum remains always *real*, as seen in *figure 1*. The reason why the same Hamiltonian can produce two different spectra is because the boundary conditions satisfied by the eigenfunctions of the Hamiltonian are different in either case. In the rotation of g used by Dyson both the Stokes wedges rotate together by the same amount and in the same direction: $\psi(x)$ vanishes in the complex-x plane as $|x| \to \infty$ in wedges at $-\pi/3 < \arg\, x < 0$ and $-4\pi/3 < \arg\, x < -\pi$. In the ϵ parameterization case, the wedges rotate by the same amount but *towards* one another: $\psi(x)$ now vanishes as $|x| \to \infty$ in wedges at $-\pi/3 < \arg\, x < 0$ and $-\pi < \arg\, x < -2\pi/3$. In this latter case, the *wedges are $\mathcal{PT}$ symmetries of one another*, and therefore onto the solu-

tion of ψ is forced the reality of the energy spectrum that the $\mathcal{PT}$ symmetry induces.

3 The Quantum Framework

The fact that classes of $\mathcal{PT}$-symmetric Hamiltonians have real energy spectra is not enough to justify their use to describe physical phenomena. Within the quantum theory, as was mentioned in *section 1*, the Hermiticity condition plays a greater role than simply ensuring that the Hamiltonian eigenvalues are real. To be able to construct an acceptable quantum framework from $\mathcal{PT}$ symmetry, that framework must also be able to construct a Hilbert space of state vectors along with an inner product whereby norms are positive; and also to construct a unitary time evolution operator, so that norms are preserved in time. Such a framework has been constructed [1], and it is presented here in comparison the that of the quantum theory. The novelty that will be found is that the $\mathcal{PT}$-symmetric framework will utilize an inner product that cannot be known *a priori* and that the Hamiltonian itself constructs!

3.1 The Inner Product

In the quantum theory, the inner product of two eigenfunctions is:

$$(\psi, \phi) \equiv \int dx\ \psi^*(x)\phi(x). \tag{30}$$

With this inner product, any two eigenfunctions of the Hamiltonian operator having different energy eigenvalues (we shall ignore the complication

of degeneracy), $\psi(x)$ and $\phi(x)$, are said to be orthonormal if:

$$(\psi, \phi) = 0, \tag{31}$$

and

$$(\psi, \psi) = (\phi, \phi) = 1. \tag{32}$$

In the $\mathcal{PT}$ framework, we can at first try to construct an inner product analogously:

$$(\psi, \phi) \equiv \int_C dx \psi^*(-x)\phi(x), \tag{33}$$

where C is a contour in the Stokes wedges shown in *figure 2*. We have chosen the factor $\psi^*(-x)$ since it corresponds to the $\mathcal{PT}$ symmetry just as the complex conjugation in (30) corresponds to the Hermiticity condition.

However, although distinct eigenfunctions are orthogonal, norms constructed with such an inner product are not guaranteed to be positive. In fact, working with the eigenfunctions of the Hamiltonian (17), we find that these $\mathcal{PT}$ norms have the result:

$$(\phi_n, \phi_m) = (-1)^n \delta_{nm}, \tag{34}$$

for all n and for all values of $\epsilon > 0$ [29]. Note that the eigenfunctions used here have been scaled $\phi_n(x) \to e^{-i\alpha/2}\phi_n(x)$, recalling (23), so that ϕ now has an eigenvalue of 1 with respect to the $\mathcal{PT}$ operator. Using these $\mathcal{PT}$-normalized

eigenfunctions, a strange completeness relation can be found:

$$\sum_{n=0}^{\infty}(-1)^n\phi_n(x)\phi_n(y) = \delta(x-y), \tag{35}$$

which has been verified numerically and analytically for all $\epsilon > 0$ [30, 31], and for which a mathematical proof has also been given [20]. It is clear that the result (35), with the aid of (34), is an acceptable representation for the identity operator since it verifies the integration rule for delta-functions: $\int dy\ \delta(x-y)\delta(y-z) = \delta(x-z)$.

Although these results themselves are not acceptable to us in forming a quantum framework, they can nonetheless still be used to create some of the usual operators and operator reconstructions in the quantum theory [1]. Using (35) we can define the parity operator in terms of the eigenstates:

$$\mathcal{P}(x,y) = \delta(x+y) = \sum_{n=0}^{\infty}(-1)^n\phi_n(x)\phi_n(-y). \tag{36}$$

And we can also reconstruct the Hamiltonian and Green's function, just as is possible in the quantum theory,

$$H(x,y) = \sum_{n=0}^{\infty}(-1)^n E_n\phi_n(x)\phi_n(y), \tag{37}$$

$$G(x,y) = \sum_{n=0}^{\infty}(-1)^n \frac{1}{E_n}\phi_n(x)\phi_n(y). \tag{38}$$

With (34), it is trivial to show that (37) satisfies the time-independent Schrödinger equation, $H\phi_n = E_n\phi_n$, and also to reproduce the statement that the Green's function is the inverse of the Hamiltonian: $\int dy\ H(x,y)G(y,z) =$

$\delta(x-z)$.

However, an inner product with positive norm is still required. The problem is that the result (34) implies that the Hilbert space of states is spanned by equal numbers of states that have a positive norm and ones that have a negative norm. This situation is analogous to the problem that Dirac faced when trying to incorporate the relativistic dispersion relation into the theory of quantum mechanics [32]; and the solution is to mirror Dirac's method of finding an interpretation for the negative norm states [1]. Since a Hamiltonian with unbroken $\mathcal{PT}$ symmetry has equal numbers of positive- and negative-norm states, there therefore exists an additional symmetry of the Hamiltonian, which may be represented by an operator that shall be called $\mathcal{C}$. The linear operator $\mathcal{C}$ can be represented in position space as a sum over the eigenfunctions as:

$$\mathcal{C}(x,y) = \sum_{n=0}^{\infty} \phi_n(x)\phi_n(y). \tag{39}$$

This $\mathcal{C}$ operator is similar to the charge conjugation operator since, with the aid of equations (34) and (35), its square can be shown to be equal to unity:

$$\int dy\ \mathcal{C}(x,y)\ \mathcal{C}(y,z) = \delta(x-z), \tag{40}$$

which implies that eigenstates ϕ of $\mathcal{C}$ have eigenvalues ± 1. It should be noted that although both the $\mathcal{C}$ operator and the parity operator $\mathcal{P}$ have squares equal to unity, they are not equivalent since the parity operator is real (as is clear from its position space representation as the delta function) whilst the $\mathcal{C}$ operator is complex (as it is constructed from complex eigenfunctions, in

position space).

Since $\mathcal{C}$ is a linear operator, and is a symmetry of H — which implies that it commutes with H — all eigenstates of H are also eigenstates of $\mathcal{C}$ with eigenvalue ± 1:

$$\mathcal{C}\phi_n(x) = \int dy\ \mathcal{C}(x,y)\phi_n(y) = \sum_{m=0}^{\infty} \phi_m(x) \int dy\ \phi_m(y)\phi_n(y) = (-1)^n \phi_n(x). \tag{41}$$

Thus, the proper interpretation of the $\mathcal{C}$ operator is that it simply represents the measurement of the sign of the $\mathcal{PT}$ norm in (34).

Having identified this $\mathcal{C}$ operator, a modified $\mathcal{CPT}$ inner product can be defined as:

$$\langle \psi | \chi \rangle^{\mathcal{CPT}} \equiv \int dx \psi^{\mathcal{CPT}}(x)\chi(x), \tag{42}$$

where $\psi^{\mathcal{CPT}}(x) \equiv \int dy\ \mathcal{C}(x,y)\psi^*(-y)$. This inner product is sufficient for our requirements [1]. Because of the presence of the complex conjugation operation, the norms are independent of the phase of the eigenstates. It is also now positive definite since the $\mathcal{C}$ operator produces an extra factor of $(-1)^n$. Norms are also preserved in time since the time evolution operator, unchanged from that of the quantum theory, e^{-iHt}, commutes with the $\mathcal{CPT}$ operator (as a result of the fact that H commutes with the $\mathcal{CPT}$ operator), and so cancels with its complex conjugate within the $\mathcal{CPT}$ inner product.

With the $\mathcal{CPT}$ operation, the completeness condition is

$$\sum_{n=0}^{\infty} \phi_n(x)[\mathcal{CPT}\phi_n(y)] = \delta(x-y), \tag{43}$$

which is perfectly analogous to the completeness relation in the quantum

theory.

In general, the $\mathcal{C}$ operator is not easy to construct via the definition (39) since it requires an evaluation of all the eigenfunctions of H. However, another procedure exists which can be readily generalizes to quantum field theory, where no simple analogue exists for the Schrödinger eigenvalue equation and its associated coordinate space eigenfunctions [1]. That procedure is detailed in the references [36], [37], [38].

Finally, it is to be noted that the $\mathcal{CPT}$ inner product (42) is independent of the choice of the integration contour as long as the contour asymptotically lies within the wedges associated with the eigenvalue problem (see *section 2.2*). In the standard quantum theory, the inner product $\int dx\ f^*(x)g(x)$ must be done over the real axis since the integration path cannot be deformed into the complex plane as the integrand is not analytic. The $\mathcal{PT}$ inner product *is* analytic in the complex plane [1], but at the cost of the loss of positive definiteness. It is therefore remarkable that the $\mathcal{CPT}$ inner product retains the path-independence of the $\mathcal{PT}$ inner product along with desirable trait of positive definiteness.

3.2 Observables

In the quantum theory, a linear operator A is an observable if A is Hermitian: $A = A^\dagger$. In the Heisenberg picture, operators evolve as $A(t) = e^{iHt}A(0)e^{-iHt}$; so, this Hermiticity condition is retained by $A(t)$ and A represents a measurement for all times. In the $\mathcal{PT}$ framework, an operator must satisfy the condition $A^T = \mathcal{CPT}\ A\ \mathcal{CPT}$, where A^T is the transpose of A [29]. This con-

dition will hold for all times if the Hamiltonian is assumed to be symmetric: $H = H^T$. The condition on A involving matrix transposition is more restrictive than is necessary [33, 22, 34], but then requires the use of biorthogonal bases: see [20] and [35].

Note that, although $\mathcal{C}$ and the Hamiltonian are observables, $\hat{x}$ and $\hat{p}$ are not [1]; and that this situation, where it makes no sense to talk of the position of a particle, mirrors that of fermionic quantum field theories, where the field is complex and has no classical limit. This analogy between $\mathcal{PT}$-symmetric quantum mechanics and quantum field theory is interesting, and it may be that $\mathcal{PT}$-symmetric quantum mechanics naturally describes extended, rather than point-like, objects [1].

3.3 Comparison with the Quantum Theory

The $\mathcal{PT}$ framework differs, interestingly, from the quantum theory in that the $\mathcal{PT}$-symmetric Hamiltonian itself chooses the Hilbert space in which it desires to live! This is in stark contrast to the standard quantum theory, where the Hilbert space and inner product are clearly defined before the Hamiltonian is even decided upon. In the $\mathcal{PT}$ framework, the inner product depends on the $\mathcal{C}$ operator, which is constructed only once the eigenfunctions of the Hamiltonian have been calculated.

Given the importance played by the $\mathcal{C}$ operator in the $\mathcal{PT}$ framework, it is interesting to note that, in some sense, it can be said to play an identical role in the standard quantum theory. In the quantum theory of Hermitian Hamiltonians, the $\mathcal{C}$ operator is, however, no longer a distinct operation, and be-

comes equivalent to the parity operator $\mathcal{P}$. The $\mathcal{CPT}$ operation then becomes equivalent to $\mathcal{T}$, which is simply the operation of complex conjugation. The $\mathcal{CPT}$ inner product thus becomes equivalent to the standard quantum theory inner product, along with reduction of the completeness relation (43) to the standard quantum theory completeness relation, $\sum_n \phi_n(x)\phi_n^*(y) = \delta(x-y)$.

4 Classical Mechanics

Having analyzed the role that $\mathcal{PT}$-symmetric Hamiltonians could play within a quantum framework, it is interesting to examine those Hamiltonians in the context of classical mechanics. Although classical mechanics is not fundamental, and so it is not necessarily correct to imbue quantum hypotheses to the classical domain, interesting results have nonetheless been discovered that warrant further investigation. A summary is presented here of several papers published in this area [39, 40, 41, 42, 43, 44, 45, 46, 47, 48].

The objective of classical mechanics is to determine trajectories of particles subject to Newton's dynamical equation, $F = ma$. These trajectories, $x(t)$, are *real* functions of a real variable, t, since their values correspond to an observable measurement for all times, t. However, $\mathcal{PT}$-symmetric Hamiltonians are in general *complex*, and describe scenarios where a particle is subject to *complex* forces. As such, the particle trajectories are not confined to the real axis, but to the complex plane. Complex analysis has been useful in providing an understanding of many problems posed in the real domain, and it is interesting to ask whether the same could be true of quantum phenomena: is it possible for hitherto purely quantum results to be understood

in terms of classical dynamics extended into the complex plane?

4.1 Energy Quantization

An illustration of the power of complex analysis can be demonstrated with the understanding that it provides for the quantization of energy [50]. Suppose we have a simple quantum system perturbed by some interaction quantified by a real parameter ϵ. Let the Hamiltonian be

$$H = \begin{pmatrix} a & 0 \\ 0 & b \end{pmatrix} + \epsilon \begin{pmatrix} 0 & c \\ c & 0 \end{pmatrix}, \tag{44}$$

where ϵ is a real parameter. This is a straightforward problem to solve, and yields two eigenvectors with eigenvalues

$$E_{\pm} = \frac{1}{2}\left[a + b \pm \sqrt{(a-b)^2 + 4\epsilon^2 c^2}\right]. \tag{45}$$

Let us now define the energy function to be

$$E(\epsilon) \equiv \frac{1}{2}\left[a + b + \sqrt{(a-b)^2 + 4\epsilon^2 c^2}\right], \tag{46}$$

and analytically continue the parameter ϵ into the complex domain. Now, E as function of complex ϵ is evidently double-valued, and so must be defined on a two-sheeted Riemann surface: the branch cut lies between the branch points of the square-root operation at values $\epsilon = \pm i(a-b)/(2c)$ in the complex-ϵ plane, as shown in *figure 3* [50]. The values of $E(\epsilon)$ on the first sheet correspond to those of the positive root, E_+, and those on the second sheet to

those of the negative root, E_-. Since the two sheets are connected smoothly

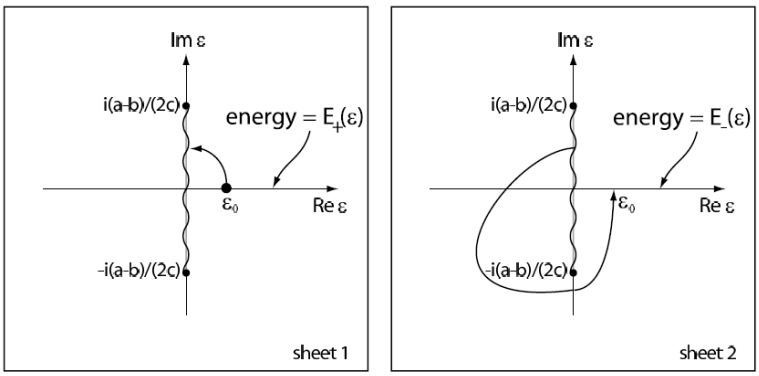

Figure 3: The two-sheeted Riemann surface for (46). The sheets are connected to one another via a branch cut (wavy line), which allows a smooth and continuous path to connect energies that would appear to be discrete if ϵ were confined to the real-ϵ axis. In this way, the observed energies of a quantum system would appear to be quantized, but are nothing more than specific energies on a path in the complex domain.

and paths across the branch cut are continuous, a path may be constructed that begins at ϵ_0 on the real-ϵ axis on the first sheet, crosses the branch cut, and ends on the corresponding point ϵ_0 on the real-ϵ axis of the second sheet. The system described by such an energy curve would appear to an observer to represent a *quantized* energy system, since only those points on the curve that cross the real-ϵ axis may be measured. Thus, the quantization of energies, which is such an abrupt departure from classical mechanics, could be explained as nothing more than the extension of an energy function into the complex domain!

Taking a cue from such a conjecture, we will analyze both conventional and strange-looking Hamiltonians, but with the dynamics not constrained to the real axis. We will start, however, by returning to the Hamiltonian in (17).

4.2 Complex Forces

In *section 2* we argued why the quantum system with Hamiltonian (17) had a real energy spectrum in terms of complex analysis and the boundary conditions on the associated coordinate-space eigenvalue problem. Let us analyze the problem classically and attempt to find a more intuitive reason why such strange systems with a $-x^4$ potential, for example, can have a positive energy spectrum.

The Hamiltonian (17), viewed classically, can be described by Hamilton's equations

$$\frac{dx}{dt} = \frac{\partial H}{\partial p} = 2p \quad \text{and} \quad \frac{dp}{dt} = -\frac{\partial H}{\partial x} = i(2+\epsilon)(ix)^{1+\epsilon}, \tag{47}$$

which can be combined to give

$$\frac{d^2x}{dt^2} = 2i(2+\epsilon)(ix)^{1+\epsilon}. \tag{48}$$

This is a Newton's second law, but describing an inherently *complex* dynamics: it is the description of a system under the influence of a *complex* force. The complex nature of the force in (48) compels us to take x as being complex, but we extend no such liberties to t, which shall remain a real variable. Integrating (48) yields:

$$\frac{1}{2}\frac{dx}{dt} = \pm\sqrt{E + (ix)^{1+\epsilon}}, \tag{49}$$

where the constant of integration, E, is the energy of the particle. Again,

this is simply a classical equation for the velocity of the particle, of which is now able to move in the complex plane.

Let us examine the system for different values of ϵ in order to see if the results of *figure 1* can be understood.

4.2.1 The Case $\epsilon = 0$

The simplest case is for $\epsilon = 0$, which corresponds to the familiar system of simple harmonic motion. Since, from *figure 1*, we know that the energy spectrum is real, we are free to choose some real energy to define the exact dynamics of the system, and without loss of generality we can take $E = 1$. In this case, the system has turning points at $x = \pm 1$, and the dynamics of a particle initially placed at any point on the real-x axis between these two turning points (except at the trivial point $x = 0$ of course) will undergo simple harmonic motion.

However, since (49) is valid for all complex x, we can take any point in the complex plane as our initial condition on x. For points not on the real-x axis, or for points on the real-x axis outside the usual bounds for the dynamics of the harmonic system, the paths traced by x are ellipses with foci at the turning points, as shown in *figure 4* [1]. The period of these trajectories can be expressed as a integral with a complex contour, which by Cauchy's theorem can be shrunk to a contour kept finite by the branch cut between the two branch points of the square-root function at $x = \pm 1$; thus, all the elliptic trajectories have periods equal to that of the usual harmonic oscillator confined to the real-x axis.

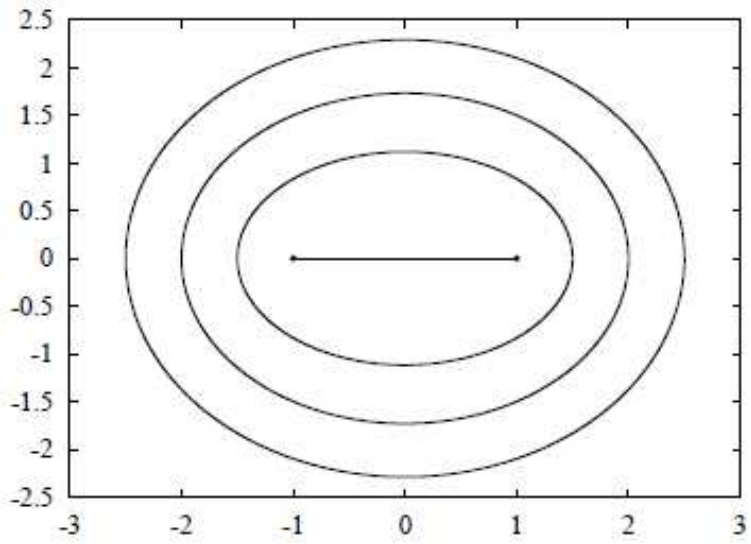

Figure 4: Classical trajectories for the simple harmonic system in the complex-x plane. The turning points at $x = \pm 1$ correspond to the familiar coordinate turning points of the simple harmonic system, and the path shown between these points is that of the familiar harmonic motion in the real-x axis. The elliptical trajectories correspond to an initial displacement off the real-x axis, or of an initial real displacement not confined to the usual region of classical motion. All trajectories have the same period by virtue of Cauchy's theorem.

4.2.2 The Case $\epsilon = 1$

Again, we may take $E = 1$ without loss of generality. With $\epsilon = 1$ in (49),

$$\frac{dx}{dt} = \pm\sqrt{1 + (ix)^3}, \tag{50}$$

(where the sign ambiguity is simply a choice of which direction to move along the trajectories) there are evidently three turning points, which occur at:

$$x_0 = i, \quad x_+ = e^{-i\pi/6}, \quad \text{and} \quad x_- = e^{-5i\pi/6}. \tag{51}$$

Similar to the $\epsilon = 1$ case, a particle placed at either of the turning points x_- or x_+ will undergo an oscillatory motion that will take the particle to the other turning point before returning to its starting displacement (see *figure 5*) [1]. Also, similarly, other initial displacements in the complex plane will follow closed elliptic-like paths around these two turning points. The difference in this case, however, is that the third turning point, x_0 acts as a sort of repelling influence: a particle placed at x_0 will travel along the imaginary-x axis to $+i\infty$ (in a finite amount of time), along an open trajectory; and particles placed on the imaginary-x axis above x_0 will either travel to $+i\infty$ directly or else move to and reach x_0 first and then move off to $+i\infty$. The turning point x_0 and the segment of the imaginary-x axis above it also "repels" the closed trajectory paths into the forms shown in *figure 5* since no trajectories may cross. Again, all closed trajectories have similar periods by virtue of Cauchy's theorem.

4.2.3 The Case $\epsilon = 2$

Again, taking $E = 1$ without loss of generality, the system will now have four turning points located at:

$$\begin{aligned} x_1 = e^{-3i\pi/4} \qquad &\text{and} \qquad x_2 = e^{-i\pi/4}, \\ x_3 = e^{i\pi/4} \qquad &\text{and} \qquad x_4 = e^{3i\pi/4}. \end{aligned} \tag{52}$$

The trajectory between the turning points x_1 and x_2 is oscillatory, as is the one between the turning points x_3 and x_4 (see *figure 6*) [1]. The trajectories with initial displacements in the negative-imaginary half of the complex-x plane are closed orbits around the turning points x_1 and x_2, whilst those

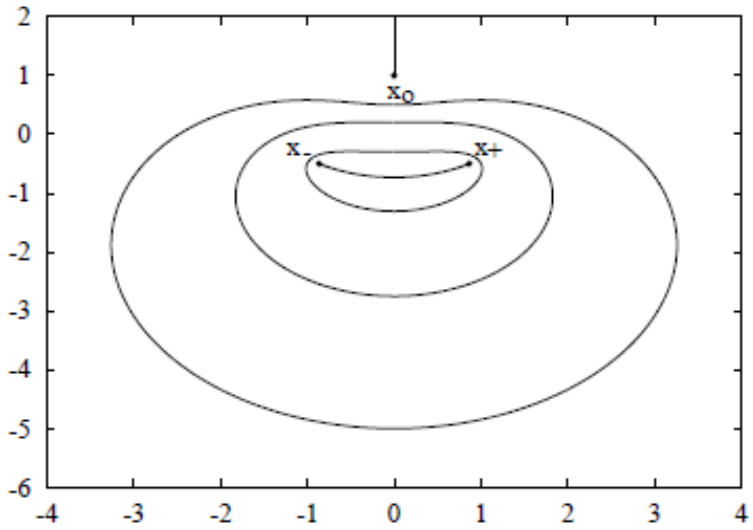

Figure 5: Classical trajectories for the Hamiltonian (17) with $\epsilon = 1$. Initial displacements at the turning points x_- or x_+ follow oscillatory trajectories to the other turning point, and all other trajectories in the plane are closed; except for those at x_0 or on the imaginary-x line above x_0, which are open.

displacements in the positive-imaginary half of the complex-x plane are closed orbits around the turning points x_3 and x_4. All these closed orbits have equal periods. A particle with an initial displacement on the real-x axis, however, will travel along an open trajectory that will end at $\pm\infty$.

4.2.4 The Energy Spectrum

Given the results of *subsections 4.2.1–4.2.3*, we can now heuristically understand the reality of the energy spectrum of *figure 1.* The trajectories of *figures 4, 5, 6* resemble those of orbits, and if it were supposed that the Hamiltonian (17) for the values $\epsilon = 0, 1, 2$ described systems of *complex* atoms, then it would be clear that such systems should have real energies. The quantization procedure one could follow could then use Bohr-Sommerfeld quantization to

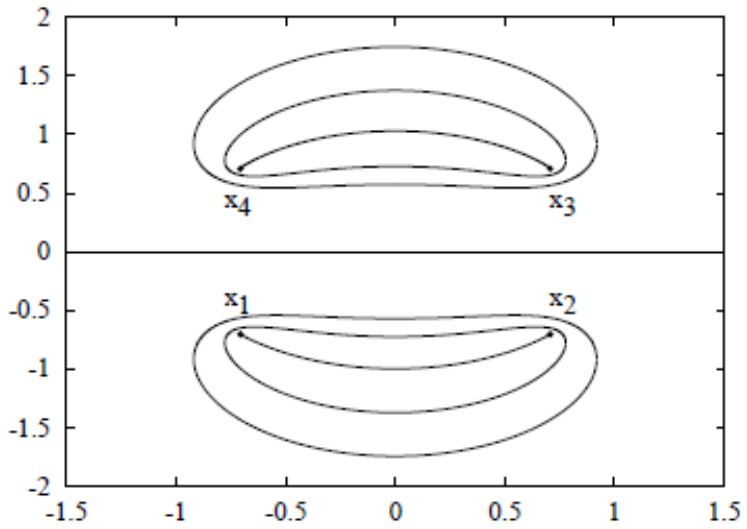

Figure 6: Classical trajectories for the Hamiltonian (17) with $\epsilon = 2$. Oscillatory motion exists for trajectories between the turning points x_1 and x_2, and between the turning points between x_3 and x_4. Trajectories are open for particles with initial displacements along the real-x axis, which end up at $\pm\infty$; and all other initial displacements in the complex plane follow closed paths without crossing the real-x line.

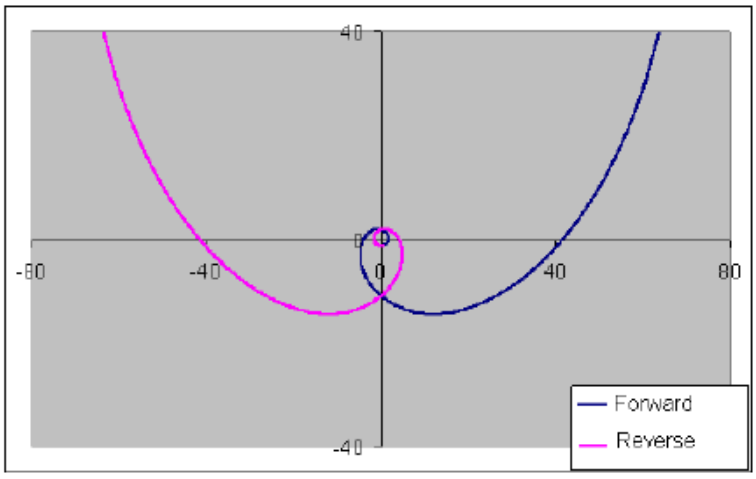

Figure 7: Classical trajectories for the Hamiltonian (17) with $\epsilon = -0.2$. The trajectories are open (and do not cross since they move on different sheets of the Riemann surface) and so no Bohr-Sommerfeld quantization (53) can be performed in order to calculate their energy.

calculate the energies of the system:

$$\oint_C dx\ p = \oint_C dx\ \sqrt{E - x^2(ix)^\epsilon} = \left(n + \frac{1}{2}\right)\pi, \tag{53}$$

where C is the classical orbit of the particle around the complex atoms. Just as with the periods of the orbits, the energies calculated with the integral (53) would be identical due to Cauchy's theorem, and also *real* because of the $\mathcal{PT}$ symmetry of the integrand.

This explanation can also be extended to the region $\epsilon < 0$. An example is given in *figure 7*, which is a plot of two trajectories for $\epsilon = -0.2$ [1]. The two trajectories are from an initial displacement just below the origin on the negative-imaginary axis, and one travels forward in time, and the other backwards in time. The trajectories are *open*, and spiral outwards to infinity. Note that the trajectories do not cross since they move on different sheets of the Riemann surface due to the branch cut of the function $(ix)^{-0.2}$, which is taken to lie on the positive-imaginary axis. Such *open* orbits, as exist when $\epsilon < 0$, mean that no Bohr-Sommerfeld quantization (53) can be performed, since the contours defined by the particle trajectories are open, and so no value for the energy can be calculated.

4.2.5 Non-Integer $\epsilon > 0$

In general, as ϵ increases from 0, the turning points at $x = \pm 1$ in *figure 4* rotate towards the negative-imaginary axis and more pairs of $\mathcal{PT}$-symmetric turning points appear, all lying on the unit circle (when the energy is taken to be $E = 1$, without loss of generality), and finite in number when ϵ is

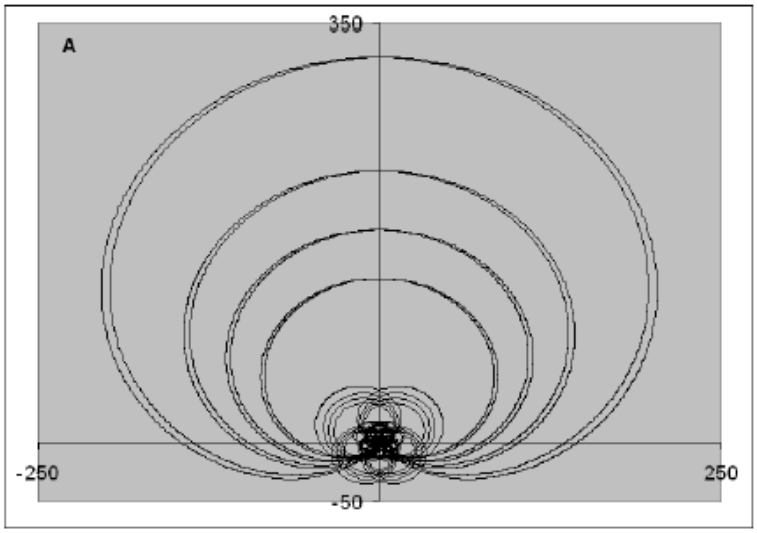

Figure 8: The classical trajectory for the Hamiltonian (17) with $\epsilon = \pi - 2$. The initial displacement is at $-7.1i$ and visits 11 sheets of the Riemann surface. The plot shown is for trajectory projected onto the principal sheet.

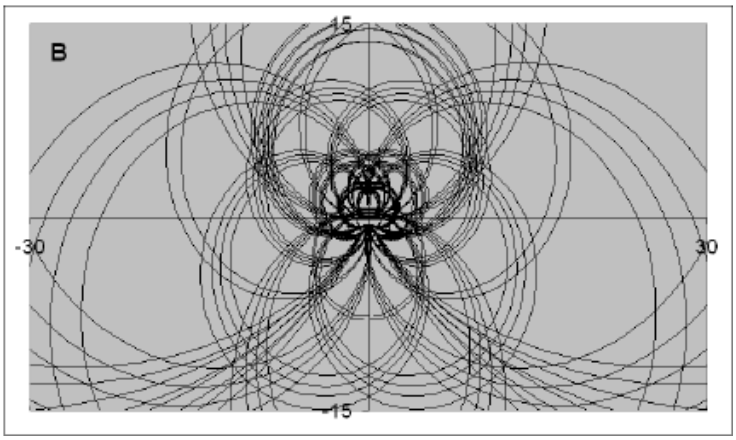

Figure 9: A close-up of the origin of *figure 8*.

rational [1]. The trajectories all remain closed, except for special cases that occur when ϵ is real (as seen in *figures 5* and *6*). Some of the trajectories are very complicated, and visit many sheets of the Riemann surface: see *figures 8* and *9* [1].

The period of the trajectories is a function the pairs of turning points

encircled by the orbits and of the number of times that they circle those turning points. The exact formula for the period is complicated, but known [41], and an analysis of the periods highlights some interesting behaviour. For any given pair of turning points the periods of the orbits that oscillate directly between those turning points may be plotted as a function of ϵ. For the turning points shown in *figure 4*, the plot of the periods versus ϵ is shown in *figure 10* [1], and for the next pair of turning points that appear — those of x_3 and x_4 in *figure 6* — in *figure 11* [1]. As is clear from *figures 10* and *11*,

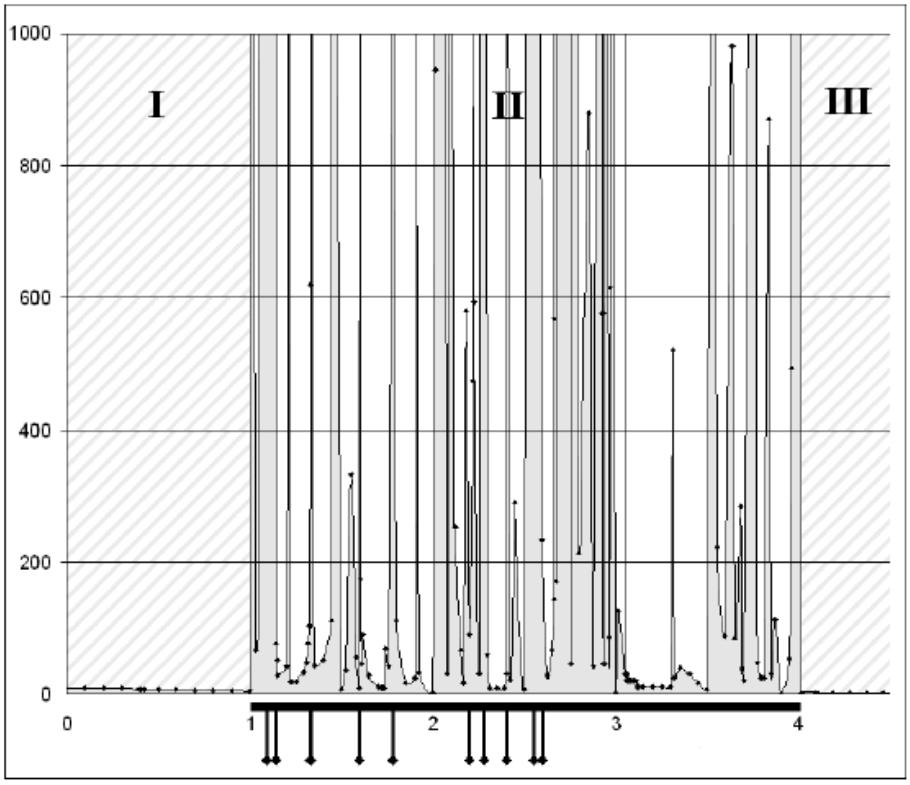

Figure 10: The period of trajectories oscillating between the turning points in *figure 4* as a function of ϵ. The region marked II is for $1 < \epsilon < 4$ and displays the erratic behaviour of the periods in this region.

the periods smoothly decrease except for a region of very erratic behaviour.

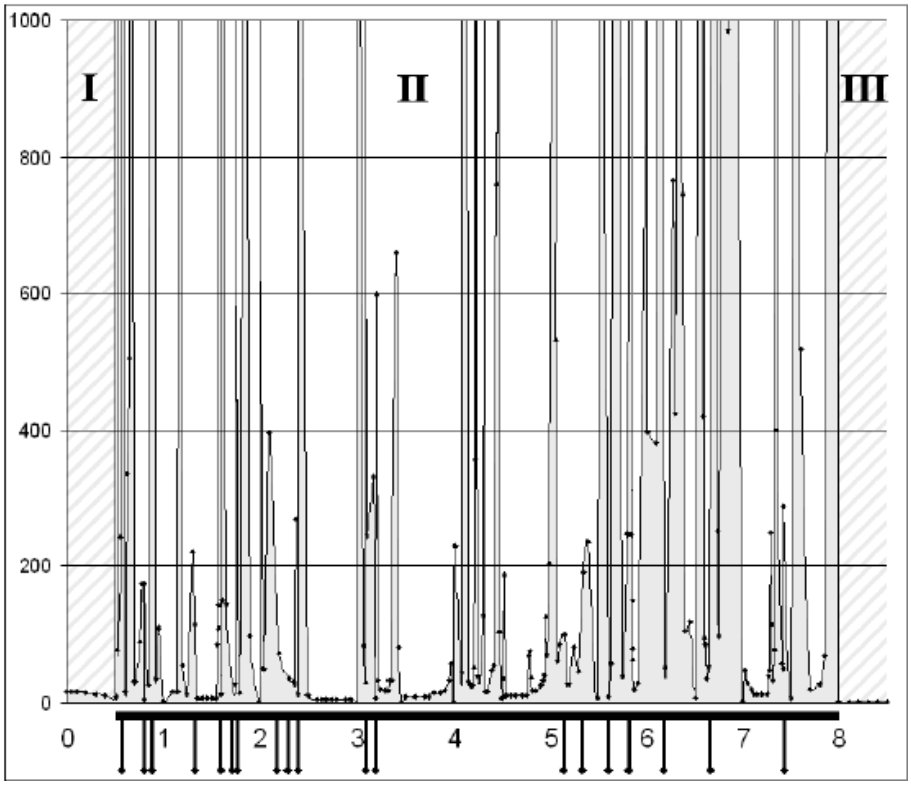

Figure 11: The period of trajectories oscillating between the turning points x_3 and x_4 in *figure 6* as a function of ϵ. The region marked II is for $\frac{1}{2} < \epsilon < 8$ and displays the erratic behaviour of the periods in this region.

If the appearance of new pairs of turning points is labelled by K, such that *figure 10* concerns the pair of turning points $K = 1$, and *figure 11* concerns the pair of turning points $K = 2$, then the region of erratic behaviour lies for the values $\frac{1}{K} < \epsilon < 4K$. Within this region, sections of small-period behaviour are broken by values of ϵ where the period grows large, and possibly infinite [1]. The values of ϵ when this occurs have been found to be always *rational* [49], and correspond to orbits that are *not* $\mathcal{PT}$-symmetric. To such cases, the $\mathcal{PT}$ symmetry is said to have been *spontaneously broken.*

The orbits at which the $\mathcal{PT}$ symmetry is spontaneously-broken coincide

with orbits that have unexpectedly hit another turning point, reflecting the particle back to its originating turning point: see *figures 12* and *13* [1]. In such cases, the trajectories must always occur between complex-conjugate pairs of turning points, leading to complex-conjugate (up-down) symmetry [1].

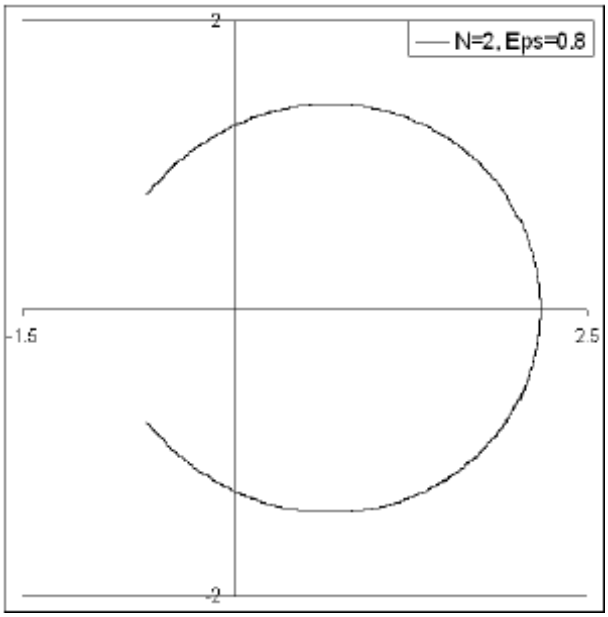

Figure 12: A spontaneously-broken $\mathcal{PT}$ symmetry trajectory at $\epsilon = \frac{4}{5}$. The symmetry is instead complex-conjugate (up-down) symmetry.

This is just a taste of the fascinating things that can occur when classical mechanics is extended into the complex domain; but the systems examined so far have only had real energies, and it is to systems with complex energies that we now turn to.

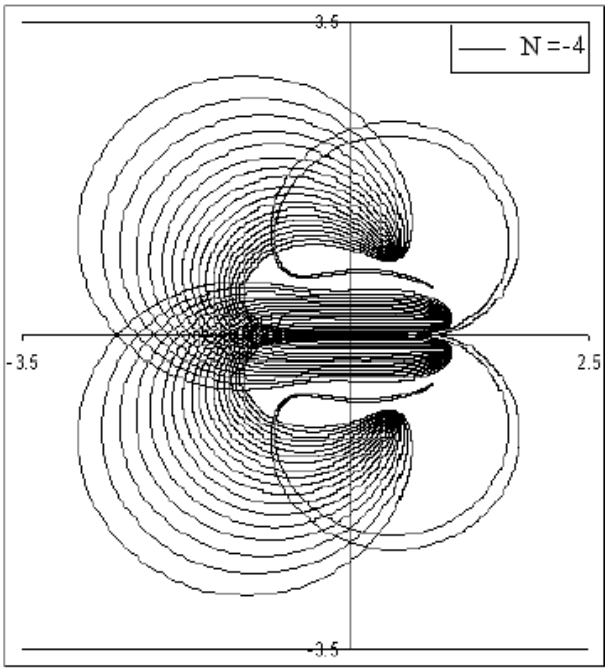

Figure 13: A more complicated trajectory where the $\mathcal{PT}$ symmetry has been spontaneously broken, his time for $\epsilon = \frac{16}{9}$. Note again the complex-conjugate symmetry.

4.3 Complex Energies

Having decided to allow the dynamical variables of a system to take complex values, it is perhaps not unjustified to ask what were to happen if the energy were allowed to take complex values as well. Indeed, it can be argued that such an assumption would not be too unprecedented given that one of the important results of the quantum theory already stipulates that the exact energy of a particle can never be known exactly — namely, Heisenberg's uncertainty principle.

Taking such a hypothesis, we look to see what effects a complex energy has on classical systems.

4.3.1 The Anharmonic Oscillator

We begin by examining the anharmonic oscillator, whose Hamiltonian is

$$H = \frac{1}{2}p^2 + x^4. \tag{54}$$

For a system with energy $E = 1$ the coordinate turning points are at $x = \pm 1, \pm i$, and the usual classical motion is the oscillatory motion along the real-x axis between the points $x = 1$ and $x = -1$. Analytically continuing the problem into the complex domain, a system with initial displacement at $\pm i$ will follow a trajectory that will take it to $\pm i\infty$ respectively, and all other initial displacements in the complex plane will follow closed ellipse-like trajectories pinched at $\pm i$, as shown in *figure 14* [50]. As usual, by Cauchy's theorem, all closed trajectories have equal periods. Let us now take a complex energy to see what trajectories the system will follow. We now take an energy $E = 1 + 0.1i$, and an initial displacement at $x = 1$; the resultant particle trajectory is shown in *figure 15* [50]. The trajectories of this system, as seen in *figure 15*, are no longer closed. In fact, the major departure from those complex classical systems of real energies to those of complex energies is that the hitherto abundance of closed trajectories disappears, and the systems begin to exhibit more interesting dynamics where the particle is apparently more free to move. As such, we will move now to a double-well potential to see if this "freedom" of movement still expresses itself.

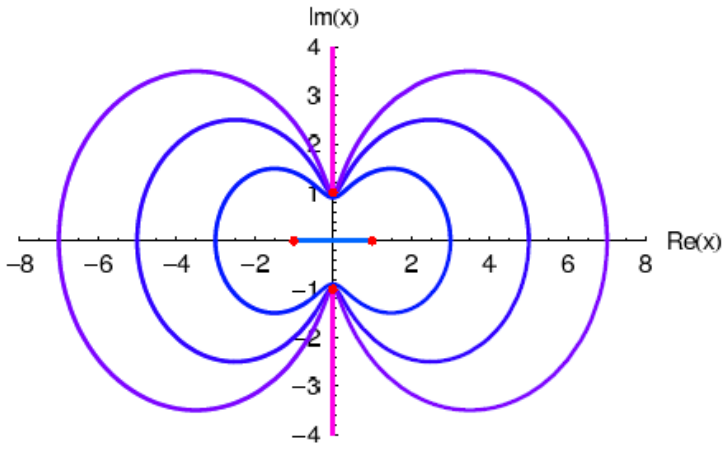

Figure 14: The trajectories of the classical anharmonic system (54) with energy $E = 1$. The oscillatory trajectory between the turning points at $x = \pm 1$ correspond to the familiar real classical motion. All other trajectories in the plane are closed, except those with initial displacements on the imaginary-x axis at and above the turning point $x = i$, and at and below the turning point $x = -i$.

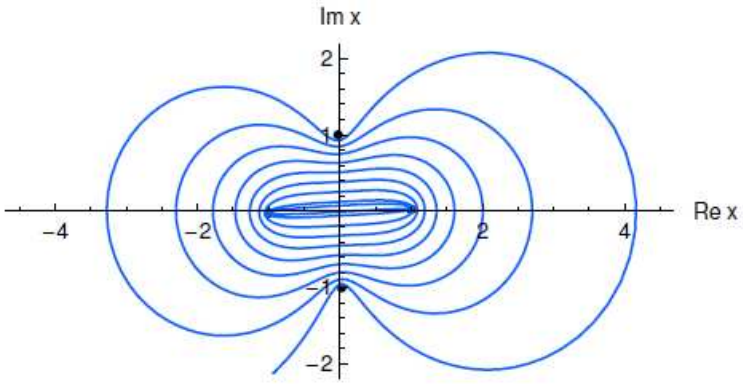

Figure 15: The classical trajectory of the anharmonic system (54) with energy $E = 1 + 0.1i$. The trajectory, as in previous examples of classical systems extended into the complex plane, does not cross itself; but is now no longer closed.

4.3.2 A Double-Well Potential

We now move onto a classical system with a double-welled potential $x^4 - 5x^2$.

A particle with energy $E = -1$ will oscillate in either of the wells of the

potential, as shown by the real-x trajectories shown in *figure 16* [50]. Again, the trajectories for complex initial displacements are also shown to be closed orbits around pairs of turning points. The double-well system for real energies

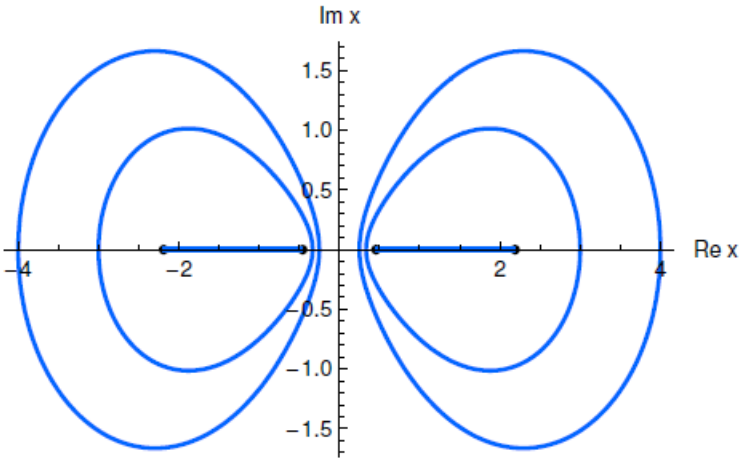

Figure 16: Classical trajectories for a system of potential $x^4 - 5x^2$ with energy $E = -1$. As seen before, the trajectories are invariably closed for all but a few special points in the plane if the energy is real. Here, six such closed trajectories are shown.

is, therefore, seemingly that of a system where the particle orbits are confined to their own local neighbourhood.

Let us now choose a complex energy and observe the particle trajectories: we will take $E = -1 - i$, and an initial displacement $x = 0$. The resultant trajectory taken is shown in *figure 17* [50]. Now, the trajectories are open and the particle is no longer confined to motion about one of the pairs of turning points. Instead, the particle revolves around one pair, spiralling outwards as it does so, crosses the imaginary-x axis, and then begins to spiral inwards about the *other* pair of turning points. The particle then turns back on itself and spirals outwards again, crosses the imaginary-x axis again and then spirals back towards the first pair of turning points. This spiralling behaviour

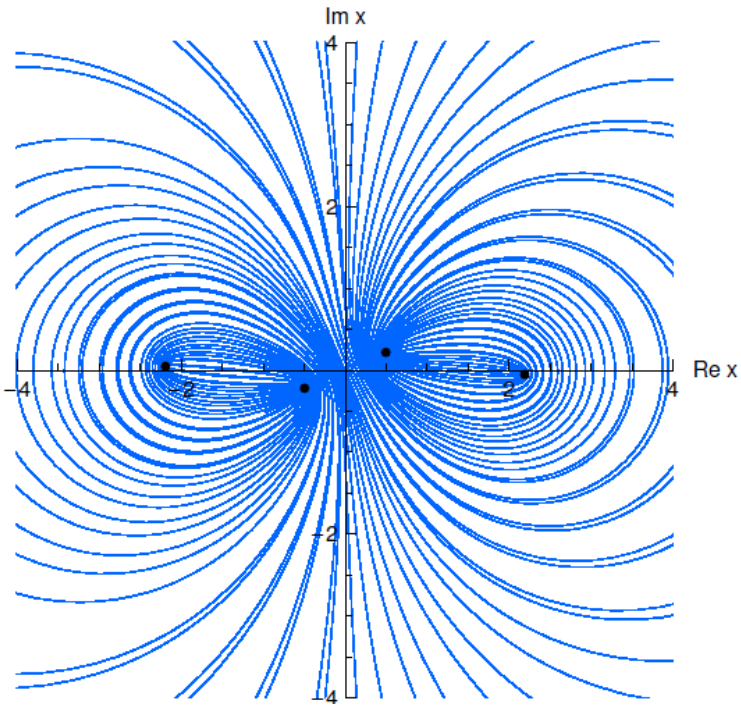

Figure 17: The classical trajectory of a particle initially placed at $x = 0$ in a double-welled potential $x^4 - 5x^2$ with *complex* energy $E = -1 - i$. We again see that the trajectory is no longer closed, but open. The path followed by this particle is particularly interesting because it appears to tunnel between the turning points in the positive-real half of the plane and those of the negative-real half of the plane.

between the two pairs of turning points continues unabated (and without crossing itself at any point), and is highly reminiscent of the tunnelling that occurs across the potential barrier in a quantum system.

We see here a classical system exhibiting what was hitherto a purely quantum effect. Whereas tunnelling is a conceptually difficult concept to understand in the quantum theory, in the complex classical system above it is merely a case of a particle moving along a complex orbit. The appearance of the particle in either well of the potential function without seemingly taking any measurable path is now a trivial consequence of motion in the

complex domain, where only real values may be actually measured.

Yet the analogy between the quantum theory and complex classical dynamics does not stop there. Stationary states of a particle wavefunction in a double-well potential have a definite parity, and the trajectory in *figure 17* also exhibits a parity of sorts. If the points at which the trajectory crosses the imaginary-x axis is recorded against the direction in which it crosses, as shown in *table 1* [50], the particle trajectory can be said to have a definite parity: if the system is parity (spatially) reflected, the directions in which the particle crosses the imaginary-x axis is also reflected; so, the trajectory in *figure 17* is said to have *odd* parity.

Let us choose another complex value for the energy of the system: let us take $E = -2-i$, and an initial displacement of $x = 0$. The trajectory is shown in *figure 18* [50]. Whilst the particle still displays a tunnelling-like behaviour, the trajectory of the particle is now confined to narrow bands. Moreover, the frequency of crossings has lessened, which is not totally unexpected since the real component of the energy has been decreased. More importantly, however, is that this trajectory appears now to have *even* parity: a spatial reflection of this system does not swap the direction in which the particle crosses the imaginary-x axis, as shown in *table 2* [50].

The case of a double-well potential has provided an intriguing analogy between complex classical systems and quantum effects. This analogy is worth exploring further, which the subsequent subsections will explore.

Imaginary crossing point	Direction	Time of crossing
$0.909592i$	$\rightarrow$	45.728640
$0.781619i$	$\leftarrow$	5.366490
$0.441760i$	$\rightarrow$	34.347705
$0.407514i$	$\leftarrow$	16.764145
$0.253436i$	$\rightarrow$	22.909889
$0.231656i$	$\leftarrow$	28.205183
$0.118499i$	$\rightarrow$	11.457463
$0.100556i$	$\leftarrow$	39.658755
$0i$	$\rightarrow$	0
$0.017057i$	$\leftarrow$	51.116500
$0.082877i$	$\rightarrow$	90.775058
$0.136772i$	$\leftarrow$	62.573579
$0.210728i$	$\rightarrow$	79.320501
$0.276231i$	$\leftarrow$	74.024673
$0.376304i$	$\rightarrow$	67.876728
$0.479881i$	$\leftarrow$	85.458656
$0.690666i$	$\rightarrow$	56.467388
$1.121155i$	$\leftarrow$	96.812583

Table 1: Table of the trajectory crossings of the imaginary-x axis in *figure 17*, along with the relative direction of the crossing, and the time at which it dis so. A parity reflection of the system (swapping the sign of the numbers in the first column and also swapping the direction of the arrows) causes the arrows to point in the opposite direction; so, the particular trajectory in *figure 17* is said to have *odd* parity.

4.3.3 A Cubic Potential

Cubic potentials provide a model for nuclear decay, since they provide a model whereby a particle confined in a potential well has the ability to tunnel through the potential barrier and escape to infinity. We find that the tunnelling behaviour seen in *section 4.3.2* also applies to cubic potentials, where we can qualitatively reproduces the quantum effect of nuclear decay.

We take a Hamiltonian $H = \frac{1}{2}p^2 + \frac{1}{2}x^2 - gx^3$, and first examine a system with $g = \frac{1}{3}$, and energy $E = 0.1$. Trajectories for this real energy are shown

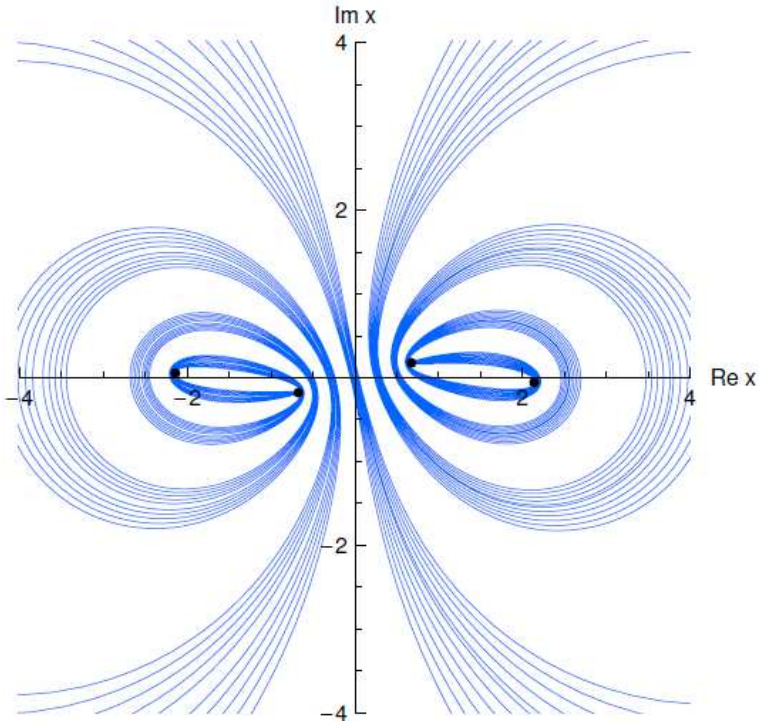

Figure 18: The classical trajectory of a particle initially placed at $x = 0$ in a double-welled potential $x^4 - 5x^2$ with complex energy $E = -2 - i$. The particle behaviour, whilst still displaying a tunnelling behaviour, is now confined to narrow bands; and the frequency of crossings has decreased, which is not unexpected since the real part of the energy has been decrease from that in *figure 16*.

in *figure 19* [50]. The trajectories are, as usual, closed except for special points where the particle moves to $+\infty$ (such behaviour is expected from a cubic potential since it is present in the case of real dynamics also).

We then take $g = 2/\sqrt{125}$ and *complex* energy of $E = 0.456 - 0.0489i$. The trajectory of a particle initially placed at $x = 0$ is shown in *figure 20* [50]. The plot on the left shows runs up to $t = 50$, and shows the particle revolving around the left two turning points, "confined" to the well defined by those two turning points. The plot on the right runs up to $t = 200$ and shows how

Imaginary crossing point	Direction	Time of crossing
$0.212966i$	$\leftarrow$	85.604840
$0.114590i$	$\leftarrow$	47.557393
$0.068159i$	$\leftarrow$	28.534298
$0.407514i$	$\leftarrow$	16.764145
$0.022623i$	$\leftarrow$	9.511410
$0i$	$\rightarrow$	0
$0.045318i$	$\rightarrow$	19.022837
$0.091223i$	$\rightarrow$	38.045810
$0.187424i$	$\rightarrow$	57.069065
$0.210728i$	$\rightarrow$	76.092765
$0.239354i$	$\rightarrow$	95.117102

Table 2: Table of the trajectory crossings of the imaginary-x axis in *figure 18*, along with the relative direction of the crossing, and the time at which it dis so. This system now exhibits *even* parity since a parity reflection of the system (swapping the sign of the numbers in the first column and also swapping the direction of the arrows) causes the arrows to point in the same direction as they do now. Also note that the number of crossing is less than before. Such a result can be explained as, since the real component of the energy has been decreased, the relative size of the barrier has increased.

the particle's trajectory now comes under the influence of the right turning point, quantitatively, at the moment that the trajectory switches from being convex, from he point of view of an observer at the right turning point, to concave. Thus, we stress that we can again say that the qualitative effect of quantum tunnelling has been reproduced in a purely classical system, albeit with complex dynamics and complex energies.

4.3.4 A Cosine Potential

Perhaps the most interesting work so far has been on a periodic potential. Such potentials provided a model for crystal lattices, which exhibit rich quantum behaviour, and it is wondered to what extent can a complex classical

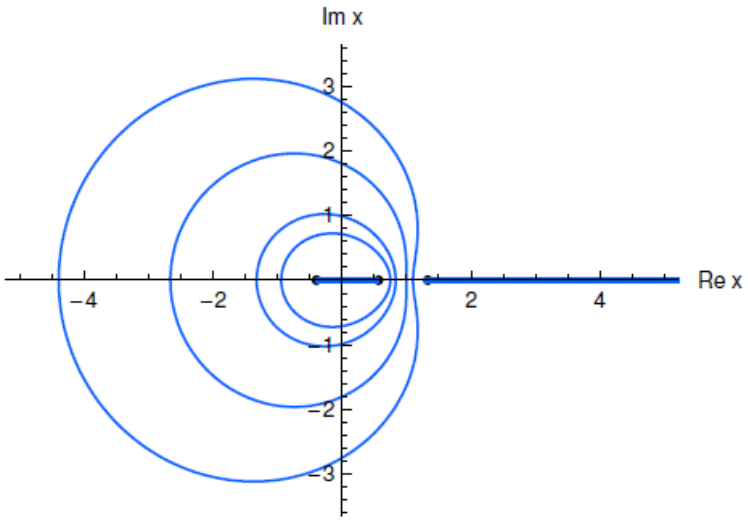

Figure 19: Classical trajectories for a system with Hamiltonian $H = \frac{1}{2}p^2 + \frac{1}{2}x^2 - \frac{1}{3}x^3$, and energy $E = 0.1$. The trajectories are all closed, representing confinement to the potential well, except for those on the real-x axis at and to the right of the rightmost turning point, which represents a particle sliding down the potential and escaping to infinity.

system qualitatively emulate it.

For a Hamiltonian $H = \frac{1}{2}p^2 - \cos(x)$ with real energy $E = -0.09754$, the trajectories are closed and localized around pairs of turning points defining successive wells in the periodic cosine potential: see *figure 21* [50].

Now, if we take a complex energy $E = -0.1 - 0.15i$ the trajectory of a particle initially located at $x = 0$ is shown in *figure 22* [50]. The particle trajectory is now open and "tunnels" between adjacent wells in the potential function by spiralling out of one site and into another before spiralling out again. Moreover, the motion of the particle exhibits a kind of deterministic "random walk" moving right twice, the left five times before moving right again. Such behaviour mirrors that of a quantum particle hopping from site to site in a crystal by tunnelling in a random direction.

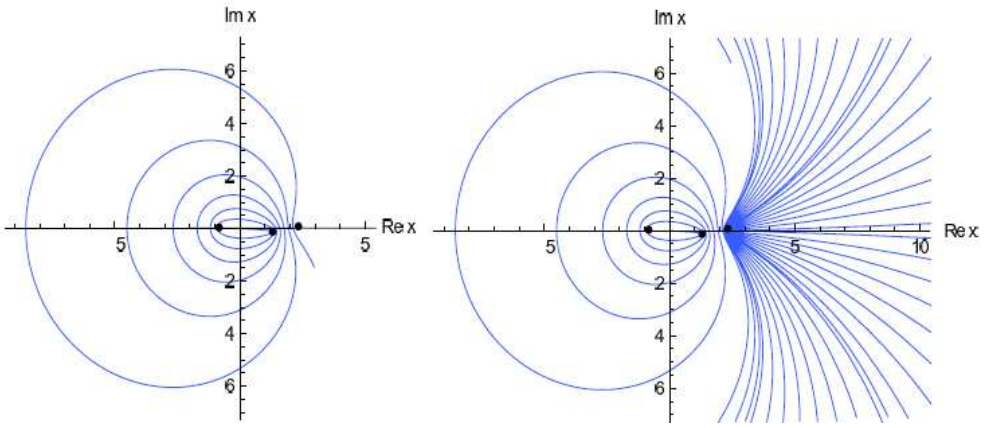

Figure 20: The classical trajectory for a system with Hamiltonian $H = \frac{1}{2}p^2 + \frac{1}{2}x^2 - 2x^3/\sqrt{125}$, and energy $E = 0.456 - 0.0489i$ at an initial displacement at $x = 0$. The plot to the left runs up to $t = 50$ and shows the particle initially under the influence of the left two turning points, before coming under the influence of the rightmost turning point, as shown in the right plot which runs up to $t = 200$. The point at which the particle comes under the influence of the rightmost turning point is a quantitative measure of when the particle can be said to have "tunnelled" from the well defined by the left two turning points.

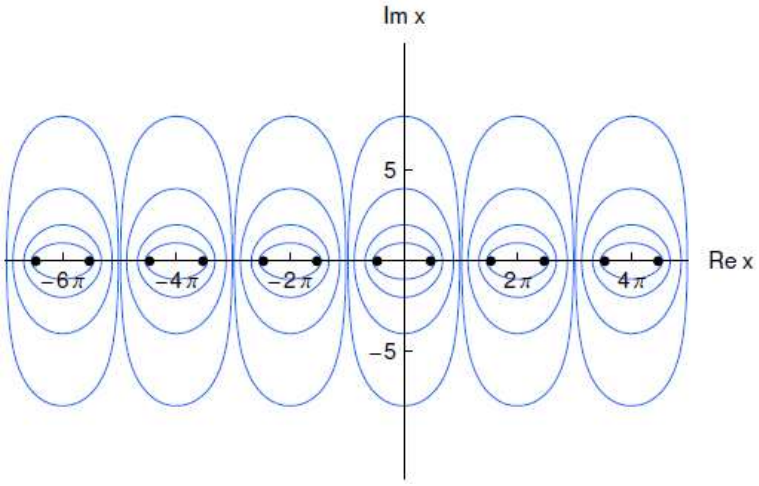

Figure 21: Classical trajectories for a system with Hamiltonian $H = \frac{1}{2}p^2 - \cos(x)$ with real energy $E = -0.09754$. The particle is localized about each well in the periodic cosine potential.

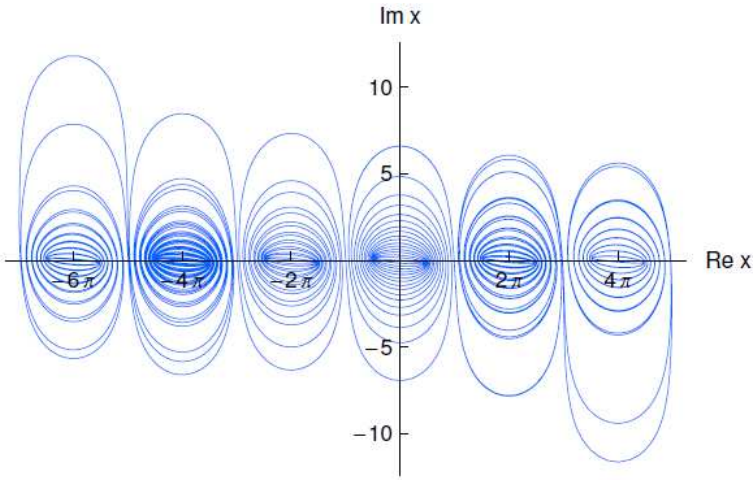

Figure 22: The classical trajectory for a $-\cos(x)$ potential with energy $E = -0.1 - 0.15i$ with an initial displacement at $x = 0$. The particle now moves in an open trajectory that spirals outwards from one well in the potential and then spirals into an adjacent well before spiralling out again. The particle moves from the well at the origin to the right, and then to right again before moving left five successive times and then right again. This "random walk" behaviour is deterministic, yet analogous to the probabilistic tunneling of a quantum particle in a crystal.

The tunnelling rate of the classical particle can also be quantified as the number of turns the particle undergoes in each site, which has been found to depend on the imaginary component of the energy. A plot of the number of turns taken by the particle versus the imaginary component of the energy is given in *figure 23*, from which it is evident that the relationship between the two is hyperbolic in nature. The time-energy Heisenberg uncertainty principle, with $\hbar = 1$, sets a lower limit of $\frac{1}{2}$ for the product of energy and time uncertainties: the product of the imaginary component of the energy, which is a measure of the uncertainty of the energy (since only real energies can be measured), and the number of turns the particle undergoes in *figure 23* is approximately 17 [50].

However, the "random walk" behaviour is not the most intriguing result found for the cosine potential. Quantum particles in a crystal can also exhibit *delocalized* behaviour whereby, for certain ranges of energies — within so called *conduction bands* — the particles are able to drift freely from site to site in one direction. Extraordinarily, such behaviour has been observed in this complex classical system too: a plot of the particle trajectory for energy $E = -0.09754 - 0.1278i$, with the particle initially located at $x = 0$, is shown in *figure 24* [50]; which shows the particle moving in only one direction at an almost constant rate.

The hopping behaviour of this classical system has been analyzed over

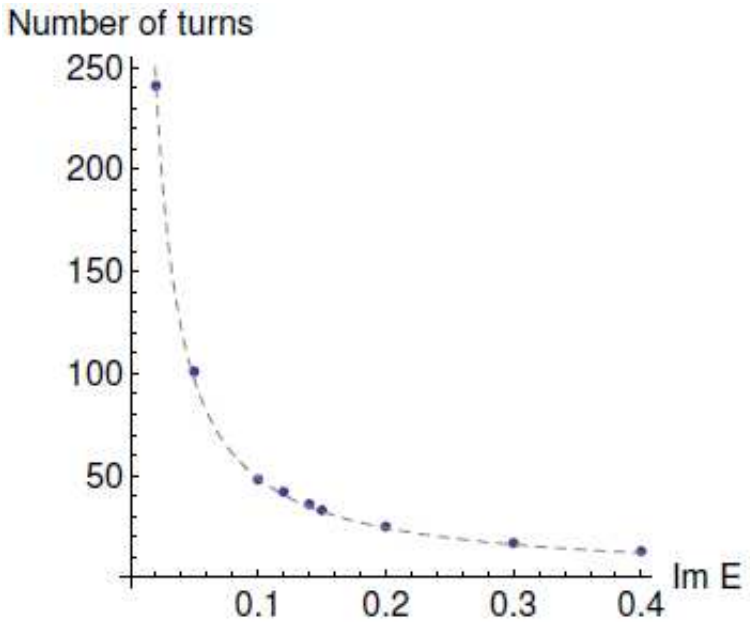

Figure 23: A graph of the number of turns the particle takes in a particular site versus the imaginary component of the energy for that trajectory. The product of the tunnelling time, as measured by the number of turns spent in a site, and the imaginary part of the energy is a constant. The time-energy Heisenberg uncertainty principle states that this product must be greater than $\frac{1}{2}$, and for this system is approximately 17.

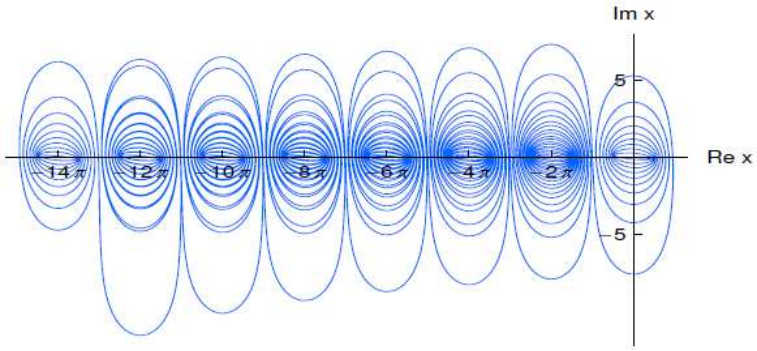

Figure 24: The classical trajectory of a particle in a $-cox(x)$ potential with energy $E = -0.09754 - 0.1278i$ at an initial displacement of $x = 0$. In this scenario the particle undergoes an almost constant drift in strictly one direction, mirroring the behaviour of a delocalized quantum particle in a crystal.

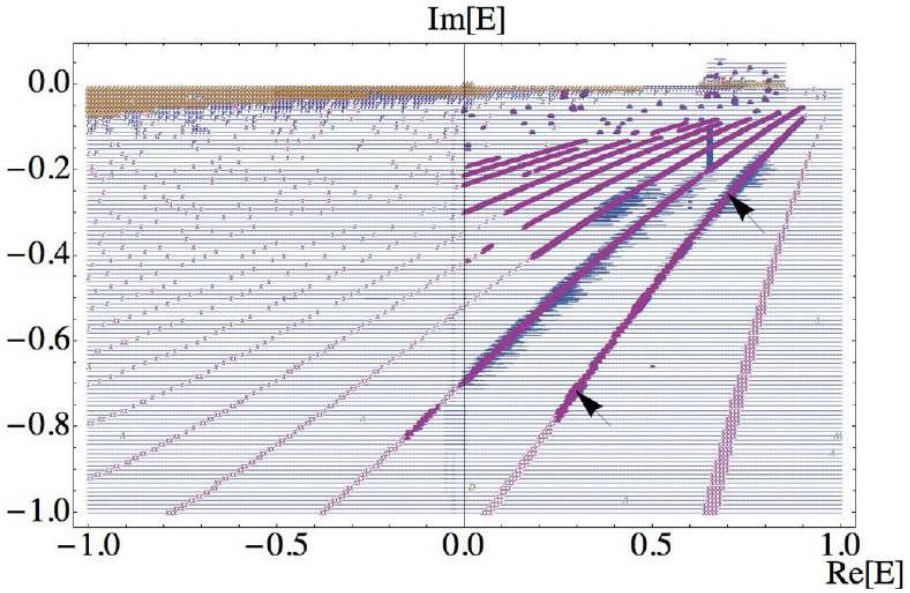

Figure 25: A graph of the hopping behaviour of classical particle trajectories for a range of energies in the complex-E plane. Delocalized behaviour is marked with a 'x', hopping behaviour with a '-', and the lack of hopping behaviour with a '&'. The "conduction bands" for which the particle behaves as if was delocalized are clearly visible, which broaden as the imaginary component of the energy decreases.

a range of energies, and bands of energies have been found at which the particle appears to behave as if is delocalized [51]. The plot in *figure 25* [51] marks the behaviour of trajectories with ten hops, and those where the hops were in one direction only are marked with a cross; the "conduction bands" are clearly visible and one such band is marked with arrows. The conduction bands are well defined, and have sharp edges — the arrowed portions of *figure 25* are shown in more detail in *figures 26* and *27* [51].

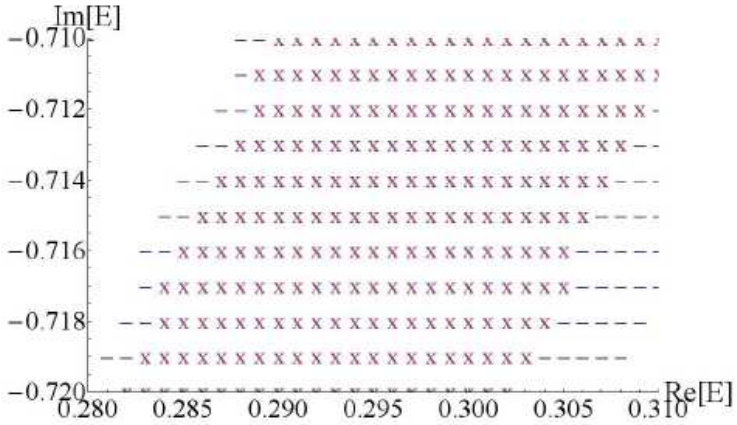

Figure 26: A detailed portion of the complex-E plane of *figure 25*. Again, energies where "delocalized" behaviour occur are marked with a 'x', and the plot shows that the bands are sharply defined.

5 An Elliptic Potential

The aim of this section is to present the findings from the analysis of a complex classical system with the cosine potential of *section 4.3.4* generalized to that of the Jacobi elliptic function $\mathrm{cn}(x, m)$ where m is the elliptic parameter.

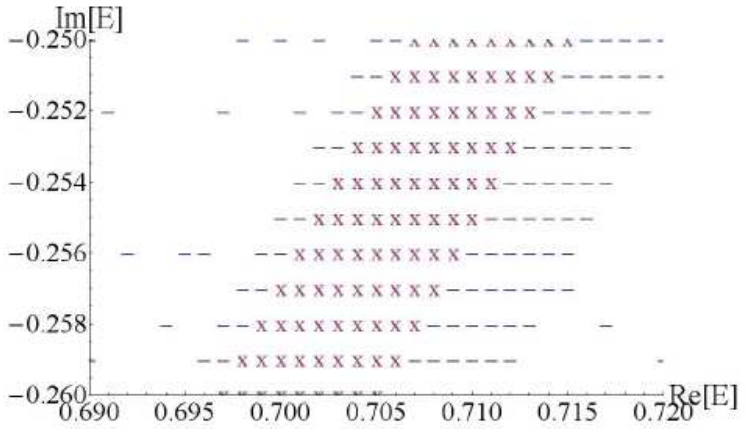

Figure 27: As in *figures 26*, this is a detailed portion of the complex-E plane where the delocalized behaviour of the classical particle can be seen; again, the conduction bands are sharply defined.

The Hamiltonian considered is:

$$H = \frac{1}{2}p^2 - \mathrm{cn}(x, m), \tag{55}$$

where, again, m is the elliptic parameter.

The elliptic function $\mathrm{cn}(x, m)$ is an interesting potential to consider for several reasons. Firstly, it is a generalization of the cosine potential, since $\mathrm{cn}(x, 0) \equiv \cos(x)$, and is periodic in two distinct directions in the complex plane. Thus, it would be interesting to see how the hopping behaviour seen for the cosine function would occur for a function that is doubly periodic. Secondly, the $\mathrm{cn}(x)$ function has singularities is the complex plane, and it would be interesting to see how this would affect trajectories for this potential.

The equation (55) is solved numerically using a Runge-Kutta iterative method, and, explicitly, a Prince-Dormand Runge-Kutta method so that

estimates for the error of an iterative step can be made in order that the step sizes can be altered. This so called adaptive step-size procedure will be important to us since we do not want to waste computing time with small iterative steps where the trajectory is not changing much.

The code is written in C++ and is presented in *appendix A*. The Runge-Kutta routine is taken directly from the source code of the GNU Scientific Library (version 1.12), and modified to use arbitrary precision data types using the GNU MPFR library (version 2.4.1) and the GNU Multiple Precision Arithmetic library (version 4.3.1). Values for the Jacobi elliptic function are provided by Mathematica (version 7.0.0), and fed to the C++ program via the MathLink library, which is provided with Mathematica: in effect, the Mathematica kernel is used as a computational engine for which the C++ program is a front-end.

The program was built on a Linux machine (kernel 2.6.28), and the various parameters needed by the simulation can be provided with runtime flags; these include the time for which to run up to, the value for the elliptic parameter, the particle's initial complex displacement, and the value for the complex energy. The program then creates some parameters needed by the Runge-Kutta routine, sets up a link with the Mathematica kernel, and begins to run the Runge-Kutta method.

The program implements the Runge-Kutta routine by calling the function *evolve_apply* (see *appendix A*) which moves the system forward in a time that is determined by calling the function *rk8pd_apply* to apply the iteration. The function *evolve_apply* then checks the errors produced by such an iteration and can call the function *h_adjust* to adjust the size of the time steps and

re-implement an iteration. Values of the Jacobi elliptic function are obtained by the function *func*, and are also called by *evolve_apply* as they are needed by the Runge-Kutta method. The function *func* obtains values of the elliptic function by sending a C++ string to the Mathematica kernel of the expression to calculate, and is likewise returned a string that contains the answer, which is then parsed for real and imaginary components and entered into the C++ data types for the system's dynamical variables.

The output produced by the program is placed directly into a text file named *data*, which can then be read by a suitable plotting program for the real and imaginary components of the system's dynamical variables. The plotting program used in this work is Gnuplot (version 4.2 patchlevel 4).

The first obstacle that the numerical simulation faced was that of time: numerical procedures for calculating complex values for elliptic functions with complex inputs are *much* slower than for the cosine potential. Another obstacle is that, with time being a significant constraint, simulations could not always be completed without large errors accruing in the trajectory: the energy of the system should remain constant, and energies that deviate from that constant value provide us with a reasonably reliable condition for knowing whether the trajectory is inaccurate. Checking that the energy of the particle agrees with what it should be would not, however, guarantee that errors have *not* accrued. Both problems are unavoidable in practical terms, but the accuracy of the simulations could be managed by taking relatively small values for the elliptic parameter m. This work presents data using only two values of m for the majority of its runs: for $m = 0.1$ and $m = 0.2$. Some data was collected for values of $m = 0.5$, but the time taken for the run

to complete and the iterative errors accumulated rendered opportunities for the collection of data for higher values of m to be limited. Indeed, even with relatively small values of m, the runs still accrue errors that are hard to avoid without spending too long a time running the simulation. On the system used in this work the runs could sometimes take up to a week to complete, and normally several days, and problems with accuracy still remain.

With computations limited by accuracy and time, interesting results were nonetheless seen, and they are described qualitatively here; and what is hoped is that these can be followed up with more detailed work. We begin by examining the case for real energies.

5.1 Real Energies

The results of previous cases of complex classical dynamics for a range of potentials, examined in *sections 4.2–4.3*, with real energies found that trajectories were typically closed, except for special cases of values for which they were open. The trajectories for an elliptic potential were also found to be closed except that, whereas before there was only a measure-zero set of open trajectories (typically, for initial displacements along a line in the complex plane), there now are now a comparable number of open trajectories as there are closed ones.

The trajectories for particles with energy $E = 0$ and elliptic parameter $m = 0.5$ are shown in *figure 28*. The closed trajectory lying wholly on the real-x axis is for an initial displacement $x = 6.5$ and shows the usual oscillatory motion of a cosine-like potential; it has a period of about 13.2

seconds. The "closed" trajectories are for initial displacements $x = 2, 2, 1, 4+3i, 6, 9.5$ and have energies that wander from $E = 0$; and so the fact that they do not close and appear to cross other particle paths can be conjectured to be only because the iterative method looses accuracy. A plot of the trajectory starting from $x = 2$ is shown in *figure 29*. The remaining trajectories are for initial displacements at $x = 2.2, 2.5, 3, 3.5, 3.6, 3.7, 3.8, 3.9, 4, 4.5, 5, 5.5$ and then for $x = 10, 10.5, 11, 11.5$ and are all clearly open; again, the fact that some paths cross is believed to be due only to the fact that the iterative method is loosing accuracy. Thus, *figure 28* clearly demonstrates some of

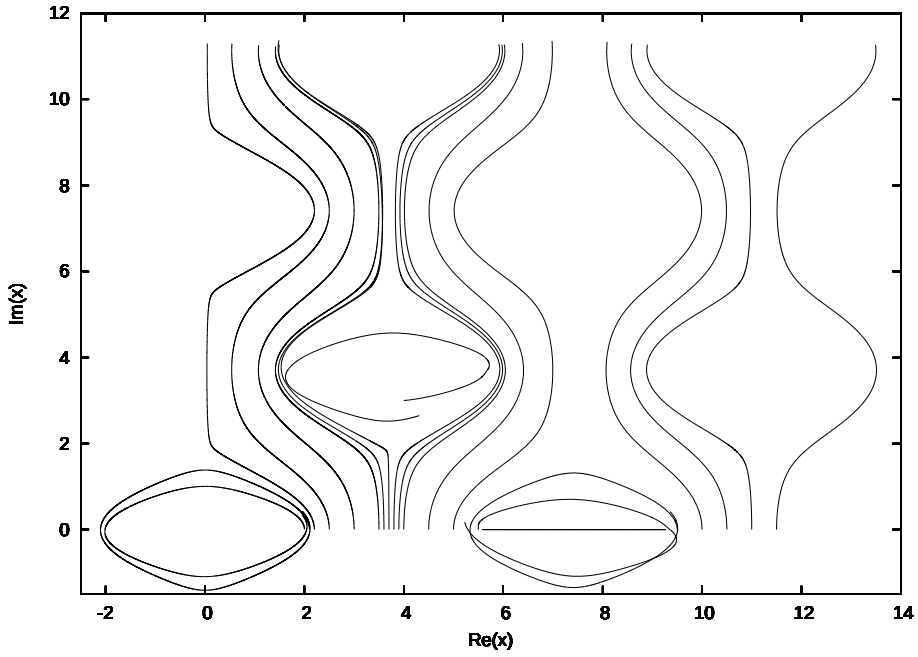

Figure 28: Classical trajectories in the complex-x plane for the system (55) with energy $E = 0$ and elliptic parameter $m = 0.5$. Visible are the open trajectories that run up-down in the plane, and the "closed" trajectories that are believed to not actually close due only to computational inaccuracies. A close-up of the "closed" trajectory for a particle placed initially at $x = 2$ is shown in *figure 29*.

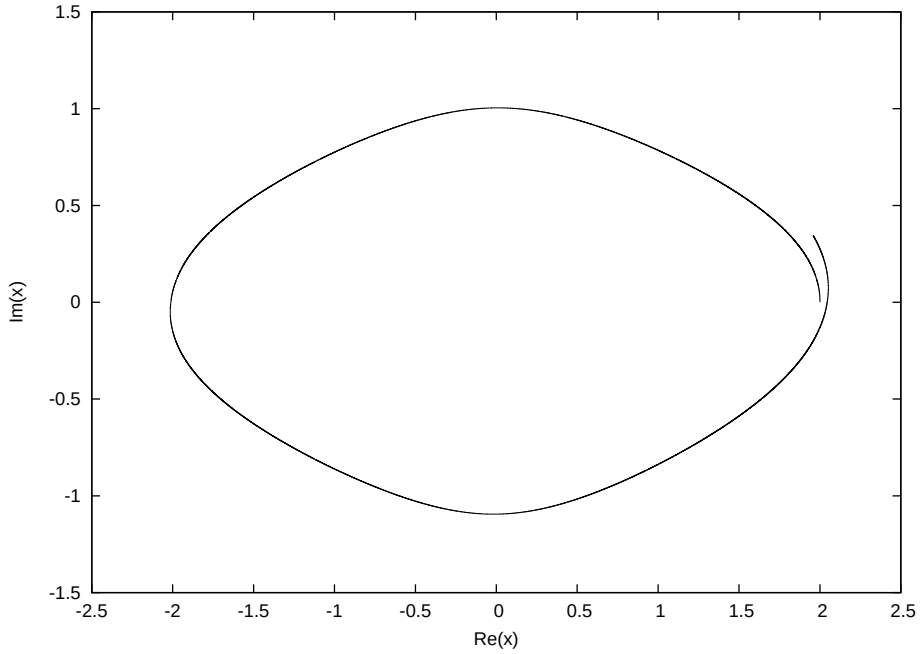

Figure 29: Classical trajectory in the complex-x plane for $E = 0$, elliptic parameter $m = 0.5$, and initial displacement $x = 2$. It is here evident some of the inaccuracy problems for higher m values since such trajectories are believed to be closed.

the accuracy problems encountered by the simulation runs.

A second plot of trajectories was taken for elliptic parameter $m = 0.1$ and energy $E = 0$, and is shown in *figure 30*. From this figure it can be see that there truly exist closed trajectories (for trajectories with initial displacements at $x = 1$, and $x = 2, 4.5$), and so it is believed that those similar trajectories in *figure 28* are also closed. The remaining open trajectories are for initial displacements at $x = 2.5, 3, 3.5, 4$.

From the trajectories in *figure 30* it can also be inferred that the existence of regions of open trajectories is not unique to a particular elliptic parameter value. It is perhaps not unexpected that there exist regions of open trajectories based on the fact that the elliptic function is doubly periodic;

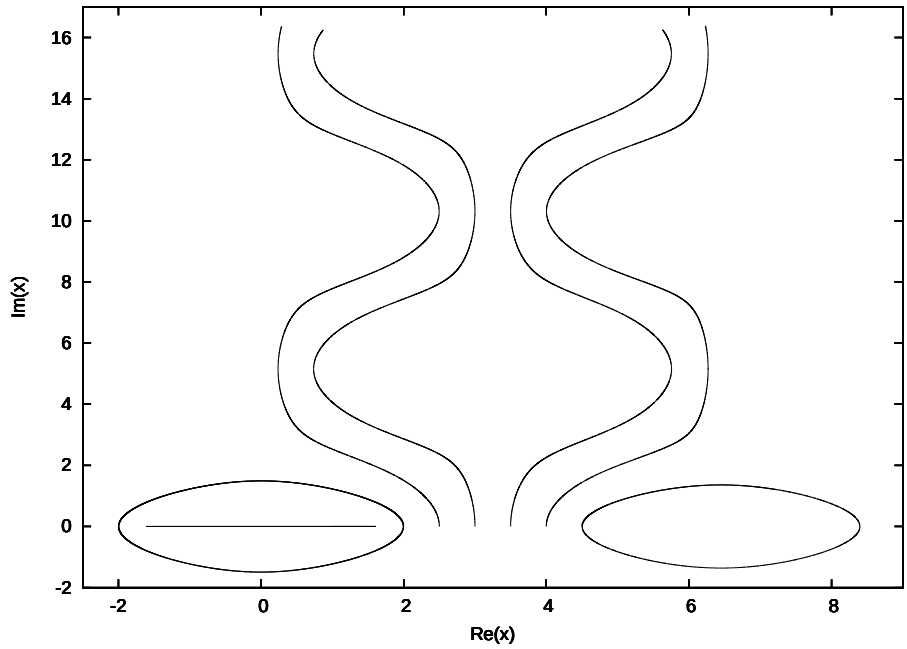

Figure 30: Classical trajectories in the complex-x plane for the system (55) with energy $E = 0$ and elliptic parameter $m = 0.1$. Here, the "closed" trajectories similar to the ones in *figure 28* are indeed closed.

but certainly the fact that there exist large portions of the complex plane for which the trajectories are open is somewhat interesting. Further work could be conducted on the points at which the open trajectories appear in order to determine if there exists some explanation for their appearance.

For the cosine potential, *figure 21* could be understood as particles confined to regions around their own respective lattice sites; now, for the elliptic potential, the open trajectories in figures *figure 28* and *30 could* represent some propensity for the particle to undergo hops between lattice sites along constant imaginary-component lines. Such a tentative hypothesis could explain the qualitative features found for trajectories followed when complex energies are specified; which is where we turn to in the next section. But,

before we do so, we lastly remark that the poles of the elliptic function in the complex plane do not seem to affect the particle trajectories.

5.2 Complex Energies

We now turn to systems with complex energies. The first plot done is shown in *figure 31* and is for a system with energy $E = 0.25 + 0.25i$, initial displacement $x = 0$ and with elliptic parameter $m = 0.1$. As expected, the trajectory is not closed; and also, as with the cosine potential, it spirals from one site to another. However, there is one striking feature of the plot and it is that it appears to only hop to and fro along one direction: the particle spirals out from the origin and skips past two sites and spirals into the third and out again (a close-up is shown in *figure 32*) before spiralling into the fourth, all of whom lie on a diagonal direction that is qualitatively from bottom-left to top-right.

To see if the same behaviour was observed for other values of complex energies, plots were generated by varying the real component of the energy, but keeping the initial displacements at $x = 0$ and the elliptic parameter of $m = 0.1$: the plot for $E = 0.75 + 0.25i$ is shown in *figure 33*, $E = 0.1 + 0.25i$ in *figure 34*, $E = -0.1 + 0.25i$ in *figure 35*, $E = -0.25 + 0.25i$ in *figure 36*, and $E = -0.75 + 0.25i$ in *figure 37*.

All the plots from *figures 33–37* display the roughly diagonal hopping behaviour seen in *figure 31*; yet, the manner in which they do so is different. In *figure 33* the particle spirals away from the origin immediately and spirals once into the site below it, and then spirals once out into the site below it

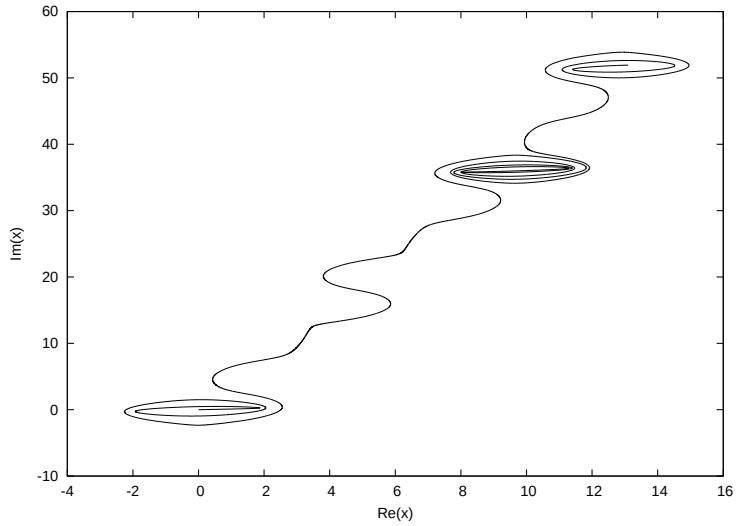

Figure 31: Classical trajectory for $E = 0.25 + 0.25i$, $m = 0.1$, and initial displacement $x = 0$. The particle appears to move only along a diagonal orientated from bottom-left to top-right. The particle also only moves along this diagonal in one direction, spiralling in and out of some sites, and bypassing others, on its way.

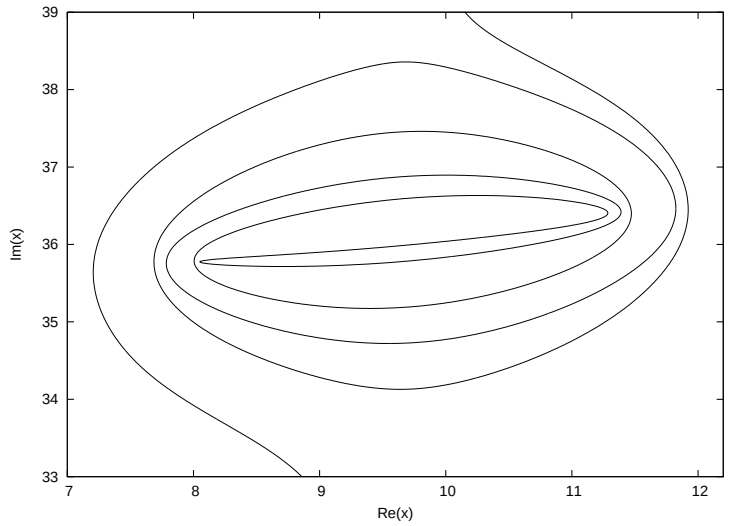

Figure 32: A close-up of *figure 31* of the spiralling in the second site spiralled into on the particles trajectory.

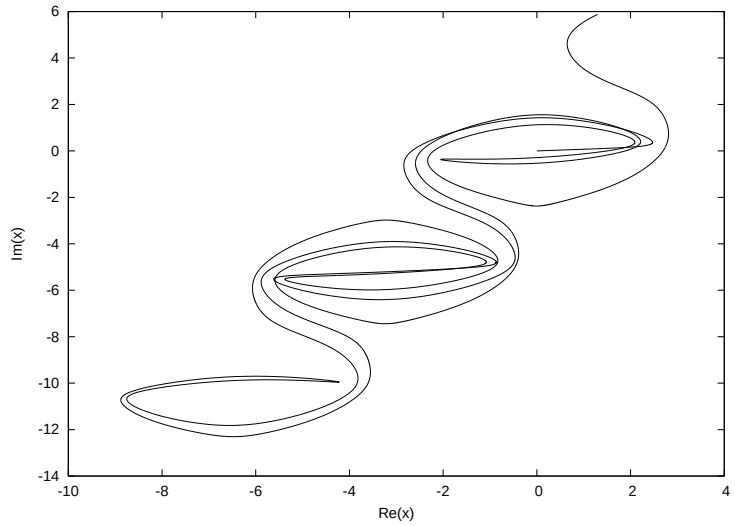

Figure 33: Classical trajectory for $E = 0.75 + 0.25i$, $m = 0.1$, and initial displacement $x = 0$. Here, the particle still spirals between sites lying on a diagonal, and spirals into two sites below it and then up past its initial site again.

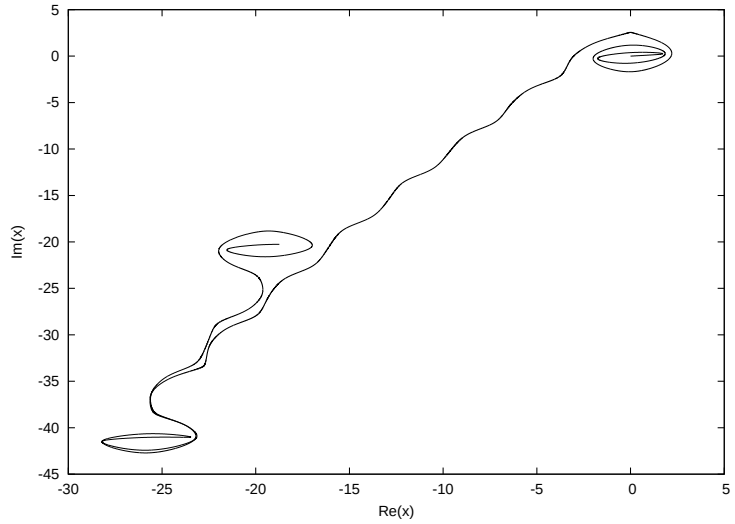

Figure 34: Classical trajectory for $E = 0.1 + 0.25i$, $m = 0.1$, and initial displacement $x = 0$. Here, the particle again moves along the same diagonal observed in *figures 31* and *33*, but now moves past many sites before spiralling into one.

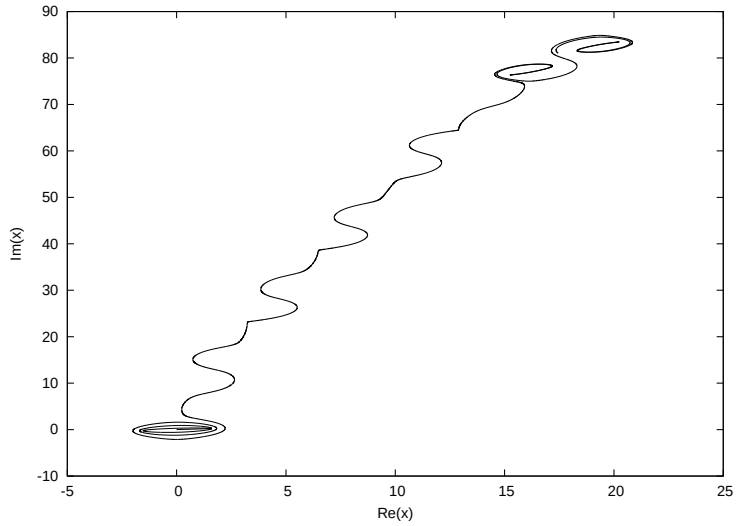

Figure 35: Classical trajectory for $E = -0.1 + 0.25i$, $m = 0.1$, and initial displacement $x = 0$. The particle trajectory is qualitatively the similar to the trajectory shown in *figure 35*, but now only ever moves along one direction along the diagonal.

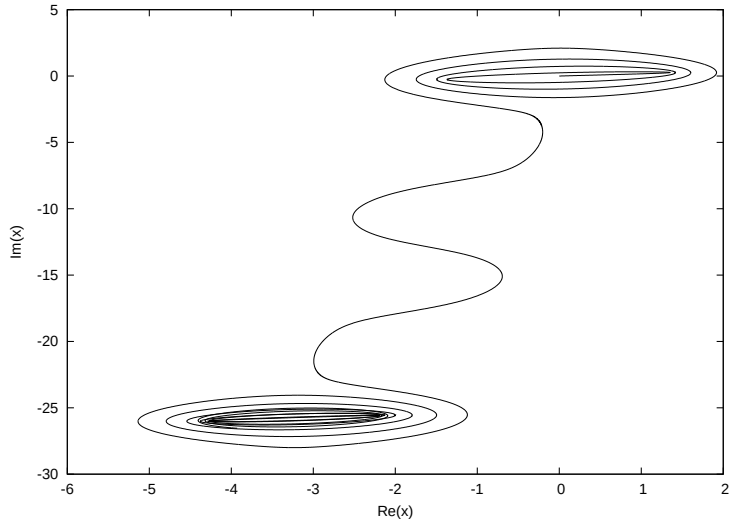

Figure 36: Classical trajectory for $E = -0.25 + 0.25i$, $m = 0.1$, and initial displacement $x = 0$. The particle here spends much more time spiralling between sites, but still remains on a bottom-left to top-right diagonal.

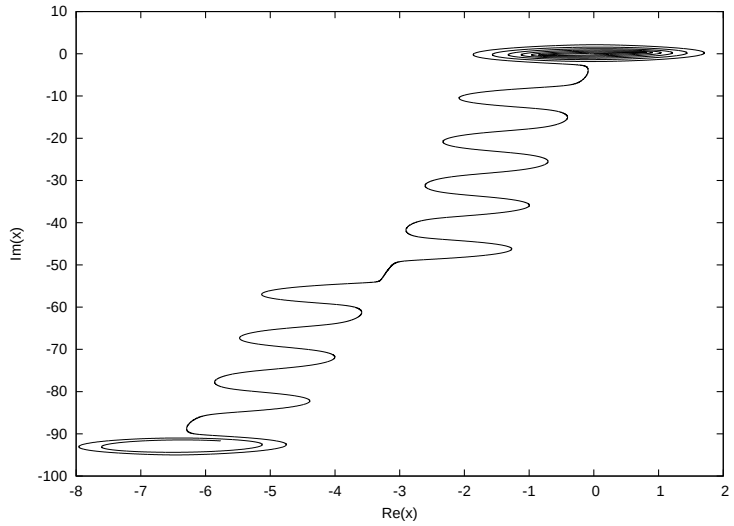

Figure 37: Classical trajectory for $E = -0.75 + 0.25i$, $m = 0.1$, and initial displacement $x = 0$. As in *figure 36*, the particle spends much more time spiralling than in *figures 34* and *35*.

before spiralling once in and once out again back past the first two sites. A close up of the intermediate site in *figure 33* is shown in *figure 38*

It should also be noted in *figure 38* that the trajectory appears to cross itself. The energy of the particle does wander away from $E = 0.75 + 0.25i$, and the crossing of the trajectory may be because the iterative method is loosing accuracy. However, it may also be that the trajectory is moving on different sheets of a Riemann surface, with branch cuts emanating from the poles of the elliptic function. More detailed runs where the accuracies of the iterative method can be kept in check are required to determine whether the trajectory is wholly reliable, but some of qualitative description of the various differences of the trajectories that the particle takes for different energies can still be tentatively made.

In *figure 34* the particle spirals out from the initial site twice before hop-

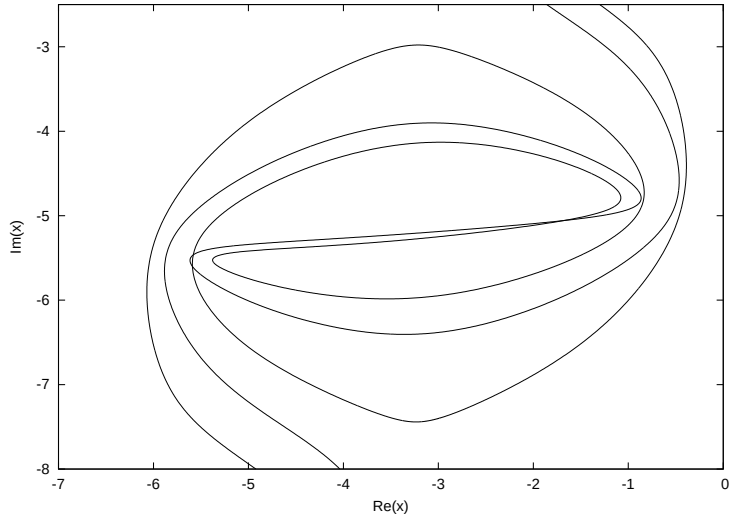

Figure 38: A close-up of the particle motion in the intermediate site of *figure 33*. The particle trajectory crosses itself, which may be due to inaccuracies in the iterative method. The trajectory could, however, also be moving on different sheets of a Riemann surface, and more accurate runs are required in order to be sure whether the trajectory truly crosses itself.

ping several times to a site further down the diagonal before hopping back up the diagonal again and then jumping to a site *not* on the diagonal.

In *figure 35* the particle moves roughly as it does in *figure 34*, but in the opposite direction: the particle spirals out three times before moving upwards along the diagonal many times before it gets to a site where it spirals in once, and then out once to the next site along before spiralling in once and out once again. Here, however, the particle never moves back to a site that it has already been to, and this behaviour is analogous to the conduction band behaviour for the cosine potential. More plots were observed with this delocalized behaviour of the particle and will be discussed in the following sections.

In *figure 36* the particle motion is different yet again. This time the

particle spirals within sites many times: it spirals three times outwards from the initial site before moving to a relatively nearby site before spiralling in five times. Similarly, in *figure 37* the particle spirals outwards six times from its initial site before moving to another one.

The differences in the qualitative nature of the trajectories is something that was not observed in the cosine potential and was worth investigating further over more values in the complex-E plane. Plots were conducted for energies

$$\begin{gathered} E = E_r + iE_i, \\ E_r, E_i \in \{-0.75, -0.5, -0.25, -0.10, 0.01, 0.1, 0.25, 0.75\}, \end{gathered} \tag{56}$$

so that any patterns across ranges of the real- and imaginary-component of the energy could be studied; and, certainly, some interesting plots were found. However, we again note that the observations being made are hounded by inaccuracies in the particle trajectories. More work is needed over longer periods of time in order to draw clear conclusions: those made here are tentative, and only indicative of some of the interesting behaviour that might be seen.

5.2.1 Hopping Behaviour

For all the plots with energies (56) the trajectories always qualitatively moved along a diagonal: at the very least the hop from the initial site is never to an adjacent site on the real-x axis. The diagonals are always bottom-left to top-right for positive-imaginary components, and top-left to bottom-right for negative-imaginary components (see *figures 39* and *40* for two such

examples). This is very curious behaviour, and it wondered whether this

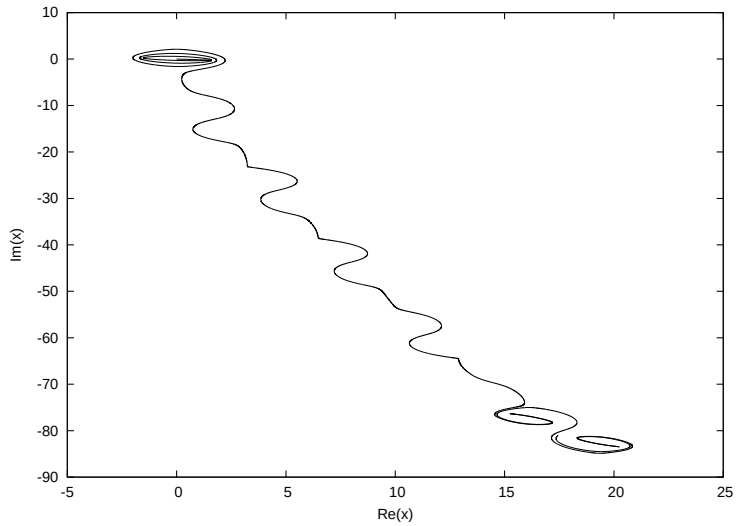

Figure 39: Classical trajectory in the complex-x plane for $E = -0.1 - 0.25i$, $m = 0.1$ and an initial displacement $x = 0$. Note that the particle still moves on a diagonal, but which is now orientated top-left to bottom-right. This is due to the sign swap of the imaginary component of the energy: negative imaginary-components all have the diagonal direction of hopping behaviour orientated in this way.

hopping behaviour and the open trajectories seen in *figures 28* and *30* for *real* energies are related. Plots were made with energies in (56) for elliptic parameter $m = 0.1$ *and* $m = 0.2$, and it appears that hops off the diagonal are more likely to occur for $m = 0.2$: see *figures 41* and *42* for two comparisons.

It is wondered whether the open trajectories observed in *figures 28* and *30* indicate some propensity to move along in the imaginary-x direction. Of course, to produce diagonal hopping motion one would also need to assume that hops along adjacent sites in the real-x direction are more likely to occur than between sites adjacent in the imaginary-x direction. The open trajec-

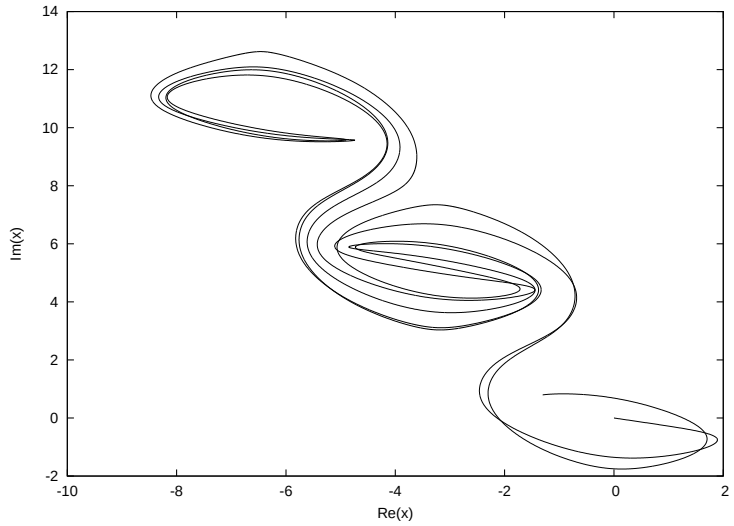

Figure 40: Classical trajectory in the complex-x plane for $E = 0.25 - 0.75i$, $m = 0.1$ and an initial displacement $x = 0$. As in *figure 39*, the negative sign of the imaginary-component of the energy means that the diagonal on which the particle generally tunnels along is orientated top-left to bottom-right.

tories seen in *figures 28* and *30* do show an "asymmetry" between what one observes moving along the real-x axis and what one observes moving along the imaginary-x axis: the open trajectories are always up-down and never left-right. Perhaps this is a manifestation of a deeper asymmetry that favours left-right hops to up-down ones? In any case, the reason why the hops appear to favour moving along diagonals, and always orientated one way for positive-imaginary components and the opposite way for negative-imaginary components, is striking and certainly deserving of more investigation.

The tentative observation that hops off the diagonal appear more frequently for those systems with elliptic parameter $m = 0.2$ than for those with elliptic parameter $m = 0.1$ may be explained by the observation that the distance between adjacent closed trajectories along the real-x axis (but *not* along the imaginary-x axis, interestingly) diminishes as m increases in

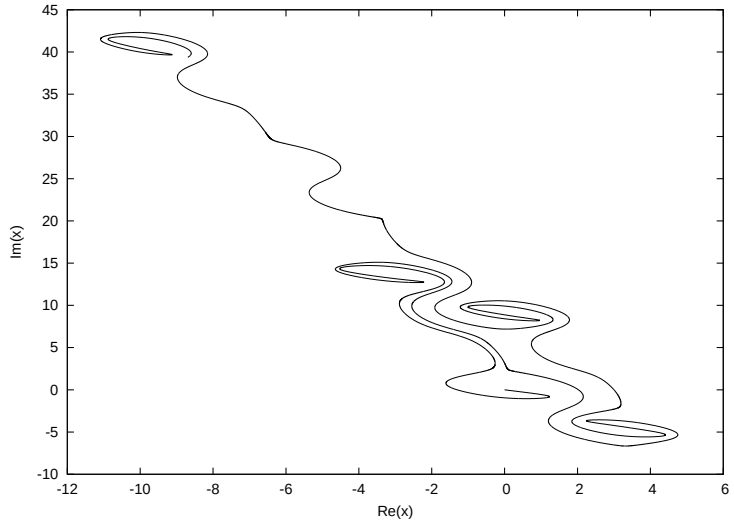

(a) $m = 0.2$

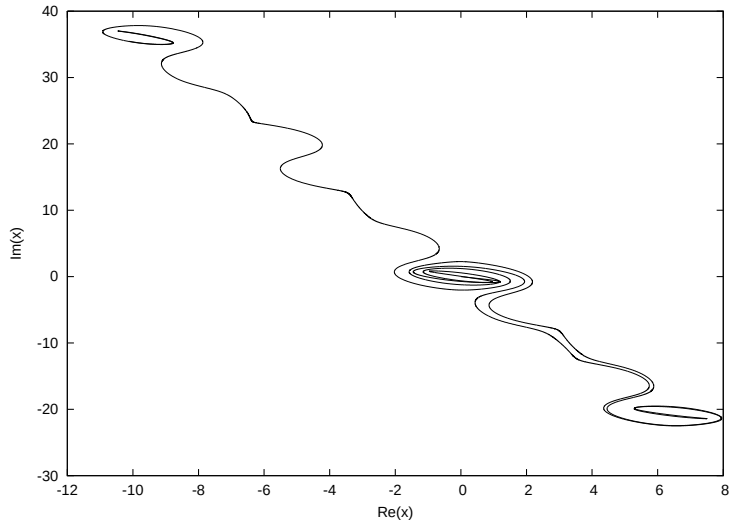

(b) $m = 0.1$

Figure 41: Trajectories for $E = -0.5 - 0.75i$ starting from $x = 0$. This is one case where the particle leaves the diagonal for a higher value of the elliptic parameter m.

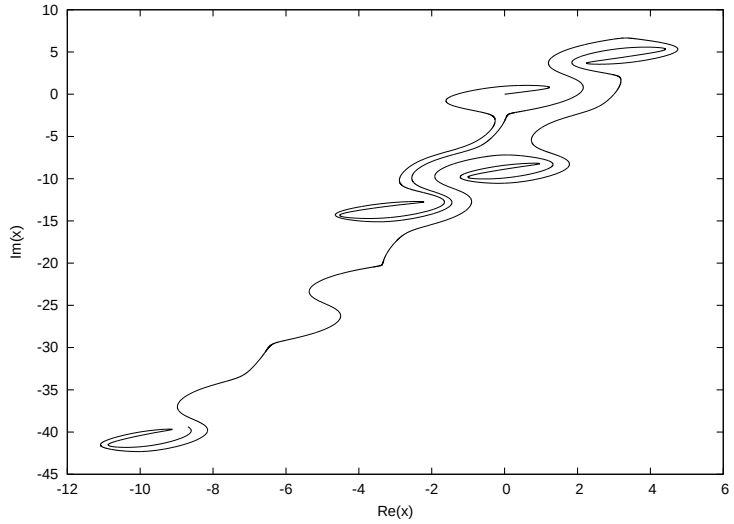

(a) $m = 0.2$

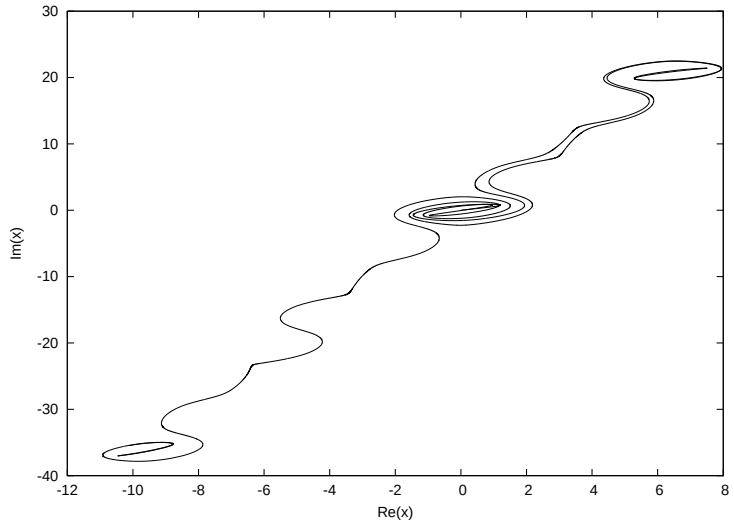

(b) $m = 0.1$

Figure 42: Trajectories for $E = -0.5+0.75i$ starting from $x = 0$. As in *figure 41*, another example where the particle appears to move off the diagonal more readily for a higher value of m.

figures *figures 28* and *30* respectively. However, such a conjecture is only tentative for now since much more data would need to be analyzed before a conclusion can be met at since, for one thing, some counter examples exist where hops off the diagonal occur for $m = 0.1$ and not for $m = 0.2$: see *figure 43* for one such example. Furthermore, these comparisons of plots of equal energies are not sufficient for any conclusion to be drawn since different values of the elliptic parameter would necessarily describe different systems. Thus, what is really required is an analysis of trajectories for a close range of energies across many elliptic parameter values, which was unfortunately not achievable here due to the prohibitive times that such an analysis would consume; but, the speculation that the elliptic parameter m might affect hops off the diagonal is certainly another area worth investigating.

5.2.2 Localized Behaviour

Another interesting behaviour that the particle undergoes is for energies where the imaginary component is close to zero. An example of such a trajectory is shown in *figure 44* for energy $E = 0.75 + 0.01i$ and elliptic parameter $m = 0.1$. Here, a particle that starts at $x = 0$ continues to spiral about its initial position never hopping to another site — the particle appears to remain "localized" but with a trajectory that is *not* closed. The particle trajectory crosses itself and, again, calculations of the energy of the particle do see it stray from its expected value. More detailed runs are required, but it is interesting to speculate that the particle may be moving on different sheets of the Riemann surface and whether it does so indefinitely on the infinitely-sheeted surface. Alternatively, it may be, however, that the

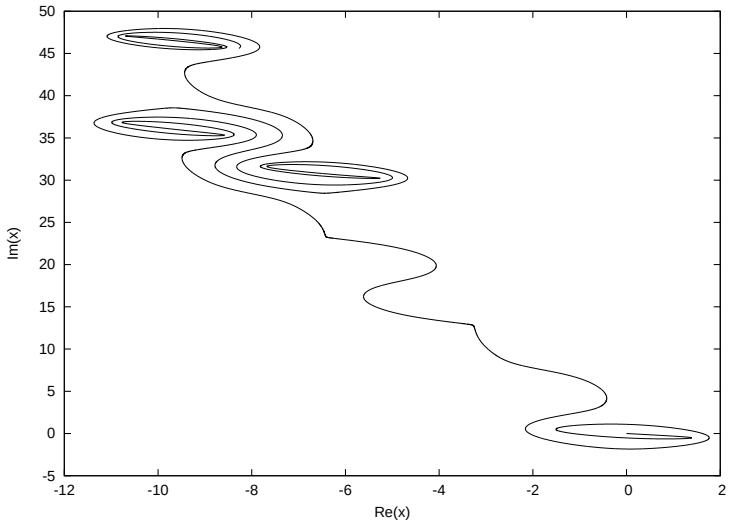

(a) $m = 0.1$

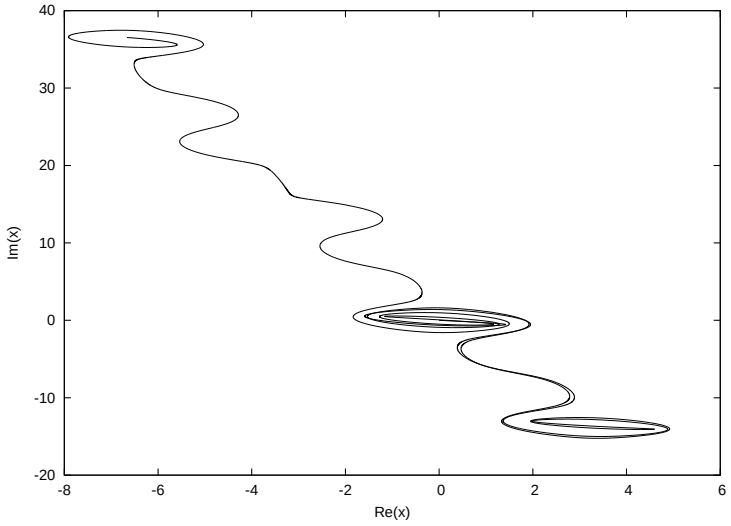

(b) $m = 0.2$

Figure 43: Trajectories for $E = -0.25 - 0.5i$ starting from $x = 0$. This is a counter-example to *figures 41* and *42* where the particle jumps off the diagonal at $m = 0.1$. This is only indicative of the more extensive study of the particle trajectories that is required before conclusions on the propensity for the particle to jump of the diagonal for higher values of m can be made.

particle is simply spiralling many times before it would eventually hop to another site. Such an alternative hypothesis would still agree with the idea that the particle is loath to tunnel from one site to another when the energies are close to being purely real.

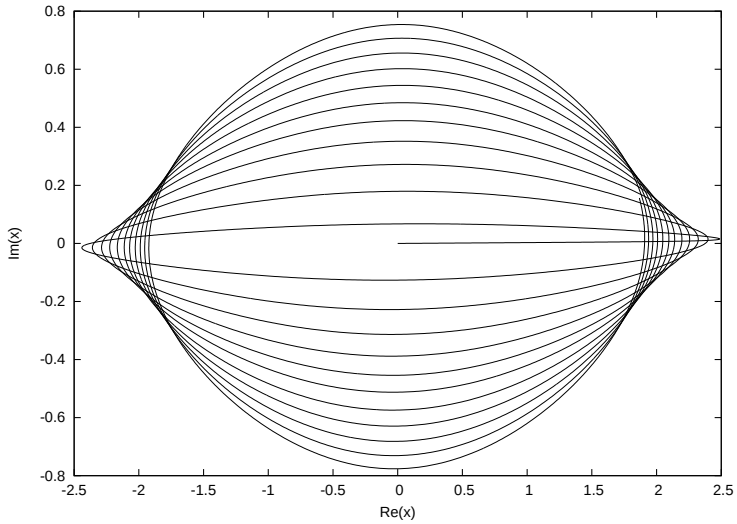

Figure 44: Classical trajectory in the complex-x plane for $E = 0.75 + 0.01i$, $m = 0.1$ and an initial displacement $x = 0$. Here the particle displays "localized" behaviour: the particle spirals many times about its initial site. The particle trajectory crosses itself, and more detailed runs are required in order to tell whether the particle stays spiralling about this one site moving indefinitely on the infinitely-sheeted Riemann surface, or whether the particle will eventually move off to another site. In any case, the particle still spirals many times about its initial site, indicating some willingness to remain where it is: the small value of the imaginary-component of the energy indicates some a difficulty that the particle shows in being able to tunnel to another site.

In any case, this same behaviour occurs across several values of the real-component of the complex energy, but with an interesting pattern: the trajectories begin to slant from bottom-left to top-right — the same orientation of the diagonal that the hops move along when the imaginary component of the energy is positive — as the *real component of the energy decreases*

with the imaginary component of the energy kept small and *positive*. For comparison to *figure 44* the trajectories for $E = -0.75 + 0.01i$ in shown in *figure 45* and for $E = -0.99 + 0.01i$ in *figure 46* (all for elliptic parameter $m = 0.1$ and initial displacements at $x = 0$).

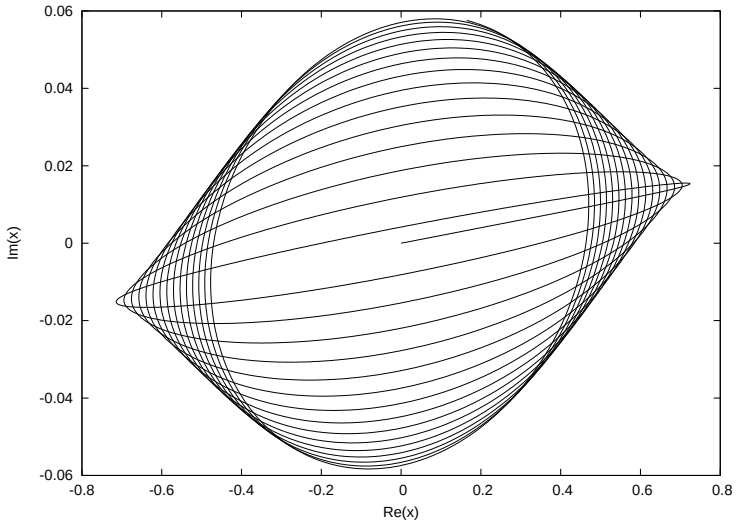

Figure 45: Classical trajectory for $E = -0.75 + 0.01i$, $m = 0.1$, and an initial displacement $x = 0$. As in *figure 44*, the particle displays "localized" behaviour. However, the decrease in the real-component of the energy causes the trajectory to slant along the diagonal that is orientated in the same way that the positive imaginary-component of the energy causes hops to occur in *figure 31*, for example.

The particle trajectory for a small *negative* imaginary component of the energy similarly slants from top-left to bottom-right as the energy is decreased, and the system with $E = -0.99 - 0.01i$ with $m = 0.1$ starting from $x = 0$ is shown in *figure 47*.

We note that the limit of energies where the imaginary component tends to zero is clearly a purely real energy. Thus, again, it is wondered whether the open trajectories found in *figures 28* and *30* have any bearing on the

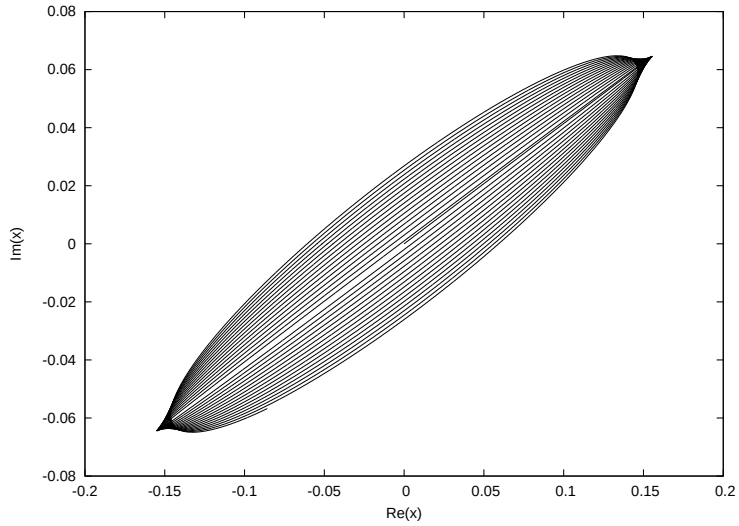

Figure 46: Classical trajectory for $E = -0.99 + 0.01i$, $m = 0.1$, and initial displacement $x = 0$. Again, we see that as the real-component of the energy decreases the particle slant becomes more pronounced.

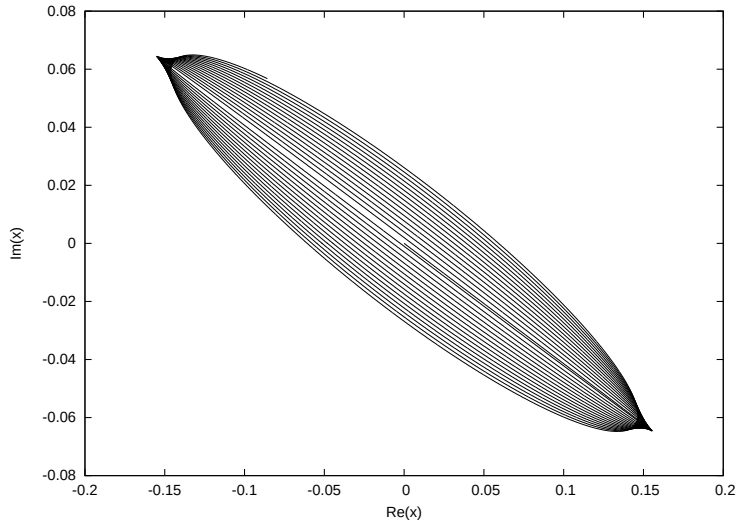

Figure 47: Classical trajectory for $E = -0.99 - 0.01i$, $m = 0.1$, and initial displacement $x = 0$. Compare to *figure 46*, where the swap in the sign of the imaginary-component of the energy causes the particle directory to slant in the opposite direction.

diagonal directions being expressed by *figures 46* and *47*.

This was not the only relationship observed with the decrease of the real component of the energy: the range of values of the imaginary component for which this "localized" behaviour of the trajectory occurs increases as the real component of the energy decreases. For example (all trajectories are with $m = 0.1$, but the qualitative results are similar for $m = 0.2$), for $E = -0.75 + 0.1i$ the particle trajectory still appears localized (see *figure 48*), but for $E = -0.1 + 0.1i$ shown in *figure 49* the particle moves in many spirals about its initial position before eventually moving off. The times are all run up to $t = 100$ in these graphs, and when we look at $E = 0.25 + 0.1i$ in *figure 50* the particle has spent less time spiralling about its initial position before moving on: the particle spirals five times in *figure 50* as opposed to nine times in *figure 49*. As we move to $E = 0.75 + 0.1i$ the particle hardly spends any time spiralling before moving to another site: see *figure 51*. This may be evidence that the particle may not be truly "localized" at all, but simply that it spirals many times before moving on. Again, only more accurate runs up to longer times will confirm this or not.

The trajectories in *figures 49* and *50* are also interesting because they seem to indicate that the particle moves some distance before spiralling many times again. This behaviour is seen across all the real components of the energy examined where the imaginary component has strayed just enough from zero to lose its "localized" behaviour: for example, *figure 52* shows the trajectory for $E = -0.25 + 0.25i$ (with $m = 0.1$ and an initial displacement at $x = 0$). It is striking that the trajectories of *figures 50* and *50* look so similar, and it is worth further investigation to see if, for longer times and more accurate

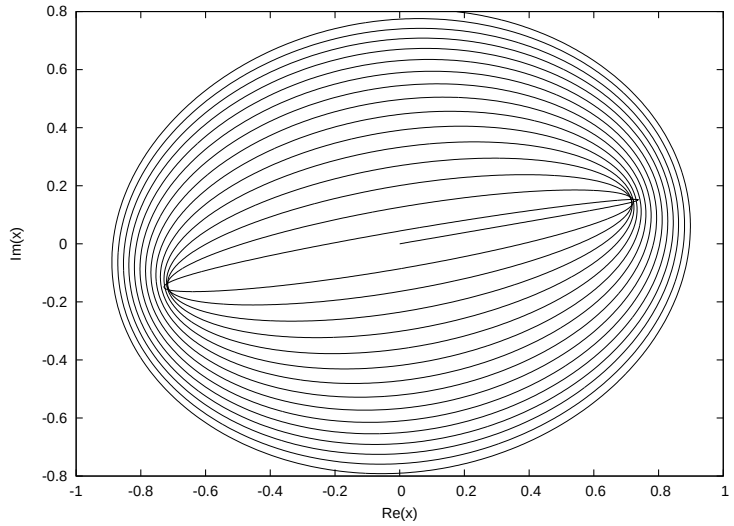

Figure 48: Classical trajectory for $E = -0.75 + 0.1i$, $m = 0.1$, and initial displacement $x = 0$. For low values of the real-component of the energy the particle still displays "localized" behaviour away from small values of the imaginary-component of the energy. Compare this with *figures 49–51* where, as the imaginary-component is kept fixed, the real-component is increased, leading to the particle to take many less spirals about its initial site.

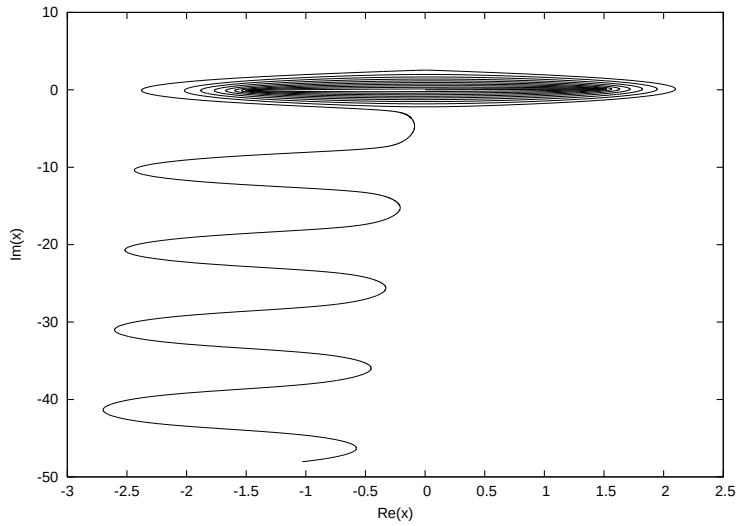

Figure 49: Classical trajectory for $E = -0.1 + 0.1i$, $m = 0.1$, and initial displacement $x = 0$. Here the particle still spirals many times about its initial site — about nine times — before tunnelling to adjacent sites.

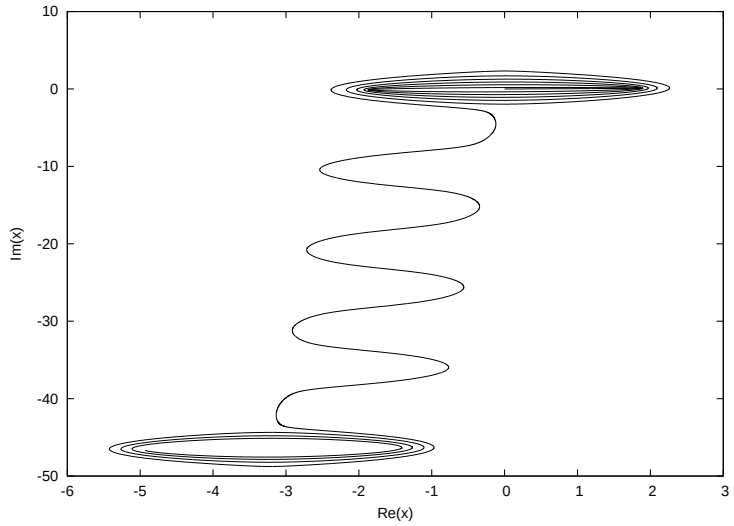

Figure 50: Classical trajectory for $E = 0.25 + 0.1i$, $m = 0.1$, and initial displacement $x = 0$. Compared to *figure 49*, the particle spirals less about its initial site — only five times now — before moving to another site.

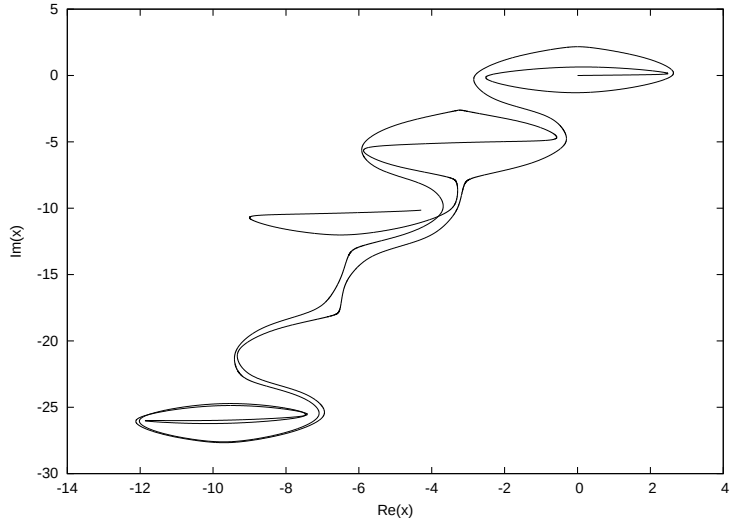

Figure 51: Classical trajectory for $E = 0.75 + 0.1i$, $m = 0.1$, and initial displacement $x = 0$. Compared to *figures 48–50*, the particle is now no longer disposed to spiral about any one site.

runs, whether the particle moves to other sites or not.

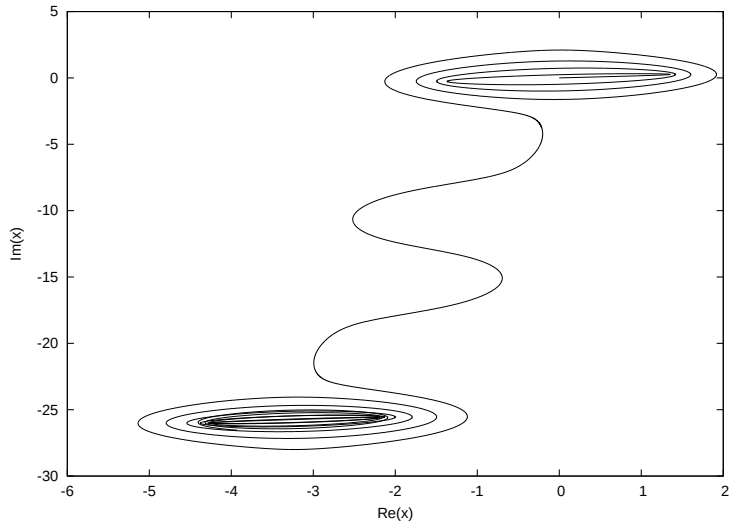

Figure 52: Classical trajectory for $E = -0.25 + 0.25i$, $m = 0.1$, and initial displacement $x = 0$. Again, we see that the particle spends much time spiralling between its initial site and another one that it tunnels to. The interesting question posed by such particle trajectories is whether the particle ever moves to other sites, and why they always look so strikingly similar.

5.2.3 Delocalized Behaviour

As for the cosine potential, energies were found for which the particle only ever moves in one direction. The energies appear at relatively diverse energies: *figure 53* is for $E = -0.25 - 0.25i$ and $m = 0.2$, *figure 54* is for $E = 0.1 - 0.75i$ and $m = 0.2$, and *figure 55* is for $E = 0.7 + 0.25i$ and $m = 0.1$ (all the *figures 53–55* run up to $t = 100$ with the particle initially at $x = 0$).

To check to see if there existed bands for which the particle behaves as if it were delocalized an energy was chosen close to the one in *figure 55*, and also ran for a longer time in order to verify that the particle was behaving as if it were delocalized. In *figure 56* the trajectory for a particle with energy $E = 0.697 + 0.25i$ is shown for $m = 0.1$ with an initial displacement at $x = 0$.

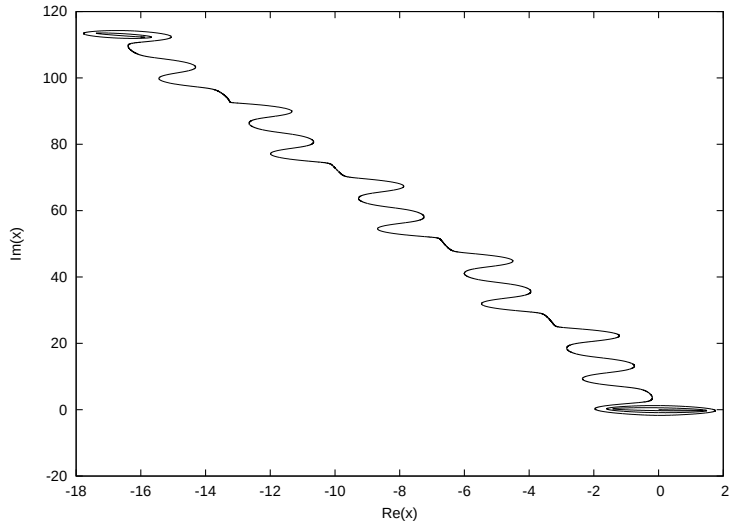

Figure 53: Classical trajectory for $E = -0.25 - 0.25i$, $m = 0.2$, and initial displacement $x = 0$. As for the cosine potential, the particle appears to behave as if it were delocalized, and only ever moves in one direction.

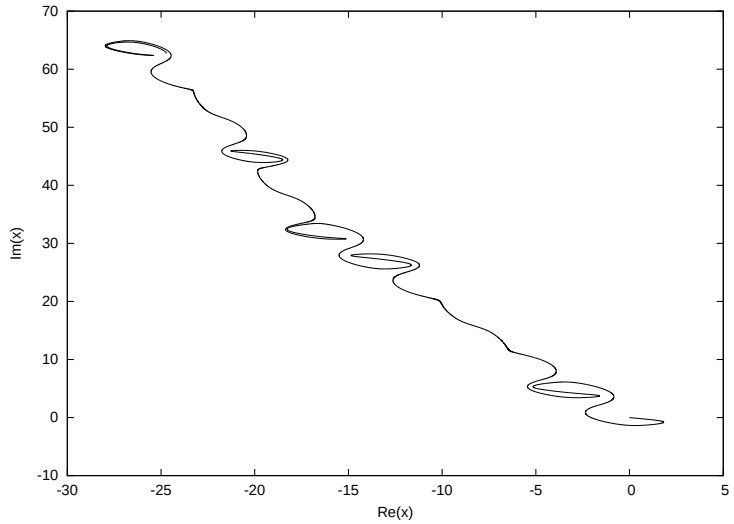

Figure 54: Another example of delocalized behaviour, this time for energy $E = 0.1 - 0.75i$, $m = 0.2$, and initial displacement $x = 0$.

The particle moves a considerable distance before turning back on itself right at the end for the first time: *figure 57* shows this more clearly. The energy of the particle in *figure 57* was checked and it does begin to diverge from its

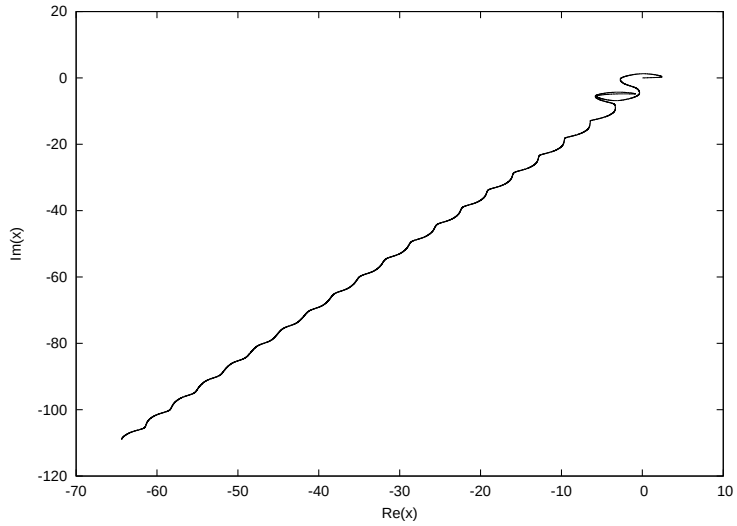

Figure 55: A further example of delocalized, this time for energy $E = 0.7 + 0.25i$, $m = 0.1$, and initial displacement $x = 0$. Compared to the values of the energies in *figures 53* and *54*, the results seems to indicate that delocalized behaviour is occurring at different regions of the complex-E range.

expected value of $E = 0.697 + 0.25i$, and so the fact that it turns back on itself it probably due to an iterative inaccuracy of the trajectory.

Just as with the cosine potential, the presence of delocalized particles in a complex *classical* system represents an extraordinary replication of quantum phenomena. However, the propensity for the trajectories to lose accuracy means that detailed runs are required in order to locate any conduction bands.

6 Conclusion

The analysis of classical complex systems with an elliptic potential hints at behaviour that is not only richer than for a cosine potential, but also more intriguing in its peculiarities. Although we stress, here, that the analysis

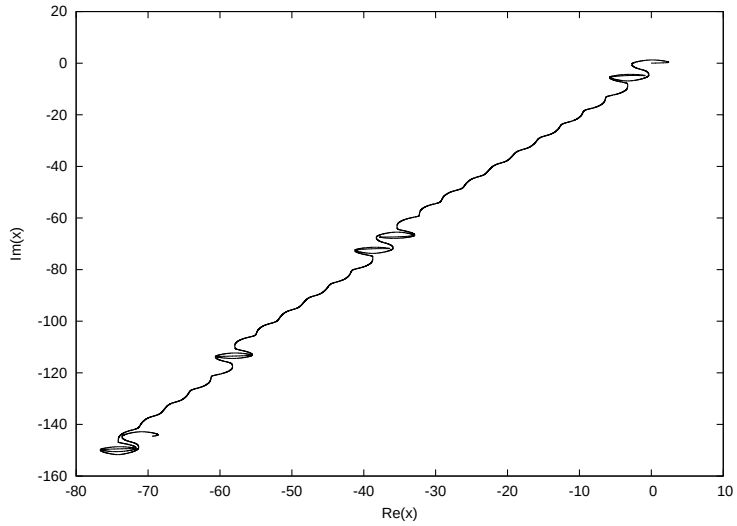

Figure 56: This the particle trajectory for energy $E = 0.697 + 0.25i$, $m = 0.1$, and initial displacement $x = 0$. As an energy close to that of *figure 55*, we see that there exist conduction bands as with the cosine potential. The trajectory does turn back on itself right at the end (see *figure 57* for a close-up), but this may be due to iterative inaccuracies since the particle's energy does begin to deviate, especially for longer times.

presented here has been constrained by time and that the runs begin to lose accuracy, it is hoped that some of the basic qualitative behaviour of the system that has been seen is enough to warrant further work.

It is a remarkable consequence of classical systems extended into the complex domain that they can reproduce what is regarded as inherently quantum behaviour. This remarkable idea of how to view classical systems, based on the work done to make $\mathcal{PT}$-symmetric Hamiltonians acceptable within a quantum framework, may provide a deeper understanding of quantum phenomena than that of the current quantum theory, and only makes the need to further study $\mathcal{PT}$-symmetric Hamiltonians more important.

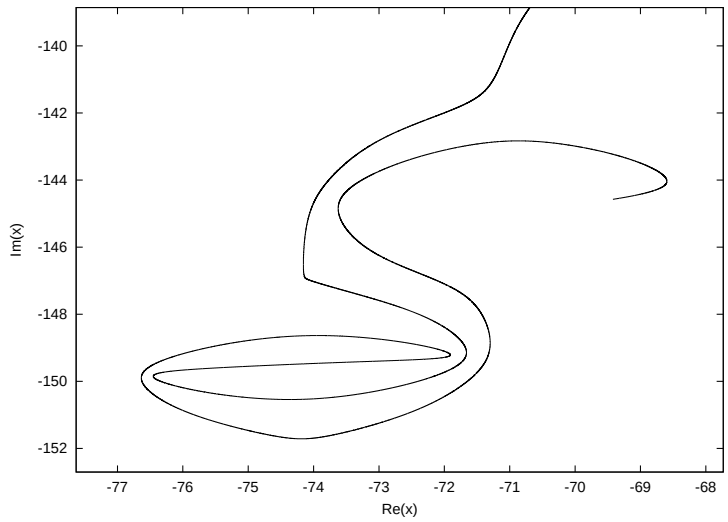

Figure 57: A close-up of the particle moving back on itself in *figure 56*. More accurate runs need to be made in order to locate conduction bands especially, since any loss in the accuracy of the particle trajectory could take it out of the conduction band energy range.

Appendices

A Source Code

The C++ source code that generated the plots in *section 5* is given here. Since it uses GNU code, it is released under the terms of the GNU General Public License version 3 or higher.

```
#include <stdio.h>
#include <iostream>
#include <string>
#include <sstream>
#include <cmath>
#include <cfloat>
#include <gmp.h>
#include <mpfr.h>
#include <mathlink.h>
using namespace std;

int evolve_apply(mpfr_t t, const mpfr_t t1, mpfr_t h, mpfr_t y[]);
```

```
int h_adjust(const mpfr_t y[], mpfr_t h);
int rk8pd_apply(mpfr_t h, mpfr_t y[]);
int func (const mpfr_t p[], mpfr_t f[]);
int init_mathlink(void);
MLEnvironment mlenv;
MLINK mlink;
int read_input(const int argc, const char* const argv[]);

//%%%%%%%%%%%%%%%%%%%%%%%%%%%%%%%%%%%%%%%%%%%%%%%%%%%%%%%%%%%%%%%%%%%%%%%%%%%%%%%
#define MPFR_PRECISION 64
#define OUTPUT_PRECISION 15
#define MATHEMATICA_PRECISION "15"
#define ABS_STEP_ERROR "1.0e-6" // allowed absolute error
#define REL_STEP_ERROR "1.0e-6" // allowed relative error
#define START_STEP_SIZE "1.0e-6" // starting step size

#ifndef END_TIME
#  define END_TIME "100.0"
#endif
#ifndef END_TIME_STEP
#  define END_TIME_STEP "100.0"
#endif
#ifndef M_PARAM
#  define M_PARAM "0.5"
#endif
#define INIT_X_R "2.0"
#define INIT_X_I "0.0"
#ifndef ENERGY
#  define ENERGY "0.0"
#endif

//%%%%%%%%%%%%%%%%%%%%%%%%%%%%%%%%%%%%%%%%%%%%%%%%%%%%%%%%%%%%%%%%%%%%%%%%%%%%%%%

class inits_t {
public:
  string end_time;
  string end_time_step;
  string init_x_r;
  string init_x_i;
  string energy;
  string param;

  inits_t(const char* const et, const char* const ets,
```

```
      const char* const ixr, const char* const ixi,
      const char* const nrg, const char* const m) :
    end_time(et),
    end_time_step(ets),
    init_x_r(ixr),
    init_x_i(ixi),
    energy(nrg),
    param(m)
  {}
  ~inits_t(void) {}
} inits(END_TIME,END_TIME_STEP,INIT_X_R,INIT_X_I,ENERGY,M_PARAM);

class temps_t {
public:
  mpfr_t t1;
  mpfr_t t2;

  temps_t(void) {
    mpfr_init2(t1,MPFR_PRECISION);
    mpfr_init2(t2,MPFR_PRECISION);
  }
  ~temps_t(void) {
    mpfr_clear(t1);
    mpfr_clear(t2);
  }
} temp;


//%%%%%%%%%%%%%%%%%%%%%%%%%%%%%%%%%%%%%%%%%%%%%%%%%%%%%%%%%%%%%%%%%%%%%%%%%%%%
int func (const mpfr_t y[], mpfr_t f[]) {

  mpfr_set(f[0],y[2],GMP_RNDN);
  mpfr_set(f[1],y[3],GMP_RNDN);


  char* c_str = 0;
  mp_exp_t exp = 0;
  c_str = mpfr_get_str(0,&exp,10,0,y[0],GMP_RNDN);
  if(!c_str) {
    cerr << "error getting mpfr value.\n";
    return 1;
  }
  string y0_str = c_str;
```

```
mpfr_free_str(c_str);
bool negative = false;
if ( y0_str[0]=='-' ) {
  y0_str.erase(0,1);
  negative = true;
}
if (exp > 0) {
  y0_str.insert(exp,".");
}
else {
  y0_str.insert(0,static_cast<size_t>(-exp),'0');
  y0_str = "0." + y0_str;
}
if(negative) y0_str = "-" + y0_str;

c_str = mpfr_get_str(0,&exp,10,0,y[1],GMP_RNDN);
if(!c_str) {
  cerr << "error getting mpfr value.\n";
  return 1;
}
string y1_str = c_str;
mpfr_free_str(c_str);
if ( y1_str[0]=='-' ) {
  y1_str.erase(0,1);
  negative = true;
}
else negative = false;
if (exp > 0) {
  y1_str.insert(exp,".");
}
else {
  y1_str.insert(0,static_cast<size_t>(-exp),'0');
  y1_str = "0." + y1_str;
}
if(negative) y1_str = "-" + y1_str;

string mathlink_string = "SetPrecision[ Chop [ -JacobiSN[ "
  + y0_str + " + " + y1_str + " I , " + inits.param
  + " ] JacobiDN[ " + y0_str + " + " + y1_str
  + " I , " + inits.param + " ] ] , "
  + MATHEMATICA_PRECISION + "]";

MLPutFunction(mlink, "EvaluatePacket", 1);
```

```
    MLPutFunction(mlink, "ToString", 1);
      MLPutFunction(mlink, "ToExpression", 1);
      MLPutString(mlink,mathlink_string.c_str());
  MLEndPacket(mlink);

  int pkt = 0;
  while( (pkt = MLNextPacket(mlink), pkt) && pkt != RETURNPKT )
    MLNewPacket(mlink);
    // if MathLink encounters an error, then it will return 0 and the
    // 'while' loop will evaluate (false && true) -- false since
    // (pkt=..., pkt) evaluates pkt, which is equal to 0 (i.e. false);
    // and true since pkt!=RETURNPKT is true.
  if(!pkt) { // pkt = 0 ==> some MathLink error occurred.
    cerr << "error: some mathlink error.\n";
    return 1;
  }


  const char* str;
  MLGetString(mlink,&str);
  string answer = str;
  size_t i_pos = answer.find('I');
  if ( i_pos == string::npos ) {
    mpfr_set_str(f[2],str,10,GMP_RNDN);
    mpfr_set_str(f[3],"0.0",10,GMP_RNDN);
  }
  else {
    size_t split = answer.find_first_of("-+",1);
    if ( split == string::npos ) {
      mpfr_set_str(f[2],"0.0",10,GMP_RNDN);
      mpfr_set_str(f[3],answer.substr(0U,i_pos-1U).c_str(),10,GMP_RNDN);
    }
    else {
      mpfr_set_str(f[2], (answer.substr(0U,split)).c_str(),10,GMP_RNDN);
      string imag = answer.substr( split, answer.length()-split-1U );
      imag.erase(1,1);
      mpfr_set_str(f[3],imag.c_str(),10,GMP_RNDN);
    }
  }
  MLDisownString(mlink,str);

#ifdef DIAG
  print("y[0]",y[0]);
```

```
  print("y[1]",y[1]);
  print("y[2]",y[2]);
  print("y[3]",y[3]);
  print("f[0]",f[0]);
  print("f[1]",f[1]);
  print("f[2]",f[2]);
  print("f[3]",f[3]);
#endif

  return 0;
}

//%%%%%%%%%%%%%%%%%%%%%%%%%%%%%%%%%%%%%%%%%%%%%%%%%%%%%%%%%%%%%%%%%%%%%%%%%%%%


class step_t {
public:
  mpfr_t k[13][4];
  mpfr_t ytmp[4];

  step_t(void) {
    for(unsigned short i=0U ; i<13U ; i++) {
      for(unsigned short j=0U ; j<4U ; j++) {
        mpfr_init2(k[i][j],MPFR_PRECISION);
      }
    }
    for(unsigned short i=0U ; i<4U ; i++) {
      mpfr_init2(ytmp[i],MPFR_PRECISION);
    }
  }
  ~step_t(void) {
    for(unsigned short i=0U ; i<13U ; i++) {
      for(unsigned short j=0U ; j<4U ; j++) {
        mpfr_clear(k[i][j]);
      }
    }
    for(unsigned short i=0U ; i<4U ; i++) {
      mpfr_clear(ytmp[i]);
    }
  }
} step;

class control_t {
```

```
public:
  mpfr_t eps_abs;
  mpfr_t eps_rel;

  control_t(const char* abs, const char* rel) {
    mpfr_init2(eps_abs,MPFR_PRECISION);
    mpfr_init2(eps_rel,MPFR_PRECISION);
    mpfr_set_str(eps_abs,abs,10,GMP_RNDN);
    mpfr_set_str(eps_rel,rel,10,GMP_RNDN);
  }
  ~control_t(void) {
    mpfr_clear(eps_abs);
    mpfr_clear(eps_rel);
  }
} control(ABS_STEP_ERROR,REL_STEP_ERROR);

class evolve_t {
public:
  mpfr_t y0[4];
  mpfr_t yerr[4];
  mpfr_t dydt_in[4];
  mpfr_t last_step;
  unsigned long int count;
  unsigned long int failed_steps;

  evolve_t(void) : count(0UL), failed_steps(0UL) {
    for(unsigned short i=0U ; i<4U ; i++) {
      mpfr_init2(y0[i],MPFR_PRECISION);
      mpfr_init2(yerr[i],MPFR_PRECISION);
      mpfr_init2(dydt_in[i],MPFR_PRECISION);
    }
    mpfr_init2(last_step,MPFR_PRECISION);
  }
  ~evolve_t(void) {
    for(unsigned short i=0U ; i<4U ; i++) {
      mpfr_clear(y0[i]);
      mpfr_clear(yerr[i]);
      mpfr_clear(dydt_in[i]);
    }
    mpfr_clear(last_step);
  }
} evolve;
```

```
class rkvars_t {
public:
  mpfr_t Abar[13];
  mpfr_t A[12];
  mpfr_t ah[10];
  mpfr_t b21;
  mpfr_t b3[2];
  mpfr_t b4[3];
  mpfr_t b5[4];
  mpfr_t b6[5];
  mpfr_t b7[6];
  mpfr_t b8[7];
  mpfr_t b9[8];
  mpfr_t b10[9];
  mpfr_t b11[10];
  mpfr_t b12[11];
  mpfr_t b13[12];

  rkvars_t(void) {
    for(unsigned short i=0U ; i<13U ; i++)
      mpfr_init2(Abar[i],MPFR_PRECISION);
    for(unsigned short i=0U ; i<12U ; i++) {
      mpfr_init2(A[i],MPFR_PRECISION);
      mpfr_init2(b13[i],MPFR_PRECISION);
    }
    for(unsigned short i=0U ; i<11U ; i++)
      mpfr_init2(b12[i],MPFR_PRECISION);
    for(unsigned short i=0U ; i<10U ; i++) {
      mpfr_init2(ah[i],MPFR_PRECISION);
      mpfr_init2(b11[i],MPFR_PRECISION);
    }
    for(unsigned short i=0U ; i<9U ; i++)
      mpfr_init2(b10[i],MPFR_PRECISION);
    for(unsigned short i=0U ; i<8U ; i++)
      mpfr_init2(b9[i],MPFR_PRECISION);
    for(unsigned short i=0U ; i<7U ; i++)
      mpfr_init2(b8[i],MPFR_PRECISION);
    for(unsigned short i=0U ; i<6U ; i++)
      mpfr_init2(b7[i],MPFR_PRECISION);
    for(unsigned short i=0U ; i<5U ; i++)
      mpfr_init2(b6[i],MPFR_PRECISION);
    for(unsigned short i=0U ; i<4U ; i++)
      mpfr_init2(b5[i],MPFR_PRECISION);
```

```
for(unsigned short i=0U ; i<3U ; i++)
  mpfr_init2(b4[i],MPFR_PRECISION);
for(unsigned short i=0U ; i<2U ; i++)
  mpfr_init2(b3[i],MPFR_PRECISION);
mpfr_init2(b21,MPFR_PRECISION);
// now, let's set them...
mpfr_set_str(temp.t1,"14005451.0",10,GMP_RNDN);
mpfr_set_str(temp.t2,"335480064.0",10,GMP_RNDN);
mpfr_div(Abar[0],temp.t1,temp.t2,GMP_RNDN);
mpfr_set_str(Abar[1],"0.0",10,GMP_RNDN);
mpfr_set_str(Abar[2],"0.0",10,GMP_RNDN);
mpfr_set_str(Abar[3],"0.0",10,GMP_RNDN);
mpfr_set_str(Abar[4],"0.0",10,GMP_RNDN);
mpfr_set_str(temp.t1,"-59238493.0",10,GMP_RNDN);
mpfr_set_str(temp.t2,"1068277825.0",10,GMP_RNDN);
mpfr_div(Abar[5],temp.t1,temp.t2,GMP_RNDN);
mpfr_set_str(temp.t1,"181606767.0",10,GMP_RNDN);
mpfr_set_str(temp.t2,"758867731.0",10,GMP_RNDN);
mpfr_div(Abar[6],temp.t1,temp.t2,GMP_RNDN);
mpfr_set_str(temp.t1,"561292985.0",10,GMP_RNDN);
mpfr_set_str(temp.t2,"797845732.0",10,GMP_RNDN);
mpfr_div(Abar[7],temp.t1,temp.t2,GMP_RNDN);
mpfr_set_str(temp.t1,"-1041891430.0",10,GMP_RNDN);
mpfr_set_str(temp.t2,"1371343529.0",10,GMP_RNDN);
mpfr_div(Abar[8],temp.t1,temp.t2,GMP_RNDN);
mpfr_set_str(temp.t1,"760417239.0",10,GMP_RNDN);
mpfr_set_str(temp.t2,"1151165299.0",10,GMP_RNDN);
mpfr_div(Abar[9],temp.t1,temp.t2,GMP_RNDN);
mpfr_set_str(temp.t1,"118820643.0",10,GMP_RNDN);
mpfr_set_str(temp.t2,"751138087.0",10,GMP_RNDN);
mpfr_div(Abar[10],temp.t1,temp.t2,GMP_RNDN);
mpfr_set_str(temp.t1,"-528747749.0",10,GMP_RNDN);
mpfr_set_str(temp.t2,"2220607170.0",10,GMP_RNDN);
mpfr_div(Abar[11],temp.t1,temp.t2,GMP_RNDN);
mpfr_set_str(Abar[12],"0.25",10,GMP_RNDN);
mpfr_set_str(temp.t1,"13451932.0",10,GMP_RNDN);
mpfr_set_str(temp.t2,"455176623.0",10,GMP_RNDN);
mpfr_div(A[0],temp.t1,temp.t2,GMP_RNDN);
mpfr_set_str(A[1],"0.0",10,GMP_RNDN);
mpfr_set_str(A[2],"0.0",10,GMP_RNDN);
mpfr_set_str(A[3],"0.0",10,GMP_RNDN);
mpfr_set_str(A[4],"0.0",10,GMP_RNDN);
mpfr_set_str(temp.t1,"-808719846.0",10,GMP_RNDN);
```

```
mpfr_set_str(temp.t2,"976000145.0",10,GMP_RNDN);
mpfr_div(A[5],temp.t1,temp.t2,GMP_RNDN);
mpfr_set_str(temp.t1,"1757004468.0",10,GMP_RNDN);
mpfr_set_str(temp.t2,"5645159321.0",10,GMP_RNDN);
mpfr_div(A[6],temp.t1,temp.t2,GMP_RNDN);
mpfr_set_str(temp.t1,"656045339.0",10,GMP_RNDN);
mpfr_set_str(temp.t2,"265891186.0",10,GMP_RNDN);
mpfr_div(A[7],temp.t1,temp.t2,GMP_RNDN);
mpfr_set_str(temp.t1,"-3867574721.0",10,GMP_RNDN);
mpfr_set_str(temp.t2,"1518517206.0",10,GMP_RNDN);
mpfr_div(A[8],temp.t1,temp.t2,GMP_RNDN);
mpfr_set_str(temp.t1,"465885868.0",10,GMP_RNDN);
mpfr_set_str(temp.t2,"322736535.0",10,GMP_RNDN);
mpfr_div(A[9],temp.t1,temp.t2,GMP_RNDN);
mpfr_set_str(temp.t1,"53011238.0",10,GMP_RNDN);
mpfr_set_str(temp.t2,"667516719.0",10,GMP_RNDN);
mpfr_div(A[10],temp.t1,temp.t2,GMP_RNDN);
mpfr_set_str(temp.t1,"2.0",10,GMP_RNDN);
mpfr_set_str(temp.t2,"45.0",10,GMP_RNDN);
mpfr_div(A[11],temp.t1,temp.t2,GMP_RNDN);
mpfr_set_str(temp.t1,"1.0",10,GMP_RNDN);
mpfr_set_str(temp.t2,"18.0",10,GMP_RNDN);
mpfr_div(ah[0],temp.t1,temp.t2,GMP_RNDN);
mpfr_set_str(temp.t1,"1.0",10,GMP_RNDN);
mpfr_set_str(temp.t2,"12.0",10,GMP_RNDN);
mpfr_div(ah[1],temp.t1,temp.t2,GMP_RNDN);
mpfr_set_str(temp.t1,"1.0",10,GMP_RNDN);
mpfr_set_str(temp.t2,"8.0",10,GMP_RNDN);
mpfr_div(ah[2],temp.t1,temp.t2,GMP_RNDN);
mpfr_set_str(temp.t1,"5.0",10,GMP_RNDN);
mpfr_set_str(temp.t2,"16.0",10,GMP_RNDN);
mpfr_div(ah[3],temp.t1,temp.t2,GMP_RNDN);
mpfr_set_str(temp.t1,"3.0",10,GMP_RNDN);
mpfr_set_str(temp.t2,"8.0",10,GMP_RNDN);
mpfr_div(ah[4],temp.t1,temp.t2,GMP_RNDN);
mpfr_set_str(temp.t1,"59.0",10,GMP_RNDN);
mpfr_set_str(temp.t2,"400.0",10,GMP_RNDN);
mpfr_div(ah[5],temp.t1,temp.t2,GMP_RNDN);
mpfr_set_str(temp.t1,"93.0",10,GMP_RNDN);
mpfr_set_str(temp.t2,"200.0",10,GMP_RNDN);
mpfr_div(ah[6],temp.t1,temp.t2,GMP_RNDN);
mpfr_set_str(temp.t1,"5490023248.0",10,GMP_RNDN);
mpfr_set_str(temp.t2,"9719169821.0",10,GMP_RNDN);
```

```
mpfr_div(ah[7],temp.t1,temp.t2,GMP_RNDN);
mpfr_set_str(temp.t1,"13.0",10,GMP_RNDN);
mpfr_set_str(temp.t2,"20.0",10,GMP_RNDN);
mpfr_div(ah[8],temp.t1,temp.t2,GMP_RNDN);
mpfr_set_str(temp.t1,"1201146811.0",10,GMP_RNDN);
mpfr_set_str(temp.t2,"1299019798.0",10,GMP_RNDN);
mpfr_div(ah[9],temp.t1,temp.t2,GMP_RNDN);
mpfr_set_str(temp.t1,"1.0",10,GMP_RNDN);
mpfr_set_str(temp.t2,"18.0",10,GMP_RNDN);
mpfr_div(b21,temp.t1,temp.t2,GMP_RNDN);
mpfr_set_str(temp.t1,"1.0",10,GMP_RNDN);
mpfr_set_str(temp.t2,"48.0",10,GMP_RNDN);
mpfr_div(b3[0],temp.t1,temp.t2,GMP_RNDN);
mpfr_set_str(temp.t1,"1.0",10,GMP_RNDN);
mpfr_set_str(temp.t2,"16.0",10,GMP_RNDN);
mpfr_div(b3[1],temp.t1,temp.t2,GMP_RNDN);
mpfr_set_str(temp.t1,"1.0",10,GMP_RNDN);
mpfr_set_str(temp.t2,"32.0",10,GMP_RNDN);
mpfr_div(b4[0],temp.t1,temp.t2,GMP_RNDN);
mpfr_set_str(b4[1],"0.0",10,GMP_RNDN);
mpfr_set_str(temp.t1,"3.0",10,GMP_RNDN);
mpfr_set_str(temp.t2,"32.0",10,GMP_RNDN);
mpfr_div(b4[2],temp.t1,temp.t2,GMP_RNDN);
mpfr_set_str(temp.t1,"5.0",10,GMP_RNDN);
mpfr_set_str(temp.t2,"16.0",10,GMP_RNDN);
mpfr_div(b5[0],temp.t1,temp.t2,GMP_RNDN);
mpfr_set_str(b5[1],"0.0",10,GMP_RNDN);
mpfr_set_str(temp.t1,"-75.0",10,GMP_RNDN);
mpfr_set_str(temp.t2,"64.0",10,GMP_RNDN);
mpfr_div(b5[2],temp.t1,temp.t2,GMP_RNDN);
mpfr_set_str(temp.t1,"75.0",10,GMP_RNDN);
mpfr_set_str(temp.t2,"64.0",10,GMP_RNDN);
mpfr_div(b5[3],temp.t1,temp.t2,GMP_RNDN);
mpfr_set_str(temp.t1,"3.0",10,GMP_RNDN);
mpfr_set_str(temp.t2,"80.0",10,GMP_RNDN);
mpfr_div(b6[0],temp.t1,temp.t2,GMP_RNDN);
mpfr_set_str(b6[1],"0.0",10,GMP_RNDN);
mpfr_set_str(b6[2],"0.0",10,GMP_RNDN);
mpfr_set_str(temp.t1,"3.0",10,GMP_RNDN);
mpfr_set_str(temp.t2,"16.0",10,GMP_RNDN);
mpfr_div(b6[3],temp.t1,temp.t2,GMP_RNDN);
mpfr_set_str(temp.t1,"3.0",10,GMP_RNDN);
mpfr_set_str(temp.t2,"20.0",10,GMP_RNDN);
```

```
mpfr_div(b6[4],temp.t1,temp.t2,GMP_RNDN);
mpfr_set_str(temp.t1,"29443841.0",10,GMP_RNDN);
mpfr_set_str(temp.t2,"614563906.0",10,GMP_RNDN);
mpfr_div(b7[0],temp.t1,temp.t2,GMP_RNDN);
mpfr_set_str(b7[1],"0.0",10,GMP_RNDN);
mpfr_set_str(b7[2],"0.0",10,GMP_RNDN);
mpfr_set_str(temp.t1,"77736538.0",10,GMP_RNDN);
mpfr_set_str(temp.t2,"692538347.0",10,GMP_RNDN);
mpfr_div(b7[3],temp.t1,temp.t2,GMP_RNDN);
mpfr_set_str(temp.t1,"-28693883.0",10,GMP_RNDN);
mpfr_set_str(temp.t2,"1125000000.0",10,GMP_RNDN);
mpfr_div(b7[4],temp.t1,temp.t2,GMP_RNDN);
mpfr_set_str(temp.t1,"23124283.0",10,GMP_RNDN);
mpfr_set_str(temp.t2,"1800000000.0",10,GMP_RNDN);
mpfr_div(b7[5],temp.t1,temp.t2,GMP_RNDN);
mpfr_set_str(temp.t1,"16016141.0",10,GMP_RNDN);
mpfr_set_str(temp.t2,"946692911.0",10,GMP_RNDN);
mpfr_div(b8[0],temp.t1,temp.t2,GMP_RNDN);
mpfr_set_str(b8[1],"0.0",10,GMP_RNDN);
mpfr_set_str(b8[2],"0.0",10,GMP_RNDN);
mpfr_set_str(temp.t1,"61564180.0",10,GMP_RNDN);
mpfr_set_str(temp.t2,"158732637.0",10,GMP_RNDN);
mpfr_div(b8[3],temp.t1,temp.t2,GMP_RNDN);
mpfr_set_str(temp.t1,"22789713.0",10,GMP_RNDN);
mpfr_set_str(temp.t2,"633445777.0",10,GMP_RNDN);
mpfr_div(b8[4],temp.t1,temp.t2,GMP_RNDN);
mpfr_set_str(temp.t1,"545815736.0",10,GMP_RNDN);
mpfr_set_str(temp.t2,"2771057229.0",10,GMP_RNDN);
mpfr_div(b8[5],temp.t1,temp.t2,GMP_RNDN);
mpfr_set_str(temp.t1,"-180193667.0",10,GMP_RNDN);
mpfr_set_str(temp.t2,"1043307555.0",10,GMP_RNDN);
mpfr_div(b8[6],temp.t1,temp.t2,GMP_RNDN);
mpfr_set_str(temp.t1,"39632708.0",10,GMP_RNDN);
mpfr_set_str(temp.t2,"573591083.0",10,GMP_RNDN);
mpfr_div(b9[0],temp.t1,temp.t2,GMP_RNDN);
mpfr_set_str(b9[1],"0.0",10,GMP_RNDN);
mpfr_set_str(b9[2],"0.0",10,GMP_RNDN);
mpfr_set_str(temp.t1,"-433636366.0",10,GMP_RNDN);
mpfr_set_str(temp.t2,"683701615.0",10,GMP_RNDN);
mpfr_div(b9[3],temp.t1,temp.t2,GMP_RNDN);
mpfr_set_str(temp.t1,"-421739975.0",10,GMP_RNDN);
mpfr_set_str(temp.t2,"2616292301.0",10,GMP_RNDN);
mpfr_div(b9[4],temp.t1,temp.t2,GMP_RNDN);
```

```
mpfr_set_str(temp.t1,"100302831.0",10,GMP_RNDN);
mpfr_set_str(temp.t2,"723423059.0",10,GMP_RNDN);
mpfr_div(b9[5],temp.t1,temp.t2,GMP_RNDN);
mpfr_set_str(temp.t1,"790204164.0",10,GMP_RNDN);
mpfr_set_str(temp.t2,"839813087.0",10,GMP_RNDN);
mpfr_div(b9[6],temp.t1,temp.t2,GMP_RNDN);
mpfr_set_str(temp.t1,"800635310.0",10,GMP_RNDN);
mpfr_set_str(temp.t2,"3783071287.0",10,GMP_RNDN);
mpfr_div(b9[7],temp.t1,temp.t2,GMP_RNDN);
mpfr_set_str(temp.t1,"246121993.0",10,GMP_RNDN);
mpfr_set_str(temp.t2,"1340847787.0",10,GMP_RNDN);
mpfr_div(b10[0],temp.t1,temp.t2,GMP_RNDN);
mpfr_set_str(b10[1],"0.0",10,GMP_RNDN);
mpfr_set_str(b10[2],"0.0",10,GMP_RNDN);
mpfr_set_str(temp.t1,"-37695042795.0",10,GMP_RNDN);
mpfr_set_str(temp.t2,"15268766246.0",10,GMP_RNDN);
mpfr_div(b10[3],temp.t1,temp.t2,GMP_RNDN);
mpfr_set_str(temp.t1,"-309121744.0",10,GMP_RNDN);
mpfr_set_str(temp.t2,"1061227803.0",10,GMP_RNDN);
mpfr_div(b10[4],temp.t1,temp.t2,GMP_RNDN);
mpfr_set_str(temp.t1,"-12992083.0",10,GMP_RNDN);
mpfr_set_str(temp.t2,"490766935.0",10,GMP_RNDN);
mpfr_div(b10[5],temp.t1,temp.t2,GMP_RNDN);
mpfr_set_str(temp.t1,"6005943493.0",10,GMP_RNDN);
mpfr_set_str(temp.t2,"2108947869.0",10,GMP_RNDN);
mpfr_div(b10[6],temp.t1,temp.t2,GMP_RNDN);
mpfr_set_str(temp.t1,"393006217.0",10,GMP_RNDN);
mpfr_set_str(temp.t2,"1396673457.0",10,GMP_RNDN);
mpfr_div(b10[7],temp.t1,temp.t2,GMP_RNDN);
mpfr_set_str(temp.t1,"123872331.0",10,GMP_RNDN);
mpfr_set_str(temp.t2,"1001029789.0",10,GMP_RNDN);
mpfr_div(b10[8],temp.t1,temp.t2,GMP_RNDN);
mpfr_set_str(temp.t1,"-1028468189.0",10,GMP_RNDN);
mpfr_set_str(temp.t2,"846180014.0",10,GMP_RNDN);
mpfr_div(b11[0],temp.t1,temp.t2,GMP_RNDN);
mpfr_set_str(b11[1],"0.0",10,GMP_RNDN);
mpfr_set_str(b11[2],"0.0",10,GMP_RNDN);
mpfr_set_str(temp.t1,"8478235783.0",10,GMP_RNDN);
mpfr_set_str(temp.t2,"508512852.0",10,GMP_RNDN);
mpfr_div(b11[3],temp.t1,temp.t2,GMP_RNDN);
mpfr_set_str(temp.t1,"1311729495.0",10,GMP_RNDN);
mpfr_set_str(temp.t2,"1432422823.0",10,GMP_RNDN);
mpfr_div(b11[4],temp.t1,temp.t2,GMP_RNDN);
```

```
mpfr_set_str(temp.t1,"-10304129995.0",10,GMP_RNDN);
mpfr_set_str(temp.t2,"1701304382.0",10,GMP_RNDN);
mpfr_div(b11[5],temp.t1,temp.t2,GMP_RNDN);
mpfr_set_str(temp.t1,"-48777925059.0",10,GMP_RNDN);
mpfr_set_str(temp.t2,"3047939560.0",10,GMP_RNDN);
mpfr_div(b11[6],temp.t1,temp.t2,GMP_RNDN);
mpfr_set_str(temp.t1,"15336726248.0",10,GMP_RNDN);
mpfr_set_str(temp.t2,"1032824649.0",10,GMP_RNDN);
mpfr_div(b11[7],temp.t1,temp.t2,GMP_RNDN);
mpfr_set_str(temp.t1,"-45442868181.0",10,GMP_RNDN);
mpfr_set_str(temp.t2,"3398467696.0",10,GMP_RNDN);
mpfr_div(b11[8],temp.t1,temp.t2,GMP_RNDN);
mpfr_set_str(temp.t1,"3065993473.0",10,GMP_RNDN);
mpfr_set_str(temp.t2,"597172653.0",10,GMP_RNDN);
mpfr_div(b11[9],temp.t1,temp.t2,GMP_RNDN);
mpfr_set_str(temp.t1,"185892177.0",10,GMP_RNDN);
mpfr_set_str(temp.t2,"718116043.0",10,GMP_RNDN);
mpfr_div(b12[0],temp.t1,temp.t2,GMP_RNDN);
mpfr_set_str(b12[1],"0.0",10,GMP_RNDN);
mpfr_set_str(b12[2],"0.0",10,GMP_RNDN);
mpfr_set_str(temp.t1,"-3185094517.0",10,GMP_RNDN);
mpfr_set_str(temp.t2,"667107341.0",10,GMP_RNDN);
mpfr_div(b12[3],temp.t1,temp.t2,GMP_RNDN);
mpfr_set_str(temp.t1,"-477755414.0",10,GMP_RNDN);
mpfr_set_str(temp.t2,"1098053517.0",10,GMP_RNDN);
mpfr_div(b12[4],temp.t1,temp.t2,GMP_RNDN);
mpfr_set_str(temp.t1,"-703635378.0",10,GMP_RNDN);
mpfr_set_str(temp.t2,"230739211.0",10,GMP_RNDN);
mpfr_div(b12[5],temp.t1,temp.t2,GMP_RNDN);
mpfr_set_str(temp.t1,"5731566787.0",10,GMP_RNDN);
mpfr_set_str(temp.t2,"1027545527.0",10,GMP_RNDN);
mpfr_div(b12[6],temp.t1,temp.t2,GMP_RNDN);
mpfr_set_str(temp.t1,"5232866602.0",10,GMP_RNDN);
mpfr_set_str(temp.t2,"850066563.0",10,GMP_RNDN);
mpfr_div(b12[7],temp.t1,temp.t2,GMP_RNDN);
mpfr_set_str(temp.t1,"-4093664535.0",10,GMP_RNDN);
mpfr_set_str(temp.t2,"808688257.0",10,GMP_RNDN);
mpfr_div(b12[8],temp.t1,temp.t2,GMP_RNDN);
mpfr_set_str(temp.t1,"3962137247.0",10,GMP_RNDN);
mpfr_set_str(temp.t2,"1805957418.0",10,GMP_RNDN);
mpfr_div(b12[9],temp.t1,temp.t2,GMP_RNDN);
mpfr_set_str(temp.t1,"65686358.0",10,GMP_RNDN);
mpfr_set_str(temp.t2,"487910083.0",10,GMP_RNDN);
```

```
  mpfr_div(b12[10],temp.t1,temp.t2,GMP_RNDN);
  mpfr_set_str(temp.t1,"403863854.0",10,GMP_RNDN);
  mpfr_set_str(temp.t2,"491063109.0",10,GMP_RNDN);
  mpfr_div(b13[0],temp.t1,temp.t2,GMP_RNDN);
  mpfr_set_str(b13[1],"0.0",10,GMP_RNDN);
  mpfr_set_str(b13[2],"0.0",10,GMP_RNDN);
  mpfr_set_str(temp.t1,"-5068492393.0",10,GMP_RNDN);
  mpfr_set_str(temp.t2,"434740067.0",10,GMP_RNDN);
  mpfr_div(b13[3],temp.t1,temp.t2,GMP_RNDN);
  mpfr_set_str(temp.t1,"-411421997.0",10,GMP_RNDN);
  mpfr_set_str(temp.t2,"543043805.0",10,GMP_RNDN);
  mpfr_div(b13[4],temp.t1,temp.t2,GMP_RNDN);
  mpfr_set_str(temp.t1,"652783627.0",10,GMP_RNDN);
  mpfr_set_str(temp.t2,"914296604.0",10,GMP_RNDN);
  mpfr_div(b13[5],temp.t1,temp.t2,GMP_RNDN);
  mpfr_set_str(temp.t1,"11173962825.0",10,GMP_RNDN);
  mpfr_set_str(temp.t2,"925320556.0",10,GMP_RNDN);
  mpfr_div(b13[6],temp.t1,temp.t2,GMP_RNDN);
  mpfr_set_str(temp.t1,"-13158990841.0",10,GMP_RNDN);
  mpfr_set_str(temp.t2,"6184727034.0",10,GMP_RNDN);
  mpfr_div(b13[7],temp.t1,temp.t2,GMP_RNDN);
  mpfr_set_str(temp.t1,"3936647629.0",10,GMP_RNDN);
  mpfr_set_str(temp.t2,"1978049680.0",10,GMP_RNDN);
  mpfr_div(b13[8],temp.t1,temp.t2,GMP_RNDN);
  mpfr_set_str(temp.t1,"-160528059.0",10,GMP_RNDN);
  mpfr_set_str(temp.t2,"685178525.0",10,GMP_RNDN);
  mpfr_div(b13[9],temp.t1,temp.t2,GMP_RNDN);
  mpfr_set_str(temp.t1,"248638103.0",10,GMP_RNDN);
  mpfr_set_str(temp.t2,"1413531060.0",10,GMP_RNDN);
  mpfr_div(b13[10],temp.t1,temp.t2,GMP_RNDN);
  mpfr_set_str(b13[11],"0.0",10,GMP_RNDN);
}
~rkvars_t(void) {
  for(unsigned short i=0U ; i<13U ; i++)
    mpfr_clear(Abar[i]);
  for(unsigned short i=0U ; i<12U ; i++) {
    mpfr_clear(A[i]);
    mpfr_clear(b13[i]);
  }
  for(unsigned short i=0U ; i<11U ; i++)
    mpfr_clear(b12[i]);
  for(unsigned short i=0U ; i<10U ; i++) {
    mpfr_clear(ah[i]);
```

```
      mpfr_clear(b11[i]);
    }
    for(unsigned short i=0U ; i<9U ; i++)
      mpfr_clear(b10[i]);
    for(unsigned short i=0U ; i<8U ; i++)
      mpfr_clear(b9[i]);
    for(unsigned short i=0U ; i<7U ; i++)
      mpfr_clear(b8[i]);
    for(unsigned short i=0U ; i<6U ; i++)
      mpfr_clear(b7[i]);
    for(unsigned short i=0U ; i<5U ; i++)
      mpfr_clear(b6[i]);
    for(unsigned short i=0U ; i<4U ; i++)
      mpfr_clear(b5[i]);
    for(unsigned short i=0U ; i<3U ; i++)
      mpfr_clear(b4[i]);
    for(unsigned short i=0U ; i<2U ; i++)
      mpfr_clear(b3[i]);
    mpfr_clear(b21);
  }
} rk;


int main(int argc, char* argv[]) {

  switch( read_input(argc,argv) ) {
  case 0: break;
  case 1: return 0;
  default:
  case 2: return 1;
  }
  if ( init_mathlink() ) return 1;

  FILE* pdata;
  pdata = fopen("data","w");

  mpfr_t   t_now, t_end, t_end_inter, t_step, h_step, y[4];

  mpfr_init2(t_now,MPFR_PRECISION);
  mpfr_set_str(t_now,"0.0",10,GMP_RNDZ);

  mpfr_init2(t_end,MPFR_PRECISION);
  mpfr_set_str(t_end,inits.end_time.c_str(),10,GMP_RNDN);
```

```
mpfr_init2(t_end_inter,MPFR_PRECISION);
mpfr_set_str(t_end_inter,inits.end_time_step.c_str(),10,GMP_RNDN);

mpfr_init2(t_step,MPFR_PRECISION);
mpfr_set_str(t_step,inits.end_time_step.c_str(),10,GMP_RNDN);

mpfr_init2(h_step,MPFR_PRECISION);
mpfr_set_str(h_step,START_STEP_SIZE,10,GMP_RNDN);

mpfr_init2(y[0],MPFR_PRECISION);
mpfr_init2(y[1],MPFR_PRECISION);
mpfr_init2(y[2],MPFR_PRECISION);
mpfr_init2(y[3],MPFR_PRECISION);
mpfr_set_str(y[0],inits.init_x_r.c_str(),10,GMP_RNDN);
mpfr_set_str(y[1],inits.init_x_i.c_str(),10,GMP_RNDN);

{ // save some memory
  stringstream ss;
  ss << "SetPrecision[ Chop [ (2(JacobiCN[ " << inits.init_x_r
    << " + " << inits.init_x_i << " I , " << inits.param
    << " ] + " << inits.energy << " ) )^0.5 ] , "
    << MATHEMATICA_PRECISION << "]";

  MLPutFunction(mlink, "EvaluatePacket", 1);
    MLPutFunction(mlink, "ToString", 1);
      MLPutFunction(mlink, "ToExpression", 1);
      MLPutString(mlink, (ss.str()).c_str() );
  MLEndPacket(mlink);

  int init_pkt = 0;
  while( (init_pkt = MLNextPacket(mlink),init_pkt)
      && init_pkt != RETURNPKT )
    MLNewPacket(mlink);
  if(!init_pkt) {
    cerr << "error: mathlink error for initial p calculation.\n";
    mpfr_clear(t_now);
    mpfr_clear(t_end);
    mpfr_clear(t_end_inter);
    mpfr_clear(t_step);
    mpfr_clear(h_step);
    mpfr_clear(y[0]);
    mpfr_clear(y[1]);
```

```
      mpfr_clear(y[2]);
      mpfr_clear(y[3]);
      mpfr_free_cache();
      MLClose(mlink);
      MLDeinitialize(mlenv);
      return 1;
    }
    const char* str;
    MLGetString(mlink,&str);
    string answer = str;
    size_t i_pos = answer.find('I');
    if ( i_pos == string::npos ) {
      mpfr_set_str(y[2],str,10,GMP_RNDN);
      mpfr_set_str(y[3],"0.0",10,GMP_RNDN);
    }
    else {
      size_t split = answer.find_first_of("-+",1);
      if ( split == string::npos ) {
        mpfr_set_str(y[2],"0.0",10,GMP_RNDN);
        mpfr_set_str(y[3],
            answer.substr(0U,i_pos-1U).c_str(),
            10,GMP_RNDN);
      }
      else {
        mpfr_set_str(y[2],
            (answer.substr(0U,split)).c_str(),
            10,GMP_RNDN);
        string imag = answer.substr( split, answer.length()-split-1U );
        imag.erase(1,1);
        mpfr_set_str(y[3],imag.c_str(),10,GMP_RNDN);
      }
    }
    MLDisownString(mlink,str);
  }

  int status = 0;
  cout << "starting...\n";
evolve_loop:
    status = evolve_apply(t_now,t_end_inter,h_step,y);
    if( status ) {
      mpfr_clear(t_now);
      mpfr_clear(t_end);
      mpfr_clear(t_end_inter);
```

```
      mpfr_clear(t_step);
      mpfr_clear(h_step);
      mpfr_clear(y[0]);
      mpfr_clear(y[1]);
      mpfr_clear(y[2]);
      mpfr_clear(y[3]);
      mpfr_free_cache();
      MLClose(mlink);
      MLDeinitialize(mlenv);
      return status;
    }

    mpfr_fprintf(pdata,"%.15RNf\t%.15RNf\t%.15RNf\t%.15RNf\t%.15RNf\n",
              t_now,y[0],y[1],y[2],y[3]);

  if ( mpfr_cmp(t_now,t_end_inter) < 0 ) goto evolve_loop;
  if ( mpfr_cmp(t_end_inter,t_end) < 0 ) {
    mpfr_add(t_end_inter,t_end_inter,t_step,GMP_RNDN);
    goto evolve_loop;
  }

  cout << "done.\n";
  mpfr_clear(t_now);
  mpfr_clear(t_end);
  mpfr_clear(t_end_inter);
  mpfr_clear(t_step);
  mpfr_clear(h_step);
  mpfr_clear(y[0]);
  mpfr_clear(y[1]);
  mpfr_clear(y[2]);
  mpfr_clear(y[3]);
  mpfr_free_cache();
  MLClose(mlink);
  MLDeinitialize(mlenv);
  return status;
}

int evolve_apply(mpfr_t t, const mpfr_t t1, mpfr_t h, mpfr_t y[]) {
  mpfr_t t0, h0, dt;

  mpfr_init2(t0,MPFR_PRECISION);
  mpfr_set(t0,t,GMP_RNDN);
```

```
  mpfr_init2(h0,MPFR_PRECISION);
  mpfr_set(h0,h,GMP_RNDN);

  mpfr_init2(dt,MPFR_PRECISION);
  mpfr_sub(dt,t1,t0,GMP_RNDN);

  int step_status;
  bool final_step = false;


  mpfr_set(evolve.y0[0],y[0],GMP_RNDN);
  mpfr_set(evolve.y0[1],y[1],GMP_RNDN);
  mpfr_set(evolve.y0[2],y[2],GMP_RNDN);
  mpfr_set(evolve.y0[3],y[3],GMP_RNDN);

  int status = func(y,evolve.dydt_in);
  if( status ) return status;

  int c1, c2;
try_step:

  c1 = mpfr_cmp_d(dt,0.0);
  c2 = mpfr_cmp(h0,dt);
  if( (c1>=0 && c2>0) || (c1<0 && c2<0) )
  {
    mpfr_set(h0,dt,GMP_RNDN);
    final_step = true;
  }
  else final_step = false;

  step_status = rk8pd_apply(h0,y);

  /* Check for stepper internal failure */
  if (step_status != 0)
    {
    mpfr_set(h,h0,GMP_RNDN);
  /* notify user of step-size which caused the failure */
      return step_status;
    }

  evolve.count++;
  mpfr_set(evolve.last_step,h0,GMP_RNDN);
```

```
  if (final_step)
    mpfr_set(t,t1,GMP_RNDN);
  else
    mpfr_add(t,t0,h0,GMP_RNDN);

      /* Check error and attempt to adjust the step. */
    const int h_adjust_status = h_adjust(y,h0);

      if (h_adjust_status == -1)
        {
          /* Step was decreased. Undo and go back to try again. */
      mpfr_set(y[0],evolve.y0[0],GMP_RNDN);
      mpfr_set(y[1],evolve.y0[1],GMP_RNDN);
      mpfr_set(y[2],evolve.y0[2],GMP_RNDN);
      mpfr_set(y[3],evolve.y0[3],GMP_RNDN);
      evolve.failed_steps++;
          goto try_step;
        }

  mpfr_set(h,h0,GMP_RNDN);
    /* suggest step size for next time-step */

  mpfr_clear(t0);
  mpfr_clear(h0);
  mpfr_clear(dt);
  return step_status;
}


int h_adjust(const mpfr_t y[], mpfr_t h) {

  mpfr_t h_old;
  mpfr_init2(h_old,MPFR_PRECISION);
  mpfr_set(h_old,h,GMP_RNDN);

  mpfr_t rmax, D0, r;
  mpfr_init2(rmax,MPFR_PRECISION);
  mpfr_set_d(rmax,LDBL_MIN,GMP_RNDN); // DBL_MIN? What else?

  mpfr_init2(D0,MPFR_PRECISION);
  mpfr_init2(r,MPFR_PRECISION);

  for(int i=0; i<4; i++) { // '4' for the dimension of the system.
```

```
     mpfr_abs(D0,y[i],GMP_RNDN);

    mpfr_mul(D0,D0,control.eps_rel,GMP_RNDN);
    mpfr_add(D0,D0,control.eps_abs,GMP_RNDN);

    mpfr_div(r,evolve.yerr[i],D0,GMP_RNDN);
    mpfr_abs(r,r,GMP_RNDN);
    mpfr_max(rmax,r,rmax,GMP_RNDN);
  }

  if ( mpfr_cmp_d(rmax,1.1) > 0 ) {
    /* decrease step, no more than factor of 5, but a fraction S more
       than scaling suggests (for better accuracy) */
    // N.B. THIS REUSES D0 AND r FROM BEFORE.
    mpfr_set_str(D0,"0.125",10,GMP_RNDN);
    mpfr_pow(D0,rmax,D0,GMP_RNDN);
    mpfr_d_div(r,0.9,D0,GMP_RNDN);

    if ( mpfr_cmp_d(r,0.2) < 0 )
      mpfr_set_str(r,"0.2",10,GMP_RNDN);

    mpfr_mul(h,r,h_old,GMP_RNDN);

//    return GSL_ODEIV_HADJ_DEC; // (-1)
    mpfr_clear(h_old);
    mpfr_clear(rmax);
    mpfr_clear(D0);
    mpfr_clear(r);
  return -1;
  }
    else if ( mpfr_cmp_d(rmax,0.5) < 0 ) {
    /* increase step, no more than factor of 5 */
      mpfr_set_str(temp.t1,"1.0",10,GMP_RNDN);
      mpfr_set_str(temp.t2,"9.0",10,GMP_RNDN);
      mpfr_div(D0,temp.t1,temp.t2,GMP_RNDN);
      mpfr_pow(D0,rmax,D0,GMP_RNDN);
      mpfr_d_div(r,0.9,D0,GMP_RNDN);

      if ( mpfr_cmp_d(r,5.0) > 0 )
      {
        mpfr_set_str(r,"5.0",10,GMP_RNDN);
      }
      else if( mpfr_cmp_d(r,1.0) < 0 )
```

```
        mpfr_set_str(r,"1.0",10,GMP_RNDN);

       mpfr_mul(h,r,h_old,GMP_RNDN);

//    return GSL_ODEIV_HADJ_INC; // (1)
    mpfr_clear(h_old);
    mpfr_clear(rmax);
    mpfr_clear(D0);
    mpfr_clear(r);
  return 1;
  }
  else {
    /* no change */
//    return GSL_ODEIV_HADJ_NIL; // (0)
    mpfr_clear(h_old);
    mpfr_clear(rmax);
    mpfr_clear(D0);
    mpfr_clear(r);
    return 0;
  }
}

int rk8pd_apply(mpfr_t h, mpfr_t y[])
{

  int status;
  // k1 step
  mpfr_set(step.k[0][0],evolve.dydt_in[0],GMP_RNDN);
  mpfr_set(step.k[0][1],evolve.dydt_in[1],GMP_RNDN);
  mpfr_set(step.k[0][2],evolve.dydt_in[2],GMP_RNDN);
  mpfr_set(step.k[0][3],evolve.dydt_in[3],GMP_RNDN);

  int i;
  for (i=0 ; i < 4 ; i++ ) {
    mpfr_mul(step.ytmp[i], h           , step.k[0][i], GMP_RNDN);
    mpfr_mul(step.ytmp[i], step.ytmp[i], rk.b21      , GMP_RNDN);
    mpfr_add(step.ytmp[i], step.ytmp[i], y[i]        , GMP_RNDN);
  }

  // k2 step
  status = func (step.ytmp, step.k[1]);
  if ( status != 0 ) return status;
```

```
for (i = 0; i < 4; i++) {
  mpfr_mul(temp.t1     , rk.b3[1]    , step.k[1][i], GMP_RNDN);
  mpfr_mul(step.ytmp[i], rk.b3[0]    , step.k[0][i], GMP_RNDN);
  mpfr_add(step.ytmp[i], step.ytmp[i], temp.t1     , GMP_RNDN);
  mpfr_mul(step.ytmp[i], step.ytmp[i], h           , GMP_RNDN);
  mpfr_add(step.ytmp[i], step.ytmp[i], y[i]        , GMP_RNDN);
}

// k3 step
status = func(step.ytmp, step.k[2]);
if ( status != 0 ) return status;

for (i = 0; i < 4; i++) {
  mpfr_mul(temp.t1     , rk.b4[2]    , step.k[2][i], GMP_RNDN);
  mpfr_mul(step.ytmp[i], rk.b4[0]    , step.k[0][i], GMP_RNDN);
  mpfr_add(step.ytmp[i], step.ytmp[i], temp.t1     , GMP_RNDN);
  mpfr_mul(step.ytmp[i], step.ytmp[i], h           , GMP_RNDN);
  mpfr_add(step.ytmp[i], step.ytmp[i], y[i]        , GMP_RNDN);
}

// k4 step
status = func(step.ytmp, step.k[3]);
if ( status != 0 ) return status;

for (i = 0; i < 4; i++) {
  mpfr_mul(temp.t1     , rk.b5[3]    , step.k[3][i], GMP_RNDN);
  mpfr_mul(step.ytmp[i], rk.b5[2]    , step.k[2][i], GMP_RNDN);
  mpfr_add(step.ytmp[i], step.ytmp[i], temp.t1     , GMP_RNDN);
  mpfr_mul(temp.t1     , rk.b5[0]    , step.k[0][i], GMP_RNDN);
  mpfr_add(step.ytmp[i], step.ytmp[i], temp.t1     , GMP_RNDN);
  mpfr_mul(step.ytmp[i], step.ytmp[i], h           , GMP_RNDN);
  mpfr_add(step.ytmp[i], step.ytmp[i], y[i]        , GMP_RNDN);
}

// k5 step
status = func(step.ytmp, step.k[4]);
if ( status != 0 ) return status;

for (i = 0; i < 4; i++) {
  mpfr_mul(temp.t1     , rk.b6[4]    , step.k[4][i], GMP_RNDN);
  mpfr_mul(step.ytmp[i], rk.b6[3]    , step.k[3][i], GMP_RNDN);
  mpfr_add(step.ytmp[i], step.ytmp[i], temp.t1     , GMP_RNDN);
  mpfr_mul(temp.t1     , rk.b6[0]    , step.k[0][i], GMP_RNDN);
```

```
  mpfr_add(step.ytmp[i], step.ytmp[i], temp.t1     , GMP_RNDN);
  mpfr_mul(step.ytmp[i], step.ytmp[i], h           , GMP_RNDN);
  mpfr_add(step.ytmp[i], step.ytmp[i], y[i]        , GMP_RNDN);
}

// k6 step
status = func(step.ytmp, step.k[5]);
if ( status != 0 ) return status;

for (i = 0; i < 4; i++) {
  mpfr_mul(temp.t1     , rk.b7[5]    , step.k[5][i], GMP_RNDN);
  mpfr_mul(step.ytmp[i], rk.b7[4]    , step.k[4][i], GMP_RNDN);
  mpfr_add(step.ytmp[i], step.ytmp[i], temp.t1     , GMP_RNDN);
  mpfr_mul(temp.t1     , rk.b7[3]    , step.k[3][i], GMP_RNDN);
  mpfr_add(step.ytmp[i], step.ytmp[i], temp.t1     , GMP_RNDN);
  mpfr_mul(temp.t1     , rk.b7[0]    , step.k[0][i], GMP_RNDN);
  mpfr_add(step.ytmp[i], step.ytmp[i], temp.t1     , GMP_RNDN);
  mpfr_mul(step.ytmp[i], step.ytmp[i], h           , GMP_RNDN);
  mpfr_add(step.ytmp[i], step.ytmp[i], y[i]        , GMP_RNDN);
}

// k7 step
status = func(step.ytmp, step.k[6]);
if ( status != 0 ) return status;

for (i = 0; i < 4; i++) {
  mpfr_mul(temp.t1     , rk.b8[6]    , step.k[6][i], GMP_RNDN);
  mpfr_mul(step.ytmp[i], rk.b8[5]    , step.k[5][i], GMP_RNDN);
  mpfr_add(step.ytmp[i], step.ytmp[i], temp.t1     , GMP_RNDN);
  mpfr_mul(temp.t1     , rk.b8[4]    , step.k[4][i], GMP_RNDN);
  mpfr_add(step.ytmp[i], step.ytmp[i], temp.t1     , GMP_RNDN);
  mpfr_mul(temp.t1     , rk.b8[3]    , step.k[3][i], GMP_RNDN);
  mpfr_add(step.ytmp[i], step.ytmp[i], temp.t1     , GMP_RNDN);
  mpfr_mul(temp.t1     , rk.b8[0]    , step.k[0][i], GMP_RNDN);
  mpfr_add(step.ytmp[i], step.ytmp[i], temp.t1     , GMP_RNDN);
  mpfr_mul(step.ytmp[i], step.ytmp[i], h           , GMP_RNDN);
  mpfr_add(step.ytmp[i], step.ytmp[i], y[i]        , GMP_RNDN);
}

// k8 step
status = func(step.ytmp, step.k[7]);
if ( status != 0 ) return status;
```

```
for (i = 0; i < 4; i++) {
  mpfr_mul(temp.t1     , rk.b9[7]    , step.k[7][i], GMP_RNDN);
  mpfr_mul(step.ytmp[i], rk.b9[6]    , step.k[6][i], GMP_RNDN);
  mpfr_add(step.ytmp[i], step.ytmp[i], temp.t1     , GMP_RNDN);
  mpfr_mul(temp.t1     , rk.b9[5]    , step.k[5][i], GMP_RNDN);
  mpfr_add(step.ytmp[i], step.ytmp[i], temp.t1     , GMP_RNDN);
  mpfr_mul(temp.t1     , rk.b9[4]    , step.k[4][i], GMP_RNDN);
  mpfr_add(step.ytmp[i], step.ytmp[i], temp.t1     , GMP_RNDN);
  mpfr_mul(temp.t1     , rk.b9[3]    , step.k[3][i], GMP_RNDN);
  mpfr_add(step.ytmp[i], step.ytmp[i], temp.t1     , GMP_RNDN);
  mpfr_mul(temp.t1     , rk.b9[0]    , step.k[0][i], GMP_RNDN);
  mpfr_add(step.ytmp[i], step.ytmp[i], temp.t1     , GMP_RNDN);
  mpfr_mul(step.ytmp[i], step.ytmp[i], h           , GMP_RNDN);
  mpfr_add(step.ytmp[i], step.ytmp[i], y[i]        , GMP_RNDN);
}

// k9 step
status = func(step.ytmp, step.k[8]);
if ( status != 0 ) return status;

for (i = 0; i < 4; i++) {
  mpfr_mul(temp.t1     , rk.b10[8]   , step.k[8][i], GMP_RNDN);
  mpfr_mul(step.ytmp[i], rk.b10[7]   , step.k[7][i], GMP_RNDN);
  mpfr_add(step.ytmp[i], step.ytmp[i], temp.t1     , GMP_RNDN);
  mpfr_mul(step.ytmp[i], rk.b10[6]   , step.k[6][i], GMP_RNDN);
  mpfr_add(step.ytmp[i], step.ytmp[i], temp.t1     , GMP_RNDN);
  mpfr_mul(temp.t1     , rk.b10[5]   , step.k[5][i], GMP_RNDN);
  mpfr_add(step.ytmp[i], step.ytmp[i], temp.t1     , GMP_RNDN);
  mpfr_mul(temp.t1     , rk.b10[4]   , step.k[4][i], GMP_RNDN);
  mpfr_add(step.ytmp[i], step.ytmp[i], temp.t1     , GMP_RNDN);
  mpfr_mul(temp.t1     , rk.b10[3]   , step.k[3][i], GMP_RNDN);
  mpfr_add(step.ytmp[i], step.ytmp[i], temp.t1     , GMP_RNDN);
  mpfr_mul(temp.t1     , rk.b10[0]   , step.k[0][i], GMP_RNDN);
  mpfr_add(step.ytmp[i], step.ytmp[i], temp.t1     , GMP_RNDN);
  mpfr_mul(step.ytmp[i], step.ytmp[i], h           , GMP_RNDN);
  mpfr_add(step.ytmp[i], step.ytmp[i], y[i]        , GMP_RNDN);
}

// k10 step
status = func(step.ytmp, step.k[9]);
if ( status != 0 ) return status;

for (i = 0; i < 4; i++) {
```

```
  mpfr_mul(temp.t1     , rk.b11[9]   , step.k[9][i], GMP_RNDN);
  mpfr_mul(step.ytmp[i], rk.b11[8]   , step.k[8][i], GMP_RNDN);
  mpfr_add(step.ytmp[i], step.ytmp[i], temp.t1     , GMP_RNDN);
  mpfr_mul(step.ytmp[i], rk.b11[7]   , step.k[7][i], GMP_RNDN);
  mpfr_add(step.ytmp[i], step.ytmp[i], temp.t1     , GMP_RNDN);
  mpfr_mul(step.ytmp[i], rk.b11[6]   , step.k[6][i], GMP_RNDN);
  mpfr_add(step.ytmp[i], step.ytmp[i], temp.t1     , GMP_RNDN);
  mpfr_mul(temp.t1     , rk.b11[5]   , step.k[5][i], GMP_RNDN);
  mpfr_add(step.ytmp[i], step.ytmp[i], temp.t1     , GMP_RNDN);
  mpfr_mul(temp.t1     , rk.b11[4]   , step.k[4][i], GMP_RNDN);
  mpfr_add(step.ytmp[i], step.ytmp[i], temp.t1     , GMP_RNDN);
  mpfr_mul(temp.t1     , rk.b11[3]   , step.k[3][i], GMP_RNDN);
  mpfr_add(step.ytmp[i], step.ytmp[i], temp.t1     , GMP_RNDN);
  mpfr_mul(temp.t1     , rk.b11[0]   , step.k[0][i], GMP_RNDN);
  mpfr_add(step.ytmp[i], step.ytmp[i], temp.t1     , GMP_RNDN);
  mpfr_mul(step.ytmp[i], step.ytmp[i], h           , GMP_RNDN);
  mpfr_add(step.ytmp[i], step.ytmp[i], y[i]        , GMP_RNDN);
}

// k11 step
status = func(step.ytmp, step.k[10]);
if ( status != 0 ) return status;

for (i = 0; i < 4; i++) {
  mpfr_mul(temp.t1     , rk.b12[10]  , step.k[10][i], GMP_RNDN);
  mpfr_mul(step.ytmp[i], rk.b12[9]   , step.k[9][i] , GMP_RNDN);
  mpfr_add(step.ytmp[i], step.ytmp[i], temp.t1      , GMP_RNDN);
  mpfr_mul(step.ytmp[i], rk.b12[8]   , step.k[8][i] , GMP_RNDN);
  mpfr_add(step.ytmp[i], step.ytmp[i], temp.t1      , GMP_RNDN);
  mpfr_mul(step.ytmp[i], rk.b12[7]   , step.k[7][i] , GMP_RNDN);
  mpfr_add(step.ytmp[i], step.ytmp[i], temp.t1      , GMP_RNDN);
  mpfr_mul(step.ytmp[i], rk.b12[6]   , step.k[6][i] , GMP_RNDN);
  mpfr_add(step.ytmp[i], step.ytmp[i], temp.t1      , GMP_RNDN);
  mpfr_mul(temp.t1     , rk.b12[5]   , step.k[5][i] , GMP_RNDN);
  mpfr_add(step.ytmp[i], step.ytmp[i], temp.t1      , GMP_RNDN);
  mpfr_mul(temp.t1     , rk.b12[4]   , step.k[4][i] , GMP_RNDN);
  mpfr_add(step.ytmp[i], step.ytmp[i], temp.t1      , GMP_RNDN);
  mpfr_mul(temp.t1     , rk.b12[3]   , step.k[3][i] , GMP_RNDN);
  mpfr_add(step.ytmp[i], step.ytmp[i], temp.t1      , GMP_RNDN);
  mpfr_mul(temp.t1     , rk.b12[0]   , step.k[0][i] , GMP_RNDN);
  mpfr_add(step.ytmp[i], step.ytmp[i], temp.t1      , GMP_RNDN);
  mpfr_mul(step.ytmp[i], step.ytmp[i], h            , GMP_RNDN);
  mpfr_add(step.ytmp[i], step.ytmp[i], y[i]         , GMP_RNDN);
```

```
}

// k12 step
status = func(step.ytmp, step.k[11]);
if ( status != 0 ) return status;

for (i = 0; i < 4; i++) {
  mpfr_mul(temp.t1     , rk.b13[11]  , step.k[11][i], GMP_RNDN);
  mpfr_mul(step.ytmp[i], rk.b13[10]  , step.k[10][i], GMP_RNDN);
  mpfr_add(step.ytmp[i], step.ytmp[i], temp.t1      , GMP_RNDN);
  mpfr_mul(step.ytmp[i], rk.b13[9]   , step.k[9][i] , GMP_RNDN);
  mpfr_add(step.ytmp[i], step.ytmp[i], temp.t1      , GMP_RNDN);
  mpfr_mul(step.ytmp[i], rk.b13[8]   , step.k[8][i] , GMP_RNDN);
  mpfr_add(step.ytmp[i], step.ytmp[i], temp.t1      , GMP_RNDN);
  mpfr_mul(step.ytmp[i], rk.b13[7]   , step.k[7][i] , GMP_RNDN);
  mpfr_add(step.ytmp[i], step.ytmp[i], temp.t1      , GMP_RNDN);
  mpfr_mul(step.ytmp[i], rk.b13[6]   , step.k[6][i] , GMP_RNDN);
  mpfr_add(step.ytmp[i], step.ytmp[i], temp.t1      , GMP_RNDN);
  mpfr_mul(temp.t1     , rk.b13[5]   , step.k[5][i] , GMP_RNDN);
  mpfr_add(step.ytmp[i], step.ytmp[i], temp.t1      , GMP_RNDN);
  mpfr_mul(temp.t1     , rk.b13[4]   , step.k[4][i] , GMP_RNDN);
  mpfr_add(step.ytmp[i], step.ytmp[i], temp.t1      , GMP_RNDN);
  mpfr_mul(temp.t1     , rk.b13[3]   , step.k[3][i] , GMP_RNDN);
  mpfr_add(step.ytmp[i], step.ytmp[i], temp.t1      , GMP_RNDN);
  mpfr_mul(temp.t1     , rk.b13[0]   , step.k[0][i] , GMP_RNDN);
  mpfr_add(step.ytmp[i], step.ytmp[i], temp.t1      , GMP_RNDN);
  mpfr_mul(step.ytmp[i], step.ytmp[i], h            , GMP_RNDN);
  mpfr_add(step.ytmp[i], step.ytmp[i], y[i]         , GMP_RNDN);
}

// k13 step
status = func(step.ytmp, step.k[12]);
if ( status != 0 ) return status;


// final sum
for (i = 0; i < 4; i++) {
  mpfr_mul(temp.t1, rk.Abar[12], step.k[12][i], GMP_RNDN);
  mpfr_mul(temp.t2, rk.Abar[11], step.k[11][i], GMP_RNDN);
  mpfr_add(temp.t2, temp.t2    , temp.t1      , GMP_RNDN);
  mpfr_mul(temp.t1, rk.Abar[10], step.k[10][i], GMP_RNDN);
  mpfr_add(temp.t2, temp.t2    , temp.t1      , GMP_RNDN);
  mpfr_mul(temp.t1, rk.Abar[9] , step.k[9][i] , GMP_RNDN);
```

```
  mpfr_add(temp.t2, temp.t2    , temp.t1      , GMP_RNDN);
  mpfr_mul(temp.t1, rk.Abar[8] , step.k[8][i] , GMP_RNDN);
  mpfr_add(temp.t2, temp.t2    , temp.t1      , GMP_RNDN);
  mpfr_mul(temp.t1, rk.Abar[7] , step.k[7][i] , GMP_RNDN);
  mpfr_add(temp.t2, temp.t2    , temp.t1      , GMP_RNDN);
  mpfr_mul(temp.t1, rk.Abar[6] , step.k[6][i] , GMP_RNDN);
  mpfr_add(temp.t2, temp.t2    , temp.t1      , GMP_RNDN);
  mpfr_mul(temp.t1, rk.Abar[5] , step.k[5][i] , GMP_RNDN);
  mpfr_add(temp.t2, temp.t2    , temp.t1      , GMP_RNDN);
  mpfr_mul(temp.t1, rk.Abar[0] , step.k[0][i] , GMP_RNDN);
  mpfr_add(temp.t2, temp.t2    , temp.t1      , GMP_RNDN);
  mpfr_mul(temp.t2, temp.t2    , h            , GMP_RNDN);
  mpfr_add(y[i]   , y[i]       , temp.t2      , GMP_RNDN);
}


// error estimate
for (i = 0; i < 4; i++) {
  mpfr_mul(temp.t1, rk.Abar[12], step.k[12][i], GMP_RNDN);
  mpfr_mul(temp.t2, rk.Abar[11], step.k[11][i], GMP_RNDN);
  mpfr_add(temp.t2, temp.t2    , temp.t1      , GMP_RNDN);
  mpfr_mul(temp.t1, rk.Abar[10], step.k[10][i], GMP_RNDN);
  mpfr_add(temp.t2, temp.t2    , temp.t1      , GMP_RNDN);
  mpfr_mul(temp.t1, rk.Abar[9] , step.k[9][i] , GMP_RNDN);
  mpfr_add(temp.t2, temp.t2    , temp.t1      , GMP_RNDN);
  mpfr_mul(temp.t1, rk.Abar[8] , step.k[8][i] , GMP_RNDN);
  mpfr_add(temp.t2, temp.t2    , temp.t1      , GMP_RNDN);
  mpfr_mul(temp.t1, rk.Abar[7] , step.k[7][i] , GMP_RNDN);
  mpfr_add(temp.t2, temp.t2    , temp.t1      , GMP_RNDN);
  mpfr_mul(temp.t1, rk.Abar[6] , step.k[6][i] , GMP_RNDN);
  mpfr_add(temp.t2, temp.t2    , temp.t1      , GMP_RNDN);
  mpfr_mul(temp.t1, rk.Abar[5] , step.k[5][i] , GMP_RNDN);
  mpfr_add(temp.t2, temp.t2    , temp.t1      , GMP_RNDN);
  mpfr_mul(temp.t1, rk.Abar[0] , step.k[0][i] , GMP_RNDN);
  mpfr_add(temp.t2, temp.t2    , temp.t1      , GMP_RNDN);

  mpfr_mul(temp.t1       , rk.A[11]      , step.k[11][i], GMP_RNDN);
  mpfr_mul(evolve.yerr[i], rk.A[10]      , step.k[10][i], GMP_RNDN);
  mpfr_add(evolve.yerr[i], evolve.yerr[i], temp.t1      , GMP_RNDN);
  mpfr_mul(temp.t1       , rk.A[9]       , step.k[9][i] , GMP_RNDN);
  mpfr_add(evolve.yerr[i], evolve.yerr[i], temp.t1      , GMP_RNDN);
  mpfr_mul(temp.t1       , rk.A[8]       , step.k[8][i] , GMP_RNDN);
  mpfr_add(evolve.yerr[i], evolve.yerr[i], temp.t1      , GMP_RNDN);
```

```
    mpfr_mul(temp.t1       , rk.A[7]       , step.k[7][i] , GMP_RNDN);
    mpfr_add(evolve.yerr[i], evolve.yerr[i], temp.t1      , GMP_RNDN);
    mpfr_mul(temp.t1       , rk.A[6]       , step.k[6][i] , GMP_RNDN);
    mpfr_add(evolve.yerr[i], evolve.yerr[i], temp.t1      , GMP_RNDN);
    mpfr_mul(temp.t1       , rk.A[5]       , step.k[5][i] , GMP_RNDN);
    mpfr_add(evolve.yerr[i], evolve.yerr[i], temp.t1      , GMP_RNDN);
    mpfr_mul(temp.t1       , rk.A[0]       , step.k[0][i] , GMP_RNDN);
    mpfr_add(evolve.yerr[i], evolve.yerr[i], temp.t1      , GMP_RNDN);

    mpfr_sub(evolve.yerr[i], evolve.yerr[i], temp.t2, GMP_RNDN);
    mpfr_mul(evolve.yerr[i], evolve.yerr[i], h      , GMP_RNDN);
  }

  return 0;
}

int init_mathlink(void) {
  mlenv = MLInitialize(0);
  if(!mlenv) {
    cout << "failed.\n";
    cerr << "error: could not initialize Mathematica.\n";
    return 1;
  }

  int ml_argc = 4;
  char ml_argv0[] = { '-', 'l', 'i', 'n', 'k',
    'n', 'a', 'm', 'e', '\0' };
  char ml_argv1[] = { 'm', 'a', 't', 'h',
    ' ', '-', 'm', 'a', 't', 'h', 'l', 'i', 'n', 'k', '\0' };
  char ml_argv2[] = {
    '-', 'l', 'i', 'n', 'k', 'm', 'o', 'd', 'e', '\0' };
  char ml_argv3[] = { 'l', 'a', 'u', 'n', 'c', 'h', '\0' };
  char* ml_argv[] = { ml_argv0 , ml_argv1 , ml_argv2 , ml_argv3 };
  mlink = MLOpen(ml_argc,ml_argv);
  if(!mlink) {
    cout << "failed.\n";
    cerr << "error: could not open MathLink.\n";
    return 1;
  }
  return 0;
}
```

```
int read_input(const int argc, const char* const argv[]) {
  for(int i=1 ; i<argc ; i++) {
    string str = argv[i];
    if(str=="-h" || str=="--help") {
      cout << argv[0] << " [options]\n\n"
         << " Options\n"
         << "  --param  <value>    enter elliptic parameter.\n"
         << "  --endt   <time>     enter end time.\n"
         << "  --endts  <time>     enter end time steps.\n"
         << "  --initxr <value>    enter initial Re(x) value.\n"
         << "  --initxi <value>    enter initial Im(x) value.\n"
         << "  --energy <value>    enter system energy.\n"
         << "  -i                  enter interactive mode.\n\n";
      return 1;
    }
    if(str=="--param") {
      if(i==argc-1) {
        cerr << "`" << str << "' needs an input.\n";
        return 2;
      }
      i++;
      string input = argv[i];
      cout << "using parameter value of `" << input << "'.\n";
      inits.param = input;
    }
    else if(str=="--endt") {
      if(i==argc-1) {
        cerr << "`" << str << "' needs an input.\n";
        return 2;
      }
      i++;
      string input = argv[i];
      cout << "using end-time value of `" << input << "'.\n";
      inits.end_time = input;
    }
    else if (str=="--endts") {
      if(i==argc-1) {
        cerr << "`" << str << "' needs an input.\n";
        return 2;
      }
      i++;
      string input = argv[i];
      cout << "using end-time step value of `" << input << "'.\n";
```

```
  inits.end_time_step = input;
}
else if(str=="--initxr") {
  if(i==argc-1) {
    cerr << "‘" << str << "’ needs an input.\n";
    return 2;
  }
  i++;
  string input = argv[i];
  cout << "using init Re(x) value of ‘" << input << "’.\n";
  inits.init_x_r = input;
}
else if(str=="--initxi") {
  if(i==argc-1) {
    cerr << "‘" << str << "’ needs an input.\n";
    return 2;
  }
  i++;
  string input = argv[i];
  cout << "using init Im(x) value of ‘" << input << "’.\n";
  inits.init_x_i = input;
}
else if(str=="--energy") {
  if(i==argc-1) {
    cerr << "‘" << str << "’ needs an input.\n";
    return 2;
  }
  i++;
  string input = argv[i];
  cout << "using energy value of ‘" << input << "’.\n";
  inits.energy = input;
}
else if(str=="-i") {
  cout << "entering interative mode...\n";
  {
    string input;
    cout << "enter end time (" << inits.end_time << "): ";
    getline(cin,input);
    if(input=="x" || input=="exit"
        || input=="quiet" || input=="q")
      return 1;
    if(!input.empty())
      inits.end_time = input;
```

```
}
{
  string input;
  cout << "enter end time steps (" << inits.end_time_step<< "): ";
  getline(cin,input);
  if(input=="x" || input=="exit" || input=="quiet" || input=="q")
    return 1;
  if(!input.empty())
    inits.end_time_step = input;
}
{
  string input;
  cout << "enter initial Re(x) (" << inits.init_x_r << "): ";
  getline(cin,input);
  if(input=="x" || input=="exit" || input=="quiet" || input=="q")
    return 1;
  if(!input.empty())
    inits.init_x_r = input;
}
{
  string input;
  cout << "enter initial Im(x) (" << inits.init_x_i << "): ";
  getline(cin,input);
  if(input=="x" || input=="exit" || input=="quiet" || input=="q")
    return 1;
  if(!input.empty())
    inits.init_x_i = input;
}
{
  string input;
  cout << "enter energy (" << inits.energy << "): ";
  getline(cin,input);
  if(input=="x" || input=="exit" || input=="quiet" || input=="q")
    return 1;
  if(!input.empty())
    inits.energy = input;
}
string input;
cout << "end time: " << inits.end_time
   << "\nend time step: " << inits.end_time_step
   << "\ninitial Re(x): " << inits.init_x_r
   << "\ninitial Im(x): " << inits.init_x_i
   << "\nenergy: " << inits.energy
```

```
         << "\nok? (y/N): ";
      getline(cin,input);
      if ( input!="y" && input!="yes" ) {
        cout << "ok, aborting...\n";
        return 1;
      }
      break;
    }
    else {
      cerr << "error: unrecognized input: `" << str << "'.\n";
      return 2;
    }
  }
  return 0;
}
```

References

[1] C. M. Bender, Rep. Prog. Phys. **70**, 947-1018 (2007).

[2] T. T. Wu, Phys. Rev. **115**, 1390 (1959).

[3] R. Brower, M. Furman, and M. Moshe, Phys. Lett. B **76**, 213 (1978); B. Harms, S. Jones, and C.-I Tan, Nucl. Phys. **171**, 392 (1980) and Phys. Lett. B **91**, 291 (1980).

[4] M. E. Fisher, Phys. Rev. Lett. **40**, 1610 1978; J. L. Cardy, *ibid.* **54**, 1345 1985; J. L. Cardy and G. Mussardo, Phys. Lett. B 225, 275 1989; A. B. Zamolodchikov, Nucl. Phys. B **348**, 619 (1991).

[5] E. Caliceti, S. Graffi, and M. Maioli, Comm. Math. Phys. **75**, 51 (1980).

[6] C. M. Bender, arXiv: quant-ph/0501052v1.

[7] A. A. Andrianov, Ann. Phys. **140**, 82 (1982).

[8] T. Hollowood, Nucl. Phys. B **384**, 523 (1992).

[9] F. G. Scholtz, H. B. Geyer, and F. J. H. Hahne, Ann. Phys. **213**, 74 (1992).

[10] R. F. Streater and A. S. Wightman, *PCT, Spin and Statistics, and All That* (Benjamin, New York, 1964).

[11] C. M. Bender, K. A. Milton, S. S. Pinsky, and L. M. Simmons, Jr., J. Math. Phys. **30**, 1447 (1989).

[12] C. M. Bender and S. Boettcher, Phys. Rev. Lett. **80**, 5243 (1998).

[13] P. Dorey, C. Dunning and R. Tateo, J. Phys. A: Math. Gen. **34**, 5679 (2001).

[14] P. Dorey, C. Dunning and R. Tateo, Czech. J. Phys. **54**, 35 (2004).

[15] K. C. Shin, J. Math. Phys. **42**, 2513 (2001); Commun. Math. Phys. **229**, 543 (2002); J. Phys. A: Math. Gen **37**, 8287 (2004); J. Math. Phys. **46**, 082110 (2005); J. Phys. A: Math. Gen **38**, 6147 (2005).

[16] F. Pham and E. Delabaere, Phys. Lett. A**250**, 25-28 (1998).

[17] E. Delabaere and F. Pham, Phys. Lett. A**250**, 29-32 (1998); E. Delabaere and D. T. Trinh, J. Phys. A: Math. Gen. **33**, 8771-8796 (2000).

[18] D. T. Trinh, PhD Thesis, University of Nice-Sophia Antipolis (2002).

[19] S. Weigert, J. Opt. B **5**, S416 (2003); J. Phys. A: Math. Gen. **39**, 235 (2006); J. Phys. A: Math. Gen. **39**, 10239 (2006).

[20] S. Weigert, Phys. Rev. A **68**, 062111 (2003).

[21] F. G. Scholtz and H. B. Geyer, Phys. Lett B**634**, 84 (2006); F. G. Scholtz and H. B. Geyer, arXiv: quant-ph/0602187.

[22] A. Mostafazadeh, J. Phys. A: Math. Gen. **38**, 3213 (2005).

[23] A. Mostafazadeh, J. Math. Phys. **43**, 205 (2002).

[24] A. Mostafazadeh, J. Math. Phys. **43**, 2814, 3944, and 6343 (2002); **44**, 943 and 974 (2003).

[25] A. Mostafazadeh, Nucl. Phys. B **640**, 419 (2002).

[26] C. M. Bender and S. A. Orszag, *Advanced Mathematical Methods for Scientists and Engineers*, (McGraw Hill, New York, 1978).

[27] C. M. Bender and A. Turbiner, Phys. Lett. A**173**, 442 (1993).

[28] F. J. Dyson, Phys. Rev. **85**, 631 (1952).

[29] C. M. Bender, D. C. Brody, and H. F. Jones, Phys. Rev. Lett. **92**, 119902 (2004).

[30] G. A. Mezincescu, J. Phys. A: Math. Gen. **33**, 4911 (2000).

[31] C. M. Bender and Q. Wang, J. Phys. A: Math. Gen. **34**, 3325 (2001).

[32] P. A. M. Dirac, Proc. R. Soc. London A **180**, 1 (1942).

[33] A. Mostafazadeh and A. Batal, J. Phys. A: Math. Gen. **37**, 11645 (2004).

[34] H. F. Jones, J. Phys. A: Math. Gen. **38**, 1741 (2005).

[35] T. Curtright and L. Mezincescu, arXiv: quant-ph/0507015.

[36] C. M. Bender, P. N. Meisinger, and Q.Wang, J. Phys. A: Math. Gen. **36**, 1973 (2003).

[37] C. M. Bender, D. C. Brody, and H. F. Jones, Phys. Rev. D **70**, 025001 (2004).

[38] C. M. Bender and H. F. Jones, Phys. Lett. A**328**, 102 (2004).

[39] C. M. Bender, S. Boettcher, and P. N. Meisinger, J. Math. Phys. **40**, 2201 (1999).

[40] A. Nanayakkara, Czech. J. Phys. **54**, 101 (2004) and J. Phys. A: Math. Gen. **37**, 4321 (2004).

[41] C. M. Bender, J.-H. Chen, D. W. Darg, and K. A. Milton, J. Phys. A: Math. Gen. **39**, 4219 (2006).

[42] C. M. Bender, D. D. Holm, and D. W. Hook, J. Phys. A: Math. Theor. **40**, F81 (2007).

[43] C. M. Bender, Contemp. Phys. **46**, 277 (2005).

[44] C. M. Bender, D. C. Brody, J.-H. Chen, and E. Furlan, J. Phys. A: Math. Theor. **40**, F153 (2007).

[45] A. Fring, J. Phys. A: Math. Theor. **40**, 4215 (2007).

[46] C. M. Bender and D. W. Darg, J. Math. Phys. **48**, 042703 (2007).

[47] C. M. Bender, Rep. Prog. Phys. **70**, 947 (2007).

[48] C. M. Bender, D. D. Holm, and D. W. Hook, J. Phys. A: Math. Theor. **40**, F793 (2007).

[49] C. M. Bender, D. D. Holm, and D. W. Hook, in preparation.

[50] C. M. Bender, D. C. Brody, and D. W. Hook, J. Phys. A: Math. Theor. **41**, 352003 (2008).

[51] T. Arpornthip and C. M. Bender, Pramana J. Phys. **73**, 2 (2009).